University of Cologne

Porting conventional tools to quantum geometrodynamics

Inaugural-Dissertation

zur

Erlangung des Doktorgrades

der Mathematisch-Naturwissenschaftlichen Fakultät

der Universität zu Köln

vorgelegt von

Yi-Fan Wang (王 一帆)

aus Sichuan, China

Diese Dissertation wurde im Jahr 2021
von der Mathematisch-Naturwissenschaftlichen Fakultät
der Universität zu Köln angenommen.

1. Gutachter: **Prof. Dr. Claus Kiefer**
Institut für Theoretische Physik
Universität zu Köln

2. Gutachter: **Jun.-Prof. Dr. Nele Callebaut**
Institut für Theoretische Physik
Universität zu Köln

Tag der mündlichen Prüfung: 19. Juli 2021.

Summary

As the prevailing theory of gravitation, the general theory of relativity successfully describes classical gravitation, but has yet to be consistently quantised, despite the efforts of generations of physicists in over a hundred years.

One of the first attempts to quantise general relativity directly is the Wheeler–DeWitt approach. It begins with the Hamiltonian formulation of this theory by Arnowitt, Deser and Misner, and applies the quantisation scheme of Dirac, designed for constrained systems, including the Dirac spinors and the Maxwell theory, among others. This approach, also known as quantum geometrodynamics, is successful in the semi-classical method of Wentzel–Kramers–Brillouin (WKB) and Born–Oppenheimer, and has been applied to quantum models of universes and black holes.

Unfortunately, because of the constrained nature of general relativity (from another perspective, its diffeomorphism invariance), its quantised version à la Dirac lacks many properties that are crucial in conventional quantum theory. Particularly, the scalar product of quantum states is difficult to define, rendering the non-existence of a Hilbert space, and of the analysis of self-adjoint operators. Moreover, the semi-classical approach described above only works for wave functions in the WKB form, which contain the classical Hamilton's principal function as a phase factor in the leading-order approximation. For wave-packets, which naturally arise in many realistic systems, even their corresponding semi-classical trajectories cannot be calculated; in conventional quantum mechanics, in contrast, one can refer to the Ehrenfest theorem if the wave-packet is sharp.

In this dissertation, we try to address these problems of the Wheeler–DeWitt approach by porting conventional tools in physics and mathematics to this context. We study a two-dimensional minisuperspace model, related to physical cosmological models, to illustrate our arguments.

Under the WKB approximation, we show that a narrow Gaussian wave-packet has "maxima" on the semi-classical trajectory, which is given by the stationary phase principle, that also governs the WKB approach. In other words, these two semi-classical approaches are consistent in the semi-classical trajectory.

By considering additional conditions, an effective Hilbert space emerges from our minisuperspace model, and the Hamiltonian, responsible for the energy spectrum, can have non-trivial self-adjoint extensions. We study its self-adjoint domains in detail and argue that these mathematical properties could lead to physical effects.

In order to maintain consistency of our new tools for both quantum gravitation and conventional quantum theory, we construct a framework of stationary wave-

packets, that make sense for both the minisuperspace Wheeler–DeWitt equation and the stationary Schrödinger equation. In doing so, we also argue for the suitable choice of amplitudes when constructing wave-packets. The framework is then tested by the model of two-dimensional hydrogen atom.

Finally, we discuss approaches to find the semi-classical trajectories from arbitrary wave-packets, which are methods for ridge-detection. We discuss different mathematical descriptions of ridge-lines, which were historically developed for Riemannian geometry with Euclidean metric signature. Then we try to generalise these descriptions to pseudo-Riemannian geometry with Lorentzian metric signature, which is the usual case of minisuperspaces. In the end, we give proposals of prospective physical applications.

Zusammenfassung

Als vorherrschende Gravitationstheorie beschreibt die Allgemeine Relativitätstheorie zwar erfolgreich die klassischen Gravitation, konnte aber trotz der Bemühungen von Generationen von Physikerinnen und Physikern in über hundert Jahren noch nicht konsistent quantisiert werden.

Einer der ersten Versuche, die Allgemeine Relativitätstheorie direkt zu quantisieren, ist der Wheeler–DeWitt-Ansatz. Er beginnt mit der Hamiltonschen Formulierung dieser Theorie von Arnowitt, Deser und Misner, und wendet das Quantisierungsschema von Dirac an, was für Systeme mit Zwangsbedingungen entworfen wurde, unter anderem für die Dirac-Spinoren und die Maxwell-Theorie. Dieser Ansatz, der auch als Quantengeometrodynamik bezeichnet wird, ist in der semiklassischen Methode von Wentzel–Kramers–Brillouin (WKB) und Born–Oppenheimer erfolgreich und auf Quantenmodelle von Universen und Schwarzen Löchern angewendet worden.

Leider fehlen ihrer quantisierten Version à la Dirac aufgrund der Zwangsbedingungen (oder der Diffeomorphismusinvarianz) der Allgemeinen Relativitätstheorie viele Eigenschaften, die in der konventionellen Quantentheorie entscheidend sind. Insbesondere ist das Skalarprodukt von Quantenzuständen schwer zu definieren, was die Nichtexistenz eines Hilbert-Raums sowie der Analyse selbstadjungierter Operatoren zur Folge hat. Außerdem funktioniert der oben beschriebene semiklassische Ansatz für Wellenfunktionen in der WKB-Form, die in der ersten Ordnung die klassische Wirkung als Phasenfaktor enthalten. Für Wellenpakete, die natürlich in vielen realistischen Systemen vorkommen, können nicht einmal die entsprechenden semi-klassischen Trajektorien berechnet werden; in der konventionellen Quantenmechanik kann man dagegen auf das Ehrenfest-Theorem zurückgreifen, wenn das Wellenpaket scharf ist.

In dieser Dissertation versuchen wir, diese Probleme des Wheeler–DeWitt-Ansatzes zu lösen, indem wir konventionelle Werkzeuge der Physik und Mathematik auf diesen Kontext übertragen. Wir untersuchen ein zweidimensionales Minisuperraum-Modell, das mit physikalischen kosmologischen Modellen verwandt ist, um unsere Argumente zu illustrieren.

Unter der WKB-Näherung zeigen wir, dass ein schmales Gaußsches Wellenpaket „Maxima“ auf der semiklassischen Trajektorie hat, die durch das stationäre Phasenprinzip gegeben ist, das auch den WKB-Ansatz steuert. Mit anderen Worten, diese beiden semiklassischen Ansätze sind auf der semiklassischen Trajektorie konsistent.

Durch die Berücksichtigung zusätzlicher Bedingungen entsteht aus unserem Minisuperraum-Modell ein effektiver Hilbert-Raum, und der für das Energiespek-

trum zuständige Hamiltonoperator kann nicht-triviale selbstadjungierte Erweiterungen haben. Wir untersuchen seine selbstadjungierten Definitionsbereiche im Detail und argumentieren, dass diese mathematischen Eigenschaften zu physikalischen Effekten führen könnten.

Um die Konsistenz unserer neuen Werkzeuge sowohl für die Quantengravitation als auch für die konventionelle Quantentheorie aufrechtzuerhalten, konstruieren wir ein Gerüst, das wir stationäre Wellenpakete nennen und das sowohl für die Minisuperraum Wheeler–DeWitt-Gleichung als auch für die stationäre Schrödinger-Gleichung sinnvoll ist. Dabei argumentieren wir auch für die geeignete Auswahl der Amplituden bei der Konstruktion von Wellenpaketen. Die Konstruktion wird dann anhand des Modells des zweidimensionalen Wasserstoffatoms getestet.

Schließlich diskutieren wir Ansätze, um die semiklassischen Trajektorien aus beliebigen Wellenpaketen zu finden, die Methoden zur Ridge-Erkennung sind. Wir diskutieren verschiedene mathematische Beschreibungen von Kammwegen, die historisch für die Riemannsche Geometrie mit euklidischer metrischer Signatur entwickelt wurden. Dann versuchen wir, diese Beschreibungen auf pseudo-Riemannsche Geometrie mit Lorentzscher metrischer Signatur zu verallgemeinern, was der übliche Fall für Minisuperräumen ist. Zum Schluss geben wir Vorschläge für mögliche physikalische Anwendungen.

Erklärung zur Dissertation

gemäß der Promotionsordnung vom 02. Februar 2006 mit den
Änderungsordnungen vom 10. Mai 2012, 16. Januar 2013 und 21. Februar 2014

Ich versichere, dass ich die von mir vorgelegte Dissertation selbständig angefertigt, die benutzten Quellen und Hilfsmittel vollständig angegeben und die Stellen der Arbeit – einschließlich Tabellen, Karten und Abbildungen –, die anderen Werken im Wortlaut oder dem Sinn nach entnommen sind, in jedem Einzelfall als Entlehnung kenntlich gemacht habe; dass diese Dissertation noch keiner anderen Fakultät oder Universität zur Prüfung vorgelegen hat; dass sie – abgesehen von unten angegebenen Teilpublikationen – noch nicht veröffentlicht worden ist, sowie, dass ich eine solche Veröffentlichung vor Abschluss des Promotionsverfahrens nicht vornehmen werde.

Die Bestimmungen der Promotionsordnung sind mir bekannt. Die von mir vorgelegte Dissertation ist von Prof. Dr. Claus Kiefer betreut worden.

Teilpublikationen

A. A. Andrianov u. a., "Integrable minisuperspace models with Liouville field: energy density self-adjointness and semiclassical wave packets", The European Physical Journal C **78**, 786 (2018), arXiv:1802.06720 [hep-th]

Datum / Unterschrift

To my beloved Qinglan Liu (劉 青藍)
Also to Don Jon (糖漿) and Cassie (開水)

Contents

List of Figures

List of Tables

1 Introduction

Among the so-called four fundamental interactions, gravitation is the earliest to be described by axiomatic mathematics, which traces back to Isaac Newton in the 17th century, but remains the last to be quantised. There are various motivations to do so, both from an experimental and theoretical point of view. To be short, consistent treatment of quantum matter with gravitational interaction needs a quantum description of the latter. Now that all other fundamental degrees of freedom are quantised, a quantum theory of gravitation is also indispensable. We refer to [91, sec. 1.1.2] for a comprehensive review of the reasons to quantise gravitation.

As is well-known, the most widely accepted classical theory of gravitation is the general theory of relativity, which was mainly developed by Albert Einstein between 1907 and 1915. Therefore, a straightforward way to quantise gravitation is to quantise general relativity, which has already been suggested by Einstein himself [51]. Although people are quite experienced in quantising matters and other interactions, gravitation remains a hard bone. Aside from the experimental difficulties that no concrete proposal to test the quantum theories of gravitation can be carried out, general relativity also differs from the other gauge interactions. The latters are all in the framework of Yang–Mills theory, which at the classical level deals with *additional* fibre-bundle structures on the space-time manifold [172]. General relativity, on the other hand, lives *in* space-time itself. For a comprehensive discussion of the gauge aspects of gravitation, see [22].

One of the oldest approaches to quantise the *full* theory of general relativity is the Wheeler–DeWitt approach, also known as quantum geometrodynamics, dating back to 1967. It handles a Hamiltonian formalism of general relativity, credited to Arnowitt, Deser and Misner in 1959 – 1962, and then applies the Dirac quantisation rules. We recommend [92] and the subsequent chapters for a recent review of the various ways to quantise general relativity and other approaches towards quantum gravitation.

1.1 The problem of lacking tools

Unfortunately, after thriving in the late 1980s and early 90s, the community of quantum gravity seems to become less interested in quantum geometrodynamics, which can be coarsely reflected in the number of citations of the establishing paper [40], see fig. 1. Although it certainly subjects to serious historical research, we believe that one reason that discourages people from working further on the Wheeler–DeWitt approach is the deep difference between this quantum theory and the conventional one, which leaves *few tools* for researchers to carry out concrete

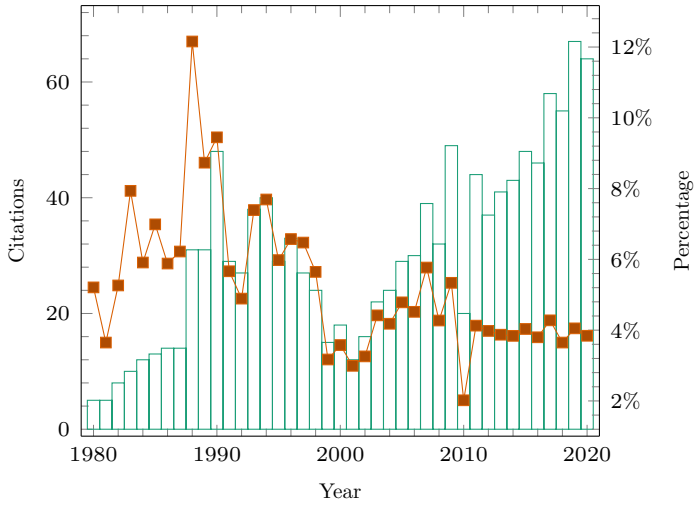

Figure 1: Citations of [40] with the keyword "quantum gravity" from 1980 to 2020. The green bar chart is the number of citations with the scale on the left, whereas the orange line chart is the percentage of citations in all papers with the keyword "quantum gravity". Source: INSPIRE.

predictions.

One such difference is reflected in the closely related problems, the lack of a Hilbert space and the absence of space-time (the problem of time). Technically, the Wheeler–DeWitt approach adapts the functional Schrödinger formalism, instead of the usual Fock-space formalism in quantum theory of fields, which starts from quantising merely the *fluctuation* of fields. Within the former formalism, an inner product is difficult to define. In contrast, the Hamiltonian in the Arnowitt–Misner–Deser formalism consists of pure constraints that are constrained to zero on shell. Upon Dirac quantisation, the wave function does not evolve with respect to a(n) (fictitious) external time, which therefore does not exist. For further discussion about these problems, see e.g. [91, ch. 5].

The lack of a Hilbert space in the Wheeler–DeWitt approach results immediately in the inability of predicting, in terms of probability amplitudes and spectra of self-adjoint operators, what play a central role in conventional quantum mechanics and quantum theory of fields. Incidentally, the self-adjointness in other quantum systems is also a focus in recent years. Since the theoretical discovery of PT-symmetric Hamiltonians that seem to be non-Hermitian but have real spectra [16], it has also been discovered in optics that systems with non-Hermitian, PT-symmetric Hamiltonian can be non-dispersive [146]. An extension of the good old Hermiticity, to the mathematical self-adjointness, is not only a theoretical fantasy, that enriches the possible systems to be studied [121], but also an experimental reality.

The deficits, caused by the missing probability amplitudes and self-adjointness,

are partially compensated by the semi-classical schemes, that study a subset of all allowed quantum states, which "has a classical correspondence". One of them is the Wentzel–Kramers–Brillouin (WKB) + Born–Oppenheimer approximation, which separates the gravitational and the matter degrees of freedom in a wave function of the universe in the WKB form. At the end of the day, the matter part of the wave function obtains a Schrödinger type of equation, and the conventional quantum theory is restored. Another one is using a narrow cosmological wave-packet, that arises heuristically by decoherence, and the classical correspondence lies on the sharp ridge of the wave-packet. In a sense, this scheme implies a probabilistic interpretation of cosmological wave functions. The two schemes mentioned above are described in [91, sec. 5.4, 90, 89] and other related chapters in these books.

The full quantum geometrodynamics, which deals with all degrees of freedom in general relativity, sometimes also with matter, is governed by functional differential equations named after Wheeler and DeWitt, and is formidable to work with. In practice, people often adapt a symmetry reduction, effectively "freeze" many of them, and study midi- and minisuperspace [117] models, if the system contains field-theoretical degrees of freedom, or only particle degrees of freedom, respectively. Applications of midi- and minisuperspace models include quantum black holes and quantum cosmology, which has been surveyed in e.g. [91, ch. 7 and 8].

1.2 Outline of the dissertation

In this dissertation, we address the above-mentioned deep difference between the conventional quantum theories and the Wheeler–DeWitt approach, within the framework of a prototype minisuperspace model in section 2, that is related to various realistic models in physics, and can also be solved exactly. Afterwards in section 3, we perform the standard WKB analysis of the model.

Since analytic results of wave-packets can be obtained both for the exact and the WKB wave packets, it makes sense to ask the following questions that have yet to be answered. First, how is the WKB approximation related to the narrow wave-packets, that both have its own classical correspondence? This question is addressed in section 3 and our answer is that they coincide. Second, does a Hilbert space make physical sense in minisuperspace models? This question is studied in section 4 in which we find that the self-adjointness of operators in quantum cosmology do have a physical effect. Third, where is the ridge of a given wave-packet? To answer this question, we first find the special wave-packets in conventional quantum mechanics that share the properties with the ones in minisuperspace models, which is done in section 5. Then we give mathematical descriptions of ridge-lines,

apply them in various examples, and discuss their advantages as well as deficits.

In the appendices we describe aspects that are either not included in the usual graduate courses, or not emphasised but are frequently used in the thesis.

The Wheeler–DeWitt approach is conservative, in the sense that it does not need much new concepts as *input*; the metric degrees of freedom and the canonical quantisation rules are all well-recognised, whereas much of the unconventional concepts are *derived* from the input. This is an advantage, in our mind, that the approach has an elegance of simplicity. On the other hand, in studying nature, *new tools* are no less important than new concepts, the former of which are unfortunately often belittled in theoretical physics, while the latter can be exaggerated.

In this dissertation, we try to provide novel tools to the old quantum geometrodynamics. More specifically, the gap between the conventional quantum theories and the Wheeler–DeWitt approach worried us, and the lacking of prediction power for wave-packets remained unsettled. Therefore, we provide a multifaceted parallel between the conventional quantum theories and quantum geometrodynamics, and pave the way towards retrieving a classical trajectory from wave-packets.

2 A two-dimensional minisuperspace model

In this section 2, we study a prototype minisuperspace model that traces back to [6, 4, 5], which is described by the Lagrangian action in minisuperspace

$$S = \mathrm{Vol}_3 \int \mathbb{d}t\, M(t) \left\{ \mathsf{s} \left(-\frac{3}{\varkappa} \frac{\dot{\gamma}^2}{M(t)^2} + \frac{\mathsf{l}}{2} \frac{\dot{\chi}^2}{M(t)^2} \right) - V \mathrm{e}^{g\chi} \right\} \tag{2.1a}$$

$$=: \int \mathbb{d}t \left\{ \frac{1}{2M(t)} \mathcal{G}_{IJ} q^I q^J - M(t) \mathcal{V}(q) \right\}, \tag{2.1b}$$

where $\mathsf{s}^2 = \mathsf{l}^2 = \mathsf{v}^2 = 1$ are signs, $\mathsf{v} := \operatorname{sgn} V$, $g > 0$ is a coupling factor; $\mathcal{G}_{IJ}$'s are the components of the *minisuperspace* DeWitt metric,[1] $\mathcal{V}$ the potential, and q^I denotes collectively the minisuperspace position variables $\{\gamma, \chi\}$. One sees that M corresponds to a lapse function and has no dynamics, whereas γ and χ are the dynamic variables.

We will see in section 2.1 that this prototype model contains several homogeneous cosmological models as its special cases. Moreover, it is exactly solvable at both the classical (section 2.2) and the quantum levels (section 2.3), which facilitates the further study of the model. These motivate the study of the minisuperspace model. As an example, we construct an exact quantum wave-packet in section 2.5.

About superspace and its mini-version In this work, the term *superspace* is coined by Wheeler (e.g. [169]), referring to the configuration space of geometrodynamics, in contrast to the somewhat more popular meaning of a supermanifold, which is central in supersymmetry. See [68] for a historical note.

Minisuperspace, on the other hand, refers to the symmetry-reduced superspace, that contains particle-like degrees of freedom, and no field-theoretical degrees of freedom. The term can at least be traced back to [117]. Such models in general relativity also contain collapse models related to black holes (e.g. [95, 150, 103, 134]).

2.1 Physical models related to the prototype

In relativistic physical cosmology, which was founded in [52], it is usually assumed that our Universe is homogeneous and isotropic at large scale. This assumption is sometimes called the *cosmological principle*, and realised as the Friedmann–Lemaître model [56, 109], equipped with the Robertson–Walker metric [143, 163], that makes a sensible exact solution of the Einstein's field equations. Starting

[1] Unfortunately, DeWitt metric in the full geometrodynamics has *upper* indices.

from here, one can then study inhomogeneities of the Universe by e.g. considering metric perturbations [76], which is out of the scope of this thesis.

Although no fundamental scalar field manifests at the classical level, it is still an easy starting point of a matter content in a cosmological model. Cases with a normal-signed kinetic term, dubbed *quintessence* [31], and with a negative-signed kinetic term, called *phantom* [30], have their applications, e.g. [39]. Extending the potential to complex numbers can give rise to a PT-symmetric scalar field [4], making more room for possible models.

Aside from the isotropic case, theoretical physicists are also interested in *an*isotropic homogeneous models, with the benefit that the extra degrees of freedom are particle-like and not field-theoretic [38, 93, 104, 94, 103]. In cosmology, the anisotropic homogeneous models in $(3+1)$-dimensions are classified into the nine Bianchi-type universes [20, 21] and the Kantowski–Sachs metric [84], the former of which are summarised in e.g. [147, 107, sec. 116].

Our prototype model in eq. (2.1a) contains several cosmological models mentioned above as special cases, described in this section 2.1 below.

2.1.1 Closed Friedmann–Lemaître–scalar model

To begin with, we consider a spatially-*closed* Friedmann–Lemaître model, minimally coupling the model to a homogeneous, isotropic, massless, free, and neutral scalar field $\phi \in \mathbb{R}$. This is a solvable model, making it a good starting point [86, 91, ch. 8].

The Robertson–Walker metric of this model is given by

$$\mathbb{d}s^2 = -N(t)^2\,\mathbb{d}t^2 + \mathrm{Len}^2\mathsf{e}^{2\alpha(t)}\Big(\mathbb{d}\xi^2 + \sin^2\xi\,\Big(\mathbb{d}\vartheta^2 + \sin^2\theta\,\mathbb{d}\varphi^2\Big)\Big)\,, \tag{2.2}$$

where $t \in \mathbb{R}$, the hyperspherical coordinates $\xi, \theta \in (0,\pi)$, $\varphi \in (0, 2\pi)$; $N(t)$ is the lapse function, and $\alpha(t)$ is the logarithm of a dimensionless scale factor. Only t and Len have the dimension of length; other variables on the right-hand side are all dimensionless.

Introducing a free neutral scalar field, and complete the spatial integration, we obtain the Lagrangian action

$$S = \mathrm{Vol}_3 \int \mathbb{d}t\, N\mathsf{e}^{3\alpha}\left\{-\frac{3}{\varkappa}\frac{\dot\alpha^2}{N^2} + \frac{\mathsf{r}}{2}\frac{\dot\phi^2}{N^2} - V_{\mathrm{cur}}\mathsf{e}^{-2\alpha}\right\}, \tag{2.3a}$$

$$\text{where} \qquad \mathsf{r}^2 = 1\,; \quad V_{\mathrm{cur}} \coloneqq \frac{3}{\varkappa \mathrm{Len}^2} > 0\,, \quad \mathrm{Vol}_3 \coloneqq 2\pi^2\mathrm{Len}^3\,. \tag{2.3b}$$

The sign r is introduced to incorporate the cases of the field with a normal-signed kinetic term $\mathsf{r} = +$ (aka quintessence) or a negative-signed kinetic term $\mathsf{r} = -$

(aka phantom).

Comparing eq. (2.3a) with eq. (2.1a), one observes that the following transformations

$$N = M\mathsf{e}^{3\alpha}\,; \qquad \alpha = \sqrt{\frac{\varkappa}{6}}\,\chi\,, \quad \phi = \sqrt{\frac{6}{\varkappa}}\,\gamma\,; \qquad g \coloneqq 2\sqrt{\frac{2\varkappa}{3}}\,. \tag{2.4}$$

gives the prototype action in eq. (2.1a) with $(\mathsf{s}, \mathsf{l}, \mathsf{v}) = (-\mathsf{r}, \mathsf{r}, +)$.

Note on the lapse function In many applications in cosmology, the Robertson–Walker metric is introduced without the lapse function $N(t)$, e.g. [165, 107, sec. 111], and one may wonder the reason to do so.

One can simply take it as a part of the Arnowitt–Deser–Misner formalism, see appendix B.2. Apart from this reason, its presence also makes the symmetry-reduced actions in eqs. (2.7), (2.3a) and (2.10a) *equivalent* to the corresponding Friedmann equations, which means the equations of motion followed by varying the actions are the same as substituting the metrics in eqs. (2.2), (2.6) and (2.9) into Einstein's field equations. Were $N(t)$ not present, the first Friedmann equation, which contains only *first-order* time derivative and is therefore a constraint, would be missing in the Euler–Lagrange equations.

Being able to derive the constraint equations from the action is important in Dirac quantisation, see section 2.3.

2.1.2 Flat Friedmann–Lemaître–Liouville model

Next, we consider a spatially-*flat* Friedmann–Lemaître model. The spatial flatness is traditionally preferred and consistent with the up-to-date observation [1]. A *Liouville* scalar field ϕ has an *exponential* potential

$$\mathcal{V}(\phi) = V\mathsf{e}^{\lambda\phi}\,, \qquad \lambda \in \mathbb{R}\,, \tag{2.5}$$

which traces back to the homonymous equation [112]; it is used nowadays in certain branches of string theory (e.g. [123]), but here we use "Liouville field" outside this context. Incidentally, the Friedmann–Lemaître–Liouville model has also been studied in the context of inflation [74, 28, 15].

The Robertson–Walker metric of the model is given by

$$\mathbb{d}s^2 = -N(t)^2\,\mathbb{d}t^2 + \mathsf{e}^{2\alpha(t)}\big(\mathbb{d}x^2 + \mathbb{d}y^2 + \mathbb{d}z^2\big)\,, \tag{2.6}$$

where the Cartesian coordinates $t, x, y, z \in \mathbb{R}$. The lapse function $N(t)$ and the logarithmic scale factor $\alpha(t)$ are dimensionless; other variables on the right-hand

side have the dimension of length.

Minimally coupling the model to a Liouville scalar field, that is homogeneous, isotropic, and neutral, and *formally* integrating out the spatial variables, we obtain the Lagrangian action [5]

$$S = \mathrm{Vol}_3 \int \mathbb{d}t\, N\mathsf{e}^{3\alpha}\left\{-\frac{3}{\varkappa}\frac{\dot{\alpha}^2}{N^2} + \frac{\mathsf{l}}{2}\frac{\dot{\phi}^2}{N^2} - V\mathsf{e}^{\lambda\phi}\right\}, \tag{2.7}$$

where $\mathrm{Vol}_3 = \int \mathbb{d}x\, \mathbb{d}y\, \mathbb{d}z$ is a formal 3-volume factor.

Comparing eq. (2.7) with eq. (2.1a), one observes that the following transformations

$$N = M\mathsf{e}^{3\alpha}\,; \tag{2.8a}$$

$$\begin{pmatrix}\alpha\\ \phi\end{pmatrix} = \pm\frac{1}{g}\begin{pmatrix}\lambda & -\mathsf{l}\mathsf{s}\varkappa\\ -6 & \mathsf{s}\lambda\end{pmatrix}\begin{pmatrix}\gamma\\ \chi\end{pmatrix}, \tag{2.8b}$$

$$\mathsf{s} := \mathrm{sgn}(\lambda^2 - 6\mathsf{l}\varkappa)\,, \qquad g := \sqrt{|\lambda^2 - 6\mathsf{l}\varkappa|}\,. \tag{2.8c}$$

give the prototype action in eq. (2.1a) if $\lambda^2 - 6\mathsf{l}\varkappa \neq 0$.

2.1.3 Vacuum Kantowski–Sachs models

Finally, we consider the Kantowski–Sachs spacetime. Without matter content, this is just the interior of Schwarzschild spacetime.

In Misner's parameterisation [60, 12], the Kantowski–Sachs metric reads

$$\begin{aligned}\mathbb{d}s^2 = &-N(t)^2\,\mathbb{d}t^2\\ &+ \mathrm{Len}^2\left[\mathsf{e}^{2\sqrt{3}\beta(t)}\,\mathbb{d}\xi^2 + \mathsf{e}^{-2\sqrt{3}(\beta(t)+\Omega(t))}\left(\mathbb{d}\theta^2 + \sin^2\theta\,\mathbb{d}\varphi^2\right)\right],\end{aligned} \tag{2.9}$$

where $t, \xi \in \mathbb{R}$. This parameterisation has an advantage for separating the kinetic term in the minisuperspace action. *In vacuum*, this metric just describes the Schwarzschild metric inside the horizon [84].

Upon formally integrating out ξ, θ, and φ, the minisuperspace action reads

$$S = \mathrm{Vol}_3 \int \mathbb{d}t\, N\mathsf{e}^{-\sqrt{3}(\beta+2\Omega)}\left\{\frac{3}{\varkappa N^2}\left(-\dot{\Omega}^2 + \dot{\beta}^2\right) + V_{\mathrm{KS}}\mathsf{e}^{2\sqrt{3}(\beta+\Omega)}\right\}, \tag{2.10a}$$

$$V_{\mathrm{KS}} := \frac{1}{\varkappa\mathrm{Len}^2}\,, \quad \mathrm{Vol}_3 := 4\pi\mathrm{Len}^3\,. \tag{2.10b}$$

The transformations

$$N = M\mathsf{e}^{-\sqrt{3}(\beta+2\Omega)}\,; \qquad \beta = \gamma\,, \quad \Omega = -\sqrt{\frac{\varkappa}{6}}\,\chi\,; \qquad g := \sqrt{2\varkappa} \tag{2.11}$$

bring the action to the prototype form in eq. (2.1a) with $(\mathsf{I}, \mathsf{s}, \mathsf{v}) = (+, -, -)$.

2.2 Classical trajectory

The minisuperspace model in eq. (2.1a) can be exactly solved by the Lagrangian approach, which is to be shown here in section 2.2. In [5, 6] the solution in the Hamiltonian approach is described; also see section 2.3 below.

The Euler–Lagrange equations of motion for (M, γ, χ) can be derived to be

$$0 = \mathsf{s}\left(\frac{3}{\varkappa}\frac{\dot{\gamma}^2}{M(t)^2} - \frac{\mathsf{I}}{2}\frac{\dot{\chi}^2}{M(t)^2}\right) - V\mathrm{e}^{g\chi}\,, \tag{2.12a}$$

$$0 = -\frac{6\mathsf{s}}{\varkappa}\frac{\mathbb{d}}{\mathbb{d}t}\frac{\dot{\gamma}}{M}\,, \tag{2.12b}$$

$$0 = -gVM\mathrm{e}^{g\chi} - \mathsf{I}\mathsf{s}\frac{\mathbb{d}}{\mathbb{d}t}\frac{\dot{\chi}}{M}\,. \tag{2.12c}$$

One readily sees that as the Euler–Lagrange equation for M, eq. (2.12a) contain only a *first*-order time derivative of M. If it were a *dynamical* equation for M, the derivative would be a *second*-order one. Instead of dynamical, the equation is a *constraint* equation, and M is *not* a dynamical variable, in contrast to γ and χ. See also the comment at the end of this subsection.

From eq. (2.12b) one sees that γ is cyclic, so that its conjugate momentum

$$p_\gamma = -\frac{6\mathsf{s}\mathrm{Vol}_3\dot{\gamma}}{\varkappa M} \tag{2.13}$$

is a first integral of the system. Using p_γ to eliminate M in the Euler–Lagrange equations, and further eliminating the parameter t, one can obtain analytic solutions of the classical, *implicit* trajectory (or *history*, if we take the model as that of a *universe*) in terms of (γ, χ),

$$\mathrm{e}^{g\chi}\,\mathrm{trig}\Big(\sqrt{\tfrac{3}{2\varkappa}}g(\gamma-\gamma_0)\Big)^2 = \frac{\varkappa p_\gamma^2}{12\mathrm{Vol}_3^2|V|}\,, \tag{2.14}$$

where γ_0 is a constant, trig a trigonometric function which depends on the four possibilities of $(\mathsf{I}, \mathsf{sv})$, see table 1. All other cases, except for the $(-,-)$, leave trajectories in the (γ, χ) space, see fig. 2.

Note that eq. (2.14) is an *implicit* equation of trajectory in configuration space, in contrast to the usual *explicit* or *parametrised* representation of path. This reflects the property of reparametrisation invariance in the system, i.e. the parametrisation of the trajectory is not a priori significant; only with additional considerations, e.g. adding a fictitious comoving observer into the universe, does a parametrisation become relevant. Moreover, it is also easier for comparison with

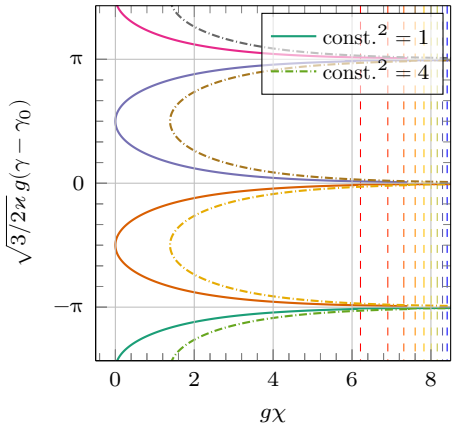

(a) $(-,+)$ with sin

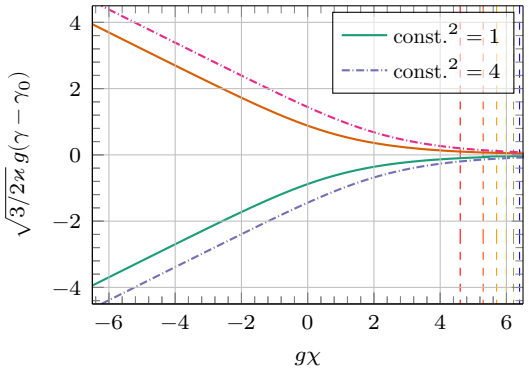

(b) $(+,-)$ with sinh

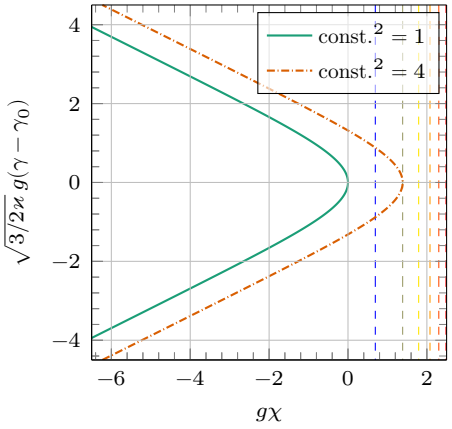

(c) $(+,+)$ with cosh

Figure 2: Three cases of the classical trajectories of the prototype model, which are given by eq. (2.14) and table 1, with p_γ such that $\frac{\varkappa p_\gamma^2}{12\mathrm{Vol}_3^2|V|} = 1$ (in solid lines) or 4 (dash-dotted lines). The contours (dashed lines) are the potential $-\mathrm{e}^{g\chi}$ (figs. 2a and 2b) or $+\mathrm{e}^{g\chi}$ (fig. 2c). Note that for the $(-,+)$ and $(+,-)$ cases, the implicit equation (2.14) contains multiple continuous trajectories: the former includes countably infinite many, whereas the latter comprises two, indicated in the plot by different colours.

(I, sv)	$\mathrm{trig}\Big(\sqrt{\frac{3}{2\varkappa}}g(\gamma-\gamma_0)\Big)^2$
$(-,-)$	$-\sin\Big(\sqrt{\frac{3}{2\varkappa}}g(\gamma-\gamma_0)\Big)^2$
$(-,+)$	$\sin\Big(\sqrt{\frac{3}{2\varkappa}}g(\gamma-\gamma_0)\Big)^2$
$(+,-)$	$\sinh\Big(\sqrt{\frac{3}{2\varkappa}}g(\gamma-\gamma_0)\Big)^2$
$(+,+)$	$\cosh\Big(\sqrt{\frac{3}{2\varkappa}}g(\gamma-\gamma_0)\Big)^2$

Table 1: Four cases of the trigonometrical function in eq. (2.14). The first case $(-,-)$ does not leave a real and physical trajectory for (γ, χ); $(-,+)$ gives infinitely many isolated trajectories due to the periodicity of the sine function, $(+,-)$ gives two, and $(+,+)$ gives one, see fig. 2.

the quantised system in the semi-classical approximation, see section 3 below.

Because of the implicity of the representation, there can be more than one trajectory contained in eq. (2.14) with the same constant γ_0. As can be seen in fig. 2, there are countably infinite trajectories in the $(I, sv) = (-,+)$ case, and two trajectory in the $(I, sv) = (+,-)$ case.

First-order differential equations as constraints We often take it for granted that the motion of a mechanical system is determined by all its positions and velocities at some point of time as the initial condition. This is sometimes known as *Newton's principle of determinacy* [9, sec. 1.1] (see also appendix B.1), and can be realised by differential equations that contain second-order (and no higher) time derivative terms. In these equations, the initial positions and velocities can be freely posed.

For an equation that contains only first-order time derivatives, its solution is determined by the initial position alone, and the initial velocities can no longer be arbitrarily given; they have to be compatible with the first-order equation. This is called a constraint, which is the case for eq. (2.12a).

2.3 Dirac quantisation

One can easily verify that the Lagrangian action in eq. (2.1a) is reparametrisation invariant, i.e. invariant under reparametrising

$$t \mapsto \tilde{t} = f(t)\,, \qquad f'(t) > 0\,. \tag{2.15}$$

For such systems that do not depend explicitly on t, it can be shown that (e.g. [91, sec. 3.1])

$$p_i \dot{q}^i - L = 0\,, \tag{2.16}$$

where (q^i, p_i) are the conjugate positions and momenta, and L the Lagrangian. One sees that the Hamiltonian of the system would be identically zero, if one were to construct it in the usual way.

Such reparametrisation-invariant systems can be shown to be *constrained* or *singular*, and the extended Hamiltonian formalism with inexpressible velocities and primary constraints are to be used. Details of this formalism are described in appendix A.1. Here in section 2.3, we give the steps that are essential for our prototype model.

To begin with, one rewrites eq. (2.1a) as *the action with inexpressible velocities and primary constraints*

$$S = \mathrm{Vol}_3 \int \mathrm{d}t \left\{ p_\gamma \dot{\gamma} + p_\chi \dot{\chi} + p_M \dot{M} - M H_\perp - p_M v^M \right\}, \tag{2.17}$$

where v^M is the *inexpressible velocity* of M, and the Hamiltonian constraint reads

$$H_\perp = H_\perp(\gamma, \chi; p_\gamma, p_\chi) = \frac{\mathsf{s}}{\mathrm{Vol}_3}\left(-\frac{\varkappa}{12} p_\gamma^2 + \frac{\mathsf{l}}{2} p_\chi^2\right) + \mathrm{Vol}_3 V \mathrm{e}^{g\chi} \tag{2.18a}$$

$$=: \frac{1}{2} \mathcal{G}^{IJ} p_I p_J + \mathcal{V}(q)\,, \tag{2.18b}$$

where $\mathcal{G}_{IJ}$'s are the components of the inverse *minisuperspace* DeWitt metric,[2] and p^I denotes collectively the minisuperspace momenta variables $\left(p_\gamma, p_\chi\right)$.

The action in eq. (2.17) is classically equivalent to the one in eq. (2.1a) in the following ways. First, varing v^M as well as the p's, and then inserting the resulting equations into eq. (2.17) gives back eq. (2.1a). Second, upon variation of all positions and momenta $\{q, p\}$ as well as the inexpressible velocity v^M, the resulting differential equations are equivalent to the equations of motion. To be more specific, the variation of p^M gives

$$v^M = \dot{M} \tag{2.19}$$

as an equation of motion; one also says that v^M is constrained to $\dot{M}$.

[2]Unfortunately, inverse DeWitt metric in the full geometrodynamics has *lower* indices.

The Hamiltonian with primary constraints in the action eq. (2.17)

$$H^{\mathrm{p}} = H^{\mathrm{p}}\big(M, \gamma, \chi; p_M, p_\gamma, p_\chi; v^M\big) = M H_\perp\big(\gamma, \chi; p_\gamma, p_\chi\big) + p_M v^M \tag{2.20}$$

is a linear combination of the primary constraint p_M and the secondary constraint $H_\perp$. At the classical level, variation of M and v^M gives

$$H_\perp = 0\,, \qquad p^M = 0\,, \tag{2.21}$$

respectively; in other words, *they are constrained to zero as a part of the equations of motion.* À la Dirac [44, 91, sec. 5.1], the constraint equations (2.21) are to be valid also at the quantum level upon acting on the wave function. This leads to the *minisuperspace Wheeler–DeWitt equation* [40]

$$0 = H_\perp\Big(\gamma, \chi; \frac{\hbar}{\mathsf{i}}\partial_\gamma, \frac{\hbar}{\mathsf{i}}\partial_\chi\Big)\psi = \Big(-\frac{\hbar^2}{2}\mathcal{G}^{IJ}\frac{\partial}{\partial q_I}\frac{\partial}{\partial q_J} + \mathcal{V}\Big)\psi \tag{2.22a}$$

$$= \Big(\mathsf{s}\frac{\hbar^2}{\mathrm{Vol}_3}\Big(+\frac{\varkappa}{12}\partial_\gamma^2 - \frac{\mathsf{l}}{2}\partial_\chi^2\Big) + \mathrm{Vol}_3 V \mathsf{e}^{g\chi}\Big)\psi(\gamma, \chi)\,, \tag{2.22b}$$

where the operator-ordering [91, sec. 5.3] is chosen such that the "kinetic energy operator"

$$-\frac{\hbar^2}{2}\mathcal{G}^{IJ}\partial_{q_I}\partial_{q_J} \tag{2.23}$$

is proportional to the Laplace operator, which sometimes is called the Laplace–Beltrami operator, named after Eugenio Beltrami, crediting his introduction of this operator in differential geometry of surfaces [154].

One sees that for $\mathsf{l} = \pm$, eq. (2.22b) is hyperbolic and elliptic, respectively. The former case is more usual for a Wheeler–DeWitt equation [87, 67, 85].

One can solve eq. (2.22b) by separating the variables. Substituting the separated test solution

$$\psi(\gamma, \chi) = \mathsf{e}^{\frac{\mathsf{i}}{\hbar}p_\gamma \gamma}\phi_{p_\gamma}(\chi) \tag{2.24}$$

into eq. (2.22b) gives

$$0 = H_\perp\Big(\gamma, \chi; \frac{\hbar}{\mathsf{i}}\partial_\gamma, \frac{\hbar}{\mathsf{i}}\partial_\chi\Big)\psi_{p_\gamma} \qquad \text{(2.22a revisited)}$$

$$= \mathsf{l}\mathsf{s}\frac{\hbar L_{\mathrm{P}}\mathsf{e}^{\frac{\mathsf{i}}{\hbar}p_\gamma\gamma}}{\mathrm{Vol}_3}\Big[-\frac{\hbar^2}{2M_{\mathrm{P}}}\frac{\mathrm{d}^2}{\mathrm{d}y^2} + \mathsf{l}\mathsf{s}\mathsf{v}U\mathsf{e}^{\frac{g}{L_{\mathrm{P}}}y} - \mathsf{l}\mathcal{E}_{p_\gamma}\Big]\phi_{p_\gamma}(y)\,, \tag{2.25a}$$

$$= \mathsf{l}\mathsf{s}\frac{\hbar^2 g^2 \mathsf{e}^{\frac{\mathsf{i}}{\hbar}p_\gamma\gamma}}{8\mathrm{Vol}_3}\Big[x^2\frac{\mathrm{d}^2}{\mathrm{d}x^2} + x\frac{\mathrm{d}}{\mathrm{d}x} + \mathsf{l}(\nu^2 - \mathsf{s}\mathsf{v}x^2)\Big]\phi_{p_\gamma}(x)\,, \tag{2.25b}$$

$(\mathit{l}, \mathit{sv})$	$\mathrm{Bessel}_\nu(x)$
$(-,-)$	$c_1 K_\nu(x) + c_2 I_\nu(x)$
$(-,+)$	$c_1 J_\nu(x) + c_2 Y_\nu(x)$
$(+,-)$	$c_1 F_{\mathrm{i}\nu}(x) + c_2 G_{\mathrm{i}\nu}(x)$
$(+,+)$	$c_1 K_{\mathrm{i}\nu}(x) + c_2 I_{\mathrm{i}\nu}(x)$

Table 2: Four cases of the Bessel function in eq. (2.27) that solves eq. (2.25b). Branches that diverge at the infinite boundary are in grey, which are to be dropped, see section 2.4. The remaining branches are all real and have no imaginary part, see fig. 3.

In eq. (2.25a), which will be used later in section 4.4,

$$\begin{aligned} L_{\mathrm{P}} &:= \sqrt{\hbar\varkappa}\,, \quad M_{\mathrm{P}} := \sqrt{\hbar/\varkappa}\,, \quad y := L_{\mathrm{P}}\chi\,; \\ U &:= \frac{\mathrm{Vol}_3^2|V|}{\hbar L_{\mathrm{P}}} > 0\,, \quad \mathcal{E} := \frac{p_\gamma^2}{12\hbar M_{\mathrm{P}}}\,. \end{aligned} \tag{2.26a}$$

In eq. (2.25b),

$$\nu := \frac{1}{\hbar g}\sqrt{\frac{2\varkappa}{3}}p_\gamma\,, \qquad x := 2\sqrt{2}\frac{\mathrm{Vol}_3\sqrt{|V|}}{\hbar g}\mathsf{e}^{g\chi/2}\,. \tag{2.26b}$$

For the moment, we focus on eq. (2.25b), which is a Bessel equation. The corresponding *complete integrals* with constant p_γ (see section 3.1), which will be called *mode functions*, read

$$\psi \propto \mathsf{e}^{\frac{\mathrm{i}}{\hbar}p_\gamma\gamma}\mathrm{Bessel}_{|\nu|}(x)\,, \tag{2.27}$$

and $\mathrm{Bessel}_\nu(x)$ is a Bessel function of order ν, the type of which depends on the signs $(\mathit{l}, \mathit{sv})$, see table 2, where $F_{\mathrm{i}\nu}(x)$ and $G_{\mathrm{i}\nu}(x)$ are the unmodified Bessel functions adapted to purely imaginary orders, defined as [46]

$$F_\nu(x) := \frac{1}{2}\Big\{\mathsf{e}^{+\nu\pi\mathrm{i}/2}H_\nu^{(1)}(x) + \mathsf{e}^{-\nu\pi\mathrm{i}/2}H_\nu^{(2)}(x)\Big\} \tag{2.28a}$$

$$\equiv \frac{1}{2}\sec\Big(\frac{\nu\pi}{2}\Big)\{J_{+\nu}(x) + J_{-\nu}(x)\}\,; \tag{2.28b}$$

$$G_\nu(x) := \frac{1}{2\mathrm{i}}\Big\{\mathsf{e}^{+\nu\pi\mathrm{i}/2}H_\nu^{(1)}(x) - \mathsf{e}^{-\nu\pi\mathrm{i}/2}H_\nu^{(2)}(x)\Big\} \tag{2.28c}$$

$$\equiv \frac{1}{2}\csc\Big(\frac{\nu\pi}{2}\Big)\{J_{+\nu}(x) - J_{-\nu}(x)\}\,. \tag{2.28d}$$

By the arguments in section 2.4, the branches that diverge as $\chi, \gamma \to \pm\infty$ are to be dropped. This removes the $(-,-)$ case completely, as was the classical

scenario; moreover, the Y_ν and $I_{\mathrm{i}\nu}$ branches in the $(-,+)$ and $(+,+)$ cases are also disqualified, respectively. Mode functions for small ν's are plotted in fig. 3.

2.4 Boundary condition at infinity

Since we do not have a Schrödinger norm that leads to a conserved probability [91, sec. 5.2.2], one may wonder whether the wave functions that diverge at the asymptotic region $\chi, \gamma \to \pm\infty$ are also allowed. From both mathematical and physical arguments, people believe that the wave functions are to be endowed with a boundary condition, that they converge to zero fast.

Mathematically, since the Wheeler–DeWitt equation is in most cases hyperbolic, and solving an initial-value problem for it also requires a boundary condition (e.g. [54, sec. 7.2]). More generally, one needs a suitable functional space, in order to perform functional analysis on the wave functions; and the easiest, simplest choice of such is a Banach space, which makes the wave functions normalisable in the, e.g. L^p sense [102]. This requirement makes the wave function fall off to zero fast enough at infinity.

Physically, a boundary condition was already suggested by DeWitt [40], so that the classical singularities can be avoided. In doing so, it is implicitly assumed that the amplitude of a Wheeler–DeWitt wave function is related to the probability, albeit the absence of a Schrödinger norm. From this perspective, the plausible requirement that the probability at infinity does not diverge also leads to a boundary condition. Moreover, in the semi-classical approximation (Born–Oppenheimer + WKB), a Hilbert space for the matter content emerges [91, sec. 5.4.2], which imposes a fall-off boundary condition to the matter wave function, rendering them belonging to L^2. This boundary condition is easier to realise, if the bulk cosmological wave function already falls off as needed at the boundary.

In the physical application of constructing wave-packets, we will also see that a norm of the mode function plays a crucial role.

2.5 An exact wave-packet

Like the stationary Schrödinger equation in conventional quantum mechanics, the Wheeler–DeWitt equation is also a linear differential equation. For a family of mode functions $\{\psi_\nu\}$, which are complete integrals of the Wheeler–DeWitt equation, one could therefore choose an amplitude $\mathcal{A}(\nu)$ and construct a *wave-packet*

$$\Psi = \int \mathbb{d}\nu \, \mathcal{A}(\nu)\psi_\nu \,, \tag{2.29}$$

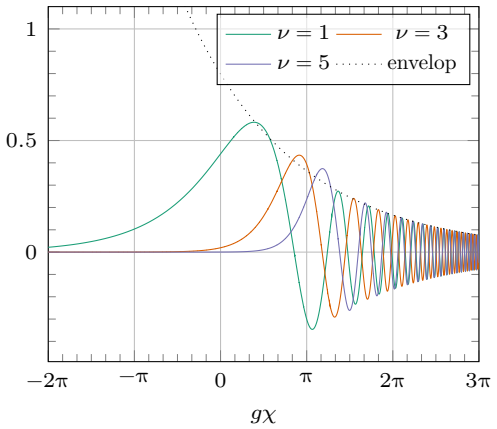

(a) $(-,+)$ with $J_\nu(x)$

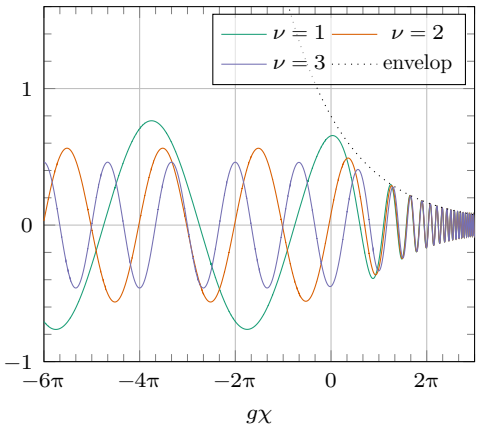

(b) $(+,-)$ with $F_{\mathrm{i}\nu}(x)$

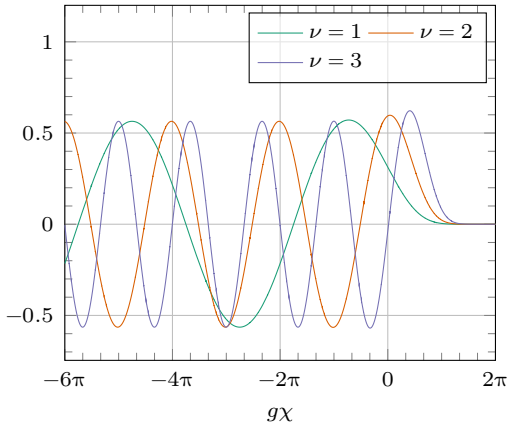

(c) $(+,+)$ with $N_{K,\nu}K_{\mathrm{i}\nu}(x)$

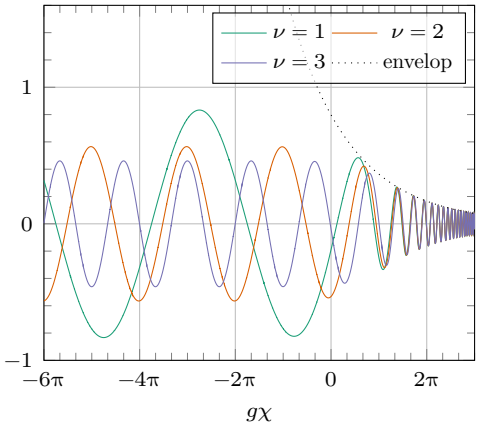

(d) $(+,-)$ with $G_{\mathrm{i}\nu}(x)$

Figure 3: Three cases of $\mathrm{Bessel}_\nu(x)$ in the mode function (2.27), which are specified in table 2. For concreteness, constants are chosen such that $x = \mathrm{e}^{g\chi/2}$. The normalisation factor $N_{K,\nu}$ is given by eq. (4.28b). The envelops, in the asymptotic sense as $x \to +\infty$, have the expression $\sqrt{2\mathrm{e}^{-x}/\pi}$, and are found by the asymptotic expansion of $\mathrm{Bessel}_\nu(x)$ with fixed ν and $x \to +\infty$, see table 6. As $g\chi \to +\infty$, one sees that the $(-,+)$ and $(+,-)$ cases in figs. 3a to 3c converges to 0 as $\sim \exp(-g\chi/4)$, but vibrates very (actually, *exponentially*) fast; the $(+,+)$ case in fig. 3d, on the other hand, converges to 0 as $\sim \exp\bigl(-\mathrm{e}^{-g\chi/2} + g\chi/4\bigr)$ and does not vibrate. As $g\chi \to -\infty$, the $(-,+)$ case in fig. 3a converges to 0, whereas the $(+,-)$ and $(+,+)$ cases in figs. 3b to 3d vibrates sinusoidally with an asymptotically constant amplitude.

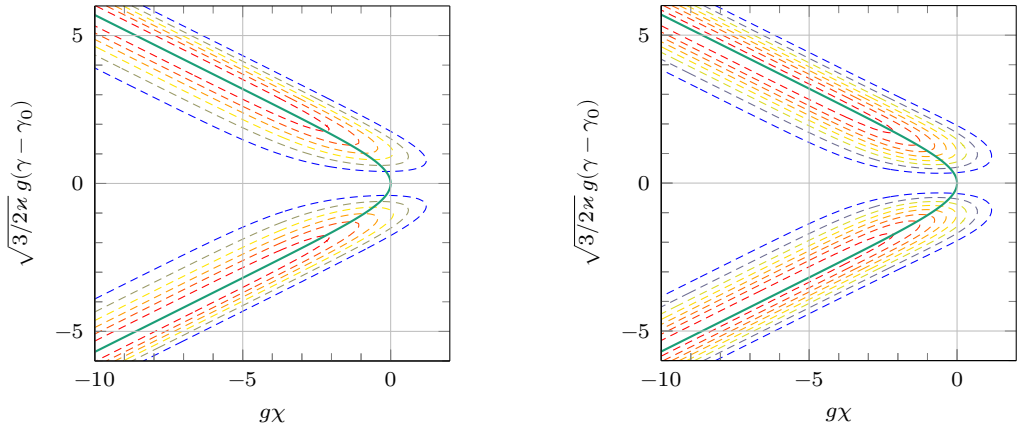

(a) $\mathcal{A}_{\text{lin}}$ (b) $\mathcal{A}_{\text{hfg}}$

Figure 4: Schrödinger profile $|\Psi|^2$ of wave-packets of the $(+,+)$-case of the prototype model, the mode-function of which is proportional to $K_{\mathrm{i}\nu}(x)$. In fig. 4a, the wave-packet is given by eq. (2.31). The solid line is the classical trajectory with $\frac{\varkappa p_\gamma^2}{12\mathrm{Vol}_3^2|V|} = 1$, which seems to lie "on the ridge" of the wave-packet. This will be studied in section 6. In fig. 4b, a half-flipped Gaussian amplitude with respect to the normalised mode function, eq. (2.37), is chosen.

which is a general solution of the Wheeler–DeWitt equation, independent of any interpretations. It is scarce that an exact expression of a wave-packet in mini-superspace models can be found. In this section 2.5 we will study such a case.

Making use of [70, eq. (6.795.3)], we have

$$\int_{-\infty}^{+\infty} \mathrm{d}\nu\, \nu \mathrm{e}^{\mathrm{i}\nu y} K_{\mathrm{i}|\nu|}(x) = \mathrm{i}\pi x \mathrm{e}^{-x\cosh y} \sinh y\,, \tag{2.30}$$

and are able to construct the exact wave-packet for the $(+,+)$-case of our prototype model,

$$\begin{aligned}\Psi_{\text{lin}}(\gamma,\chi) \propto{}& \mathrm{e}^{\frac{g\chi}{2}} \sinh\left[\sqrt{\tfrac{3}{2\varkappa}}\, g(\gamma-\gamma_0)\right] \\ &\cdot \exp\left\{-\frac{2\sqrt{2}\,\mathrm{Vol}_3\sqrt{|V|}}{\hbar g}\mathrm{e}^{\frac{g\chi}{2}} \cosh\left[\sqrt{\tfrac{3}{2\varkappa}}\, g(\gamma-\gamma_0)\right]\right\},\end{aligned} \tag{2.31}$$

with an amplitude that "seems to be" $\mathcal{A}_{\text{lin}}(\nu) \propto p_\gamma \propto \nu$ (c.f. eq. (2.26b)). This is a typical profile of the norm square $|\Psi|^2$ of a wave-packet in Wheeler–DeWitt quantum cosmology, which form a tube around some classical trajectory in the asymptotic region, see fig. 4a.

One may wonder how an amplitude that is proportional to the "wave number" ν can lead to a smooth wave-packet that makes physical sense. For example, if

one naively takes plane waves $(2\pi)^{-1/2}\mathsf{e}^{\mathsf{i}kx}$ and uses a linear amplitude, one finds

$$\frac{1}{\sqrt{2\pi}}\int_{-M}^{+M} \mathbb{d}k\, k\mathsf{e}^{\mathsf{i}kx} = -\mathsf{i}\sqrt{\frac{2(1+M^2x^2)}{\pi}}\frac{1}{x^2}\cos\left(Mx + \arctan\frac{1}{Mx}\right) \tag{2.32a}$$

$$\to -\mathsf{i}\sqrt{2\pi}\delta'(x) \qquad M \to +\infty\,, \tag{2.32b}$$

which is 0 for $x \neq 0$, and in no ways resembles the plot in fig. 4a.

The doubts can be dispelled if one considers the *Schrödinger normalisation* of $\mathsf{i}|\nu|(x)$, which is given in eq. (4.28b), leading to the true amplitude

$$\mathcal{A}_{\text{lin}}(\nu) \propto \frac{\nu}{N_{K,\nu}} \propto \sqrt{\frac{\nu}{\sinh(\nu)}}\,\operatorname{sgn}\nu\,. \tag{2.33}$$

In turn, the normalisation condition for the amplitude $\int_{-\infty}^{+\infty}\mathbb{d}\nu\,|\mathcal{A}_{\text{lin}}(\nu)| = 1$ gives

$$\mathcal{A}_{\text{lin}}(\nu) = \sqrt{\frac{2\nu}{\sinh(\nu)}}\,\operatorname{sgn}\nu\,. \tag{2.34}$$

See fig. 5 for the amplitude and probability density.

To understand more about $\mathcal{A}_{\text{lin}}$, one can turn to the *Gaussian amplitude* that is popular in the literature, and compare the former with a modified version of the latter, which is flipped with respect to the x-axis for $\nu < 0$ and has the same second moment $\langle\nu^2\rangle$ as $\mathcal{A}_{\text{lin}}$. The second moment for the "linear" amplitude in eq. (2.34) reads

$$\int_{-\infty}^{+\infty}\mathbb{d}\nu\,\nu^2|\mathcal{A}_{\text{lin}}(\nu)|^2 = \frac{1}{2}. \tag{2.35}$$

One therefore uses the *one-dimensional Gaussian distribution* (c.f. eq. (3.22b))

$$\text{GD}_1\left(0, \sigma^2 = \frac{1}{2}; \nu\right) = \pi^{-1/2}\mathsf{e}^{-\nu^2} \tag{2.36}$$

and constructs the amplitude as

$$\mathcal{A}_{\text{hfg}}(\nu) = \sqrt{\text{GD}_1\left(0, \sigma^2 = \frac{1}{2}; \nu\right)}\,\operatorname{sgn}\nu = \pi^{-1/4}\mathsf{e}^{-\frac{\nu^2}{2}}\operatorname{sgn}\nu\,, \tag{2.37}$$

see figs. 5a and 5b. The corresponding wave-packet, which is constructed numerically, is plotted in fig. 4b. One sees that it indeed resembles that with $\mathcal{A}_{\text{lin}}$ in fig. 4a.

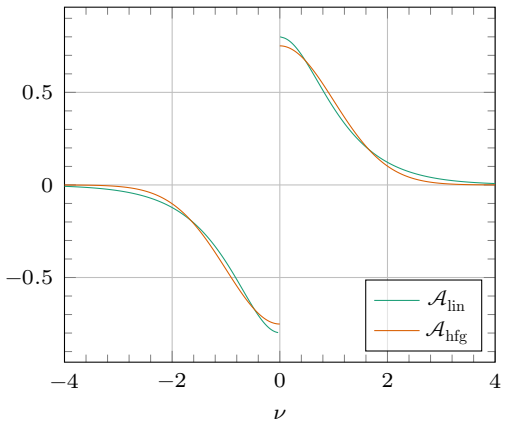

(a) Amplitudes

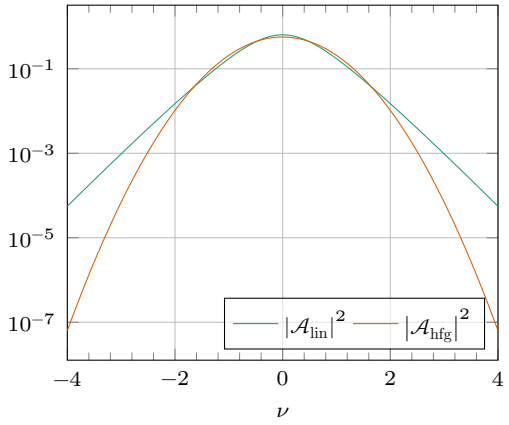

(b) Densities

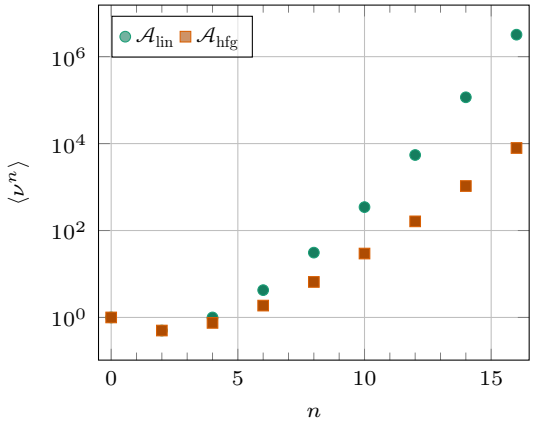

(c) Moments

Figure 5: Comparison of $\mathcal{A}_{\text{lin}}$ and $\mathcal{A}_{\text{hfg}}$, in terms of the amplitudes (5a), densities (fig. 5b) and moments (5c). In the linear-scaled plot in fig. 5a, the difference between $\mathcal{A}_{\text{lin}}$ and $\mathcal{A}_{\text{hfg}}$ seems small. In the logarithm-scaled plot in fig. 5b, one sees that $|\mathcal{A}_{\text{lin}}|^2$ approaches a straight line as $\nu \to \pm\infty$, whereas $\left|\mathcal{A}_{\text{hfg}}\right|^2$ remains parabolic, hence their difference becomes "asymptotically infinitely large" in terms of orders of magnitude. In fig. 5c one sees that their moments are the same for $n = 0$ and 2, then become exponentially different as the order increases.

The difference of $\mathcal{A}_{\text{lin}}$ and $\mathcal{A}_{\text{hfg}}$ can also be seen with the higher moments,

$$\int_{-\infty}^{+\infty} \mathbb{d}\nu\, \nu^{2n} \big|\mathcal{A}_{\text{lin}}(\nu)\big|^2 = \frac{(-2)^n(4^{n+1}-1)}{n+1} B_{2n+2}\,, \tag{2.38a}$$

$$\int_{-\infty}^{+\infty} \mathbb{d}\nu\, \nu^{2n} \big|\mathcal{A}_{\text{hfg}}(\nu)\big|^2 = \pi^{-1/2}\Gamma\left(n+\frac{1}{2}\right), \tag{2.38b}$$

where B_n is the nth Bernoulli–Seki number [45, sec. 24.1, 71, sec. 6.5].[3] See fig. 5c.

One may wonder that the wave-packet in fig. 4a, though exact in its mathematical form, is somewhat artificially constructed, and can hardly arise in Nature. In section 5.3 we will indeed argue for this. Moreover, the wave-packets that are more relevant to the real world will be numerically constructed in section 4.5.

Finally, one may ask about a possible classical correspondence of this wave-packet, which many other wave-packets do have, see sections 3.5, 4.5 and 5.2. Generally speaking, the familiar scenario would be that the wave-packet is constructed by superposing mode functions with quantum number $\nu \in \mathbb{R}$ by a normal Gaussian amplitude, that is centred at ν_0. Then the claim is that, this wave-packet corresponds to the classical trajectory with a classical first-integral $\propto \nu$, see also [5, 94]. This approach is not viable here, since the amplitude is by no means a normal Gaussian one. We will focus on the issue of digging a classical trajectory out of a generic wave-packet in section 6.

[3] These numbers were discovered independently by Jacob Bernoulli and Seki Takakazu at about the same time. See [152] for the second mathematician.

3 Semi-classical approach of WKB

The WKB approach, named after Wentzel, Kramers and Brillouin [168, 99, 27], is an important approximation in conventional quantum mechanics that separates the rapidly varying phase from the slowly varying amplitude [91, sec. 5.3.2, 105, ch. 7]. It is also one of the standard ways to connect quantum geometrodynamics with classical general relativity.

In contrast, the connection between the quantum and classical gravitational theories in the scenario of *wave-packets*, is not very clear, and mostly *ad hoc* case by case, shown with plots [5, 88, 94]. In [61], the author observed that a superposition of WKB states can be chosen to have support only in a thin "tube" around a classical trajectory. Moreover, in [78], it was suggested that in the WKB approximation, an integral across a narrow section near a classical trajectory is related to the lapse function. Furthermore, in [110], the author interpreted WKB wave-packets as containing higher-order WKB effects. And finally in [127], it was suggested that the wave function of the universe forms a narrow wave-packet in the classical region.

It is common to construct a wave-packet by superposing mode functions with an amplitude that refers to a quantum number, e.g. superposing plane waves with a Gaussian amplitude that refers to the momenta of the plane waves. At the classical level, the quantum numbers correspond to first integrals, and using the former implies the existence of the latter. Therefore, this practice implicitly assumes that the system is *Liouville integrable* [9, sec. 49], containing a number of first integrals. Systems that do not have sufficient first integrals belong to the regime of classical and quantum chaos [171], and will not be studied here. For a criterion of integrable systems that can be separated in the Hamilton–Jacobi formulation, see [161].

In this section 3, we will first describe the general WKB theory in mathematics and minisuperspace models, and explain the relation between the WKB mode functions and the classical trajectories in section 3.1. Then we will derive the WKB approximation for our prototype minisuperspace model, both by analysing the obtained exact solution in section 3.2, and by working the WKB mode functions out from scratch in section 3.3. Observing that these mode functions all contain a quantum number, we will show in section 3.4 that these quantum numbers have their correspondence at the classical level as first integrals of the system, and the phase of the WKB mode functions is just the Hamilton's principal function. Finally, we will apply the theory established in section 3.4 to wave-packets in section 3.5. We will show that these wave-packets, if constructed by superposing the WKB mode functions with a narrow Gaussian amplitude, necessarily peak near a classical trajectory, which has the first integrals corresponding to the centre

of the Gaussian amplitude.

3.1 General theory

This section 3.1 briefly introduces the WKB approximation in mathematics and the Wheeler–DeWitt approach.

Mathematically, the WKB approximation belongs to the class of *global* approximations to the solution of a linear differential equation, in which the highest derivative is controlled by a small parameter δ [17, ch. 10], with respect to which the solution $y = y(x)$ is expanded as a formal power series on the exponent:

$$\phi(x) \sim \exp\left(\frac{1}{\delta}\sum_{n=0}^{+\infty}\delta^n S_n(x)\right), \qquad \delta \to 0\,. \tag{3.1}$$

In conventional quantum mechanics as well as in the Wheeler–DeWitt approach of quantum gravitation, the highest derivatives are controlled by the reduced Planck constant $\hbar$. The meaning of a power expansion with respect to such a *dimensionful* quantity is questioned at the end of this subsection.

At the next-to-leading order, the WKB wave function is often taken as the test solution [94]

$$\psi \approx \sqrt{D}\,\mathsf{e}^{\frac{\mathrm{i}}{\hbar}S}\,, \tag{3.2}$$

where S is the leading order term, $D = \mathsf{e}^{2\hbar^0 S_1}$ corresponds to the real part of the next-to-leading order term, which is called *Van Vleck factor*, named after its eponymous founder [159].[4] In the minisuperspace models, inserting eq. (3.2) into the Hamiltonian in the form of eq. (2.20), the resulting equations read [94]

$$0 = H_\perp\left(\chi,\gamma;\frac{\partial S_0}{\partial\chi},\frac{\partial S_0}{\partial\gamma}\right) = \frac{1}{2}\mathcal{G}^{IJ}\frac{\partial S}{\partial q^I}\frac{\partial S}{\partial q^J} + \mathcal{V}(q)\,, \tag{3.3a}$$

$$\mathcal{G}^{IJ}\frac{\partial S}{\partial q^I}\frac{\partial D}{\partial q^J} = -(\Box S)D\,. \tag{3.3b}$$

Results for the next orders can be found in e.g. [91, sec. 5.4.1], which are not needed here.

Equation (3.3a) is just the *Hamilton–Jacobi equation* for the singular system described by eq. (2.17).

Expansion with the dimensionful $\hbar$ One may wonder how a physical quantity, that has a *unit*, can be called small. More specifically, upon going to the

[4] See [132, ch. 7] for a viable introduction of the Van Vleck factor; for historical remarks, see [160, 170].

natural unit, we have $\hbar = 1$, and a formal power expansion with $\hbar^2 \equiv 1$ does not make sense.

In our opinion, one way out is to compare $\hbar^2$ with the other quantities in eq. (2.22b), i.e. to use $\hbar^2/\big(\mathrm{Vol}_3^2 V\big)$ as the small parameter. But once this is fixed and found to be small, one could absorb the denominator into the expansion coefficient, rending the usual power series with respect to $\hbar$.

3.2 Asymptotic expansion as a WKB approximation

In our prototype model, the exact solution of the minisuperspace Wheeler–DeWitt equation (2.22b) is known. The WKB approach can therefore be realised in two ways. One can start with the generic WKB result, which means the Hamilton–Jacobi equation in (3.3a), and then solve S_0 for it. This approach will be illustrated later in section 3.3. Alternatively, one can also begin with the mode functions in eq. (2.27) which are exact solutions, and find an approximation for the Bessel functions that have the form of eq. (3.1). We will follow this approach in this section 3.2.

Since $\nu, x \propto \hbar^{-1}$ (c.f. eq. (2.26b)), an approximation at *small* $\hbar$ means asymptotic expansion of the Bessel functions at *large* ν *and* x. Note that

$$\left(\frac{\nu}{x}\right)^2 = \frac{\varkappa p_\gamma^2}{12\mathrm{Vol}_3^2 |V| \mathsf{e}^{g\chi}} \tag{3.4a}$$

$$= \mathrm{trig}\left(\sqrt{\frac{3}{2\varkappa}} g(\gamma - \gamma_0)\right)^2 \qquad \text{by substituting eq. (2.14).} \tag{3.4b}$$

Equation (3.4b) makes sense *if* we want to study the behaviour of the mode functions *near* a classical trajectory.

In such a case of fixed ν/x, the asymptotic representations belong to the "Debye" type [114, sec. 3.14.2]. In the following we give the leading order results. For the $(-,+)$ case with $J_\nu(x)$, the Debye expansion reads [45, eq. (10.19.6)]

$$\begin{aligned} J_\nu(x) = {} & \sqrt{\frac{2}{\pi}} (x^2 - \nu^2)^{-1/4} \\ & \cdot \left\{ \sin\left[\sqrt{x^2 - \nu^2} - \nu \arccos\frac{\nu}{x} + \frac{\pi}{4} \right] + O(x^{-1}) \right\} \qquad x > \nu \,, \end{aligned} \tag{3.5}$$

where $x > \nu$ holds because $\mathrm{trig} = \sin$ for $(-,+)$, and $x = \nu$ is excluded because it is not contained in the trajectories, see fig. 2a. The mode function $\mathsf{e}^{\frac{\mathrm{i}}{\hbar} p_\gamma (\gamma - \tilde{\gamma}_0)} J_\nu(x)$ contains therefore *two* WKB branches $\sim \mathsf{e}^{\frac{\mathrm{i}}{\hbar} S_\pm}$,

$$\frac{S_\pm}{\hbar} := \frac{p_\gamma}{\hbar}(\gamma - \tilde{\gamma}_0) \pm \left(\sqrt{x^2 - \nu^2} - \nu \arccos\frac{\nu}{x} + \frac{\pi}{4} \right), \tag{3.6}$$

see fig. 6a. Note we have introduced an additive constant $\tilde{\gamma}_0$ to cancel the extra constant factors and match the classical constant γ_0, which is also related to eqs. (3.16a) and (3.16b). By using eq. (3.16a), one gets

$$0 = \frac{1}{\hbar}\frac{\partial S_{\pm}}{\partial p_{\gamma}} = (\gamma - \gamma_0) \mp \sqrt{\frac{2\varkappa}{3}}\,\frac{1}{g}\arccos\sqrt{\frac{\varkappa p_{\gamma}^2}{12\mathrm{Vol}_3^2|V|\mathsf{e}^{g\chi}}}\,, \tag{3.7}$$

which leads to eq. (2.14) with trig = sin.

For the $(+,-)$ case with $F_{\mathrm{i}\nu}(x)$ and $G_{\mathrm{i}\nu}(x)$, the Debye expansions at leading order read [46, eqs. (5.15) and (5.16)]

$$\begin{aligned} F_{\mathrm{i}\nu}(x) = {} & \sqrt{\frac{2}{\pi}}(x^2+\nu^2)^{-1/4} \\ & \cdot\Big\{\sin\Big[\sqrt{x^2+\nu^2} - \nu\,\mathrm{arsinh}\,\frac{\nu}{x} + \frac{\pi}{4}\Big] + O(x^{-1})\Big\}\,, \end{aligned} \tag{3.8a}$$

$$\begin{aligned} G_{\mathrm{i}\nu}(x) = {} & -\sqrt{\frac{2}{\pi}}(x^2+\nu^2)^{-1/4} \\ & \cdot\Big\{\cos\Big[\sqrt{x^2+\nu^2} - \nu\,\mathrm{arsinh}\,\frac{\nu}{x} + \frac{\pi}{4}\Big] + O(x^{-1})\Big\}\,, \end{aligned} \tag{3.8b}$$

where $x, \nu \in \mathbb{R}^+$ are arbitrary. Both cases contain two WKB branches. Take $F_{\mathrm{i}\nu}(x)$ as an example, one has

$$\frac{S_{\pm}}{\hbar} = \frac{p_{\gamma}}{\hbar}(\gamma - \tilde{\gamma}_0) \pm \Big(\sqrt{x^2+\nu^2} - \nu\,\mathrm{arsinh}\,\frac{\nu}{x} + \frac{\pi}{4}\Big)\,, \tag{3.9}$$

$$0 = \frac{1}{\hbar}\frac{\partial S_{\pm}}{\partial p_{\gamma}} = (\gamma - \gamma_0) \mp \sqrt{\frac{2\varkappa}{3}}\,\frac{1}{g}\,\mathrm{arsinh}\sqrt{\frac{\varkappa p_{\gamma}^2}{12\mathrm{Vol}_3^2|V|\mathsf{e}^{g\chi}}}\,, \tag{3.10}$$

which also leads to eq. (2.14) with trig = sinh. The calculation for $G_{\mathrm{i}\nu}(x)$ is essentially the same, with an extra constant phase shift $\pi/2$.

Finally, for the $(+,+)$ case, the expansion at leading order reads [114, p. 141–142]

$$\begin{aligned} K_{\mathrm{i}\nu}(x) = {} & \sqrt{\frac{2\pi}{\mathsf{e}^{\pi\nu}}}(\nu^2-x^2)^{-1/4} \\ & \cdot\Big\{\cos\Big[\sqrt{\nu^2-x^2} - \nu\,\mathrm{arcosh}\,\frac{\nu}{x} + \frac{\pi}{4}\Big] + O(x^{-1})\Big\} \qquad \nu > x\,, \end{aligned} \tag{3.11}$$

where $\nu > x$ holds because trig = cosh for $(+,+)$. Equation (3.11) contains, once

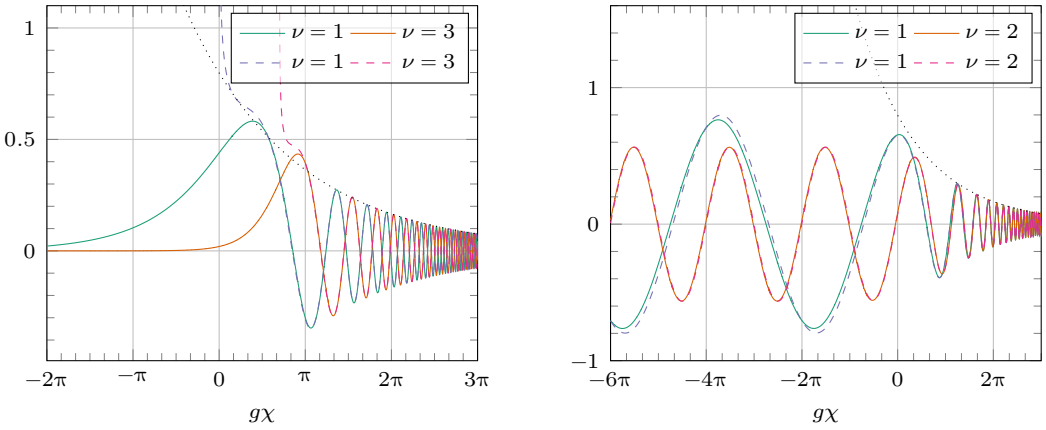

(a) $(-,+)$ with $J_\nu(x)$

(b) $(+,-)$ with $F_{\mathrm{i}\nu}(x)$

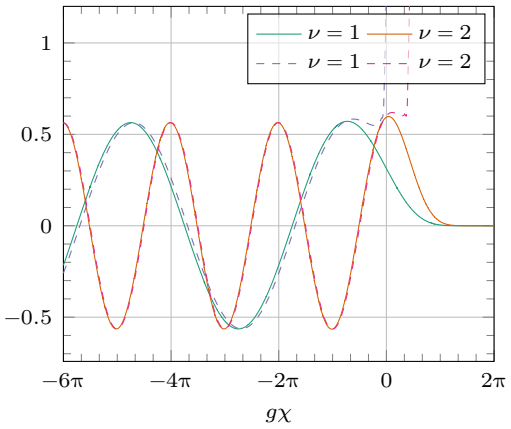

(c) $(+,+)$ with $N_{K,\nu}K_{\mathrm{i}\nu}(x)$

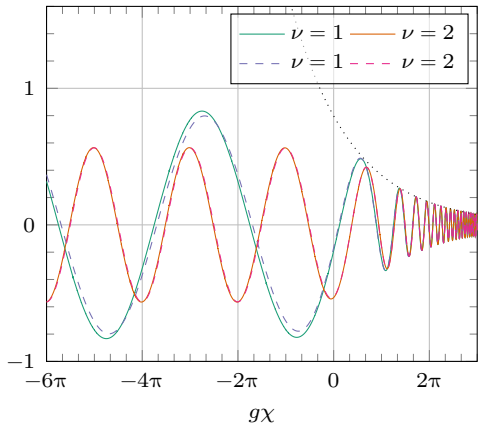

(d) $(+,-)$ with $G_{\mathrm{i}\nu}(x)$

Figure 6: Asymptotic expansions of $\mathrm{Bessel}_\nu(x)$ of the "Debye" type. The exact functions are plotted with solid lines, whereas the asymptotic expressions are shown with dashed lines. The constants, normalisation factors and envelops are chosen in the same way as in fig. 3. One sees that even for such small ν's, the asymptotic expressions fit well with the exact functions over a large range. More specifically, the asymptotics for $F_{\mathrm{i}\nu}(x)$ and $G_{\mathrm{i}\nu}(x)$ work for $g\chi \in \mathbb{R}$. As for $J_\nu(x)$, the asymptotic works for $\mathrm{e}^{g\chi/2} \gg \nu$, and $K_{\mathrm{i}\nu}(x)$ for $\mathrm{e}^{g\chi/2} \ll \nu$. For the latter two cases, the asymptotics blow up at a certain value. This is related to the fact that the WKB approximation fails at the classical turning point. At the other side of the "blowing-up walls", there is another branch of asymptotic expression, which fits the decaying part of the exact function, but is not needed here.

(I, sv)	$D_{\pm}$
$(-,-)$	no solution
$(-,+)$	$(+x^2-\nu^2)^{-1/2} D_0\Big(\sqrt{\frac{3}{2\varkappa}}\, g\gamma \mp \arccos\frac{\nu}{x}\Big)$
$(+,-)$	$(+x^2+\nu^2)^{-1/2} D_0\Big(\sqrt{\frac{3}{2\varkappa}}\, g\gamma \mp \operatorname{arsinh}\frac{\nu}{x}\Big)$
$(+,+)$	$(-x^2+\nu^2)^{-1/2} D_0\Big(\sqrt{\frac{3}{2\varkappa}}\, g\gamma \mp \operatorname{arcosh}\frac{\nu}{x}\Big)$

Table 3: General integrals of the Van Vleck factor $D_{\pm}$ that are solutions to eq. (3.14) and correspond to $S_{\pm}$. The pre-factors are in accordance with those in eqs. (3.5), (3.11), (3.8a) and (3.8b). The arbitrary function D_0 can be argued to be a constant.

again, two WKB branches, and one has

$$\frac{S_{\pm}}{\hbar} = \frac{p_\gamma}{\hbar}(\gamma - \tilde{\gamma}_0) \pm \Big(\sqrt{\nu^2 - x^2} - \nu \operatorname{arcosh}\frac{\nu}{x} + \frac{\pi}{4}\Big)\,, \tag{3.12}$$

$$0 = \frac{1}{\hbar}\frac{\partial S_{\pm}}{\partial p_\gamma} = (\gamma - \gamma_0) \mp \sqrt{\frac{2\varkappa}{3}}\,\frac{1}{g} \operatorname{arcosh}\sqrt{\frac{\varkappa p_\gamma^2}{12\mathrm{Vol}_3^2 |V| \mathrm{e}^{g\chi}}}\,, \tag{3.13}$$

which, again, lead to eq. (2.14) with trig = cosh.

The WKB phases in eqs. (3.6), (3.9) and (3.12) can also be compared to the classical trajectories, see fig. 7.

3.3 WKB approximation by direct calculation

In this section 3.3, we obtain the WKB phase S and the van Vleck factor D directly from eqs. (3.3a) and (3.3b).

To begin with, one can verify that the $S_{\pm}$ given by eqs. (3.6), (3.9) and (3.12) are indeed complete integrals of the Hamilton–Jacobi equation (3.3a), which is a *non-linear* first-order partial differential equation by itself.

The transport equation (3.3b) in our prototype model reads

$$\mathsf{s}\frac{\hbar}{\mathrm{Vol}_3}\Big(-\frac{\varkappa}{6}\frac{\partial S}{\partial\gamma}\frac{\partial D}{\partial\gamma} + I\frac{\partial S}{\partial\chi}\frac{\partial D}{\partial\chi}\Big) = -\frac{\mathsf{s}}{\mathrm{Vol}_3}\Big(-\frac{\varkappa}{6}\frac{\partial^2 S}{\partial\gamma^2} + I\frac{\partial^2 S}{\partial\chi^2}\Big)D\,, \tag{3.14}$$

which is a first-order *linear* partial differential equation. By using the transformation in eq. (2.26b), we are able to derive the *general* integral, which contains an arbitrary *function* D_0, in contrary to the *complete* integrals for S, where merely arbitrary *constants* are present. See table 3.

Since $S_{\pm}$'s are complete integrals that result from separation test solutions (see eq. (3.18) below), the full Van Vlack factor should also be in a separated form, which would render D_0 constant, because it mixes γ with χ otherwise. This can

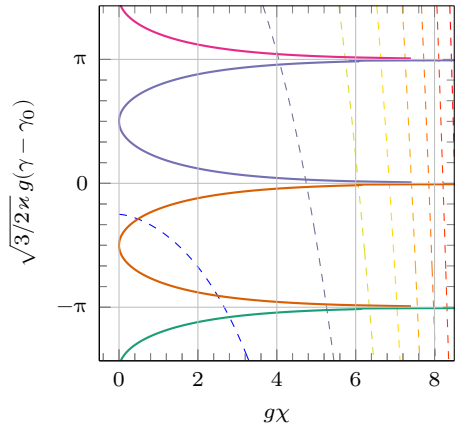

(a) $(-,+)$ with S_+

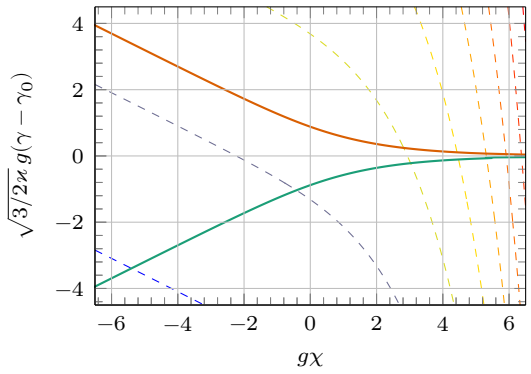

(b) $(+,-)$ with S_+

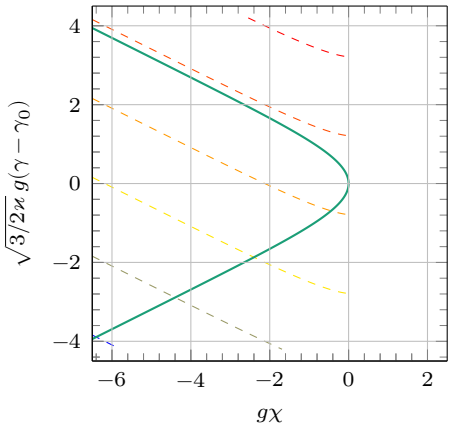

(c) $(+,+)$ with S_+

Figure 7: The WKB phases S_+ in eqs. (3.5), (3.11), (3.8a) and (3.8b) as dashed contours, and the corresponding classical trajectories given by eq. (2.14) and table 1. One sees that in the region where the mode function is asymptotically sinusoidal with a constant amplitude (see fig. 6), the WKB phase fronts align asymptotically with the classical trajectory. This happens for $(+,-)$ as $g\chi \to -\infty, \sqrt{\frac{3}{2\varkappa}}\, g(\gamma-\gamma_0) \to +\infty$ (7b) and $(+,+)$ as $g\chi \to -\infty, \sqrt{\frac{3}{2\varkappa}}\, g(\gamma-\gamma_0) \to -\infty$ (7c). For $(-,+)$ (7a), the mode function is never a sinusoidal form, and the wave fronts do not match the classical trajectories.

be verified if one begins from scratch by inserting the WKB wave function in eq. (3.2) into the Wheeler–DeWitt equation (2.22b), and then adapts a separation test solution. An ordinary differential equation in χ would arise, from which one could find the second terms of $S_{\pm}$'s in eqs. (3.5), (3.11), (3.8a) and (3.8b) that only contain γ, and the corresponding $D_{\pm}$'s are solved by the pre-factors in table 3, with no place for the arbitrary function D_0.

We conclude that eqs. (3.3b) and (3.14) may not be the best starting point to solve for the Van Vleck factor for systems with multiple degrees of freedom.

3.4 WKB phase as a complete integral

In this section 3.4, we study the WKB mode functions and their phases. We will see that the mode functions can be chosen, such that they are labelled with quantum numbers, which are related to classical integrals of motion. Correspondingly, their phases are complete integrals of the classical Hamilton–Jacobi equation, which contain the classical integrals mentions above.

For the Hamilton–Jacobi equation (3.3a), the useful family of solutions is the *complete solution* or *complete integral* [106, sec. 47, 54, sec. 3.1, 9, sec. 9.4], that containing integral constants, e.g.

$$S = S(q^i; \alpha_1, \dots, \alpha_{n-1}) + \alpha_n \,, \tag{3.15}$$

where α_i are constants, $i = 1, 2, \dots, n$. A classical trajectory that corresponds to this WKB solution can then be obtained by the *principle of constructive interference* [61] as

$$\frac{\partial S}{\partial \alpha_i} = 0 \,. \tag{3.16a}$$

Meanwhile, in the classical Hamilton–Jacobi formalism, the related equations are

$$\frac{\partial S}{\partial \alpha_i} = \beta_i \,, \tag{3.16b}$$

where $\{\alpha_i\}$'s are the constants contained in the complete integral S, and $\{\beta_i\}$'s are another set of constants [106, sec. 47].

Now, if S is a complete integral in the form of eq. (3.15), a stationary wave-packet can be constructed by smearing out each constant with an amplitude, see e.g. section 3.5.

In practice, it has been shown in [61] that, in order to be able to derive the Hamilton equations for the canonical momenta in full geometrodynamics, it is sufficient and necessary that S is a complete integral of the Hamilton–Jacobi equation,

containing a number of constants that is equal to the physical degrees of freedom.

In the following we give a construction, in which the phase factor S in eq. (3.2) is indeed of a form close to the expression in eq. (3.15). Let the system be such that $m \leq n-1$ variables can be iteratively separated [106, sec. 48], so that the following equations can be obtained along a classical trajectory

$$\begin{aligned} \phi_1\Big(q^1, \frac{\mathbb{d}S_1}{\mathbb{d}q^1}\Big) =: \alpha_1\,, \qquad \phi_2\Big(q^2, \frac{\mathbb{d}S_2}{\mathbb{d}q^2}; \alpha_1\Big) =: \alpha_2\,, \dots\,, \\ \phi_m\Big(q^m, \frac{\mathbb{d}S_n}{\mathbb{d}q^m}; \alpha_1, \dots, \alpha_{m-1}\Big) =: \alpha_m\,, \end{aligned} \tag{3.17}$$

and the corresponding complete integral, (3.15), reads

$$\begin{aligned} S(q^1, \dots, q^n; \alpha_1, \dots \alpha_m) = S_1(q^1; \alpha_1) + \dots + S_m(q^m; \alpha_1, \dots, \alpha_m) \\ + S_{m+1}(q^{m+1} \dots q^n; \alpha_1, \dots, \alpha_m)\,. \end{aligned} \tag{3.18}$$

From the Hamilton–Jacobi theory, we know that $\big\{\phi_j(q^j, p_j)\big\}$'s are *in involution* [9, sec. 10.1] with $H_\perp$, i.e. the Poisson brackets vanish,

$$\big[\phi_j(q^j, p_j), H_\perp(q^1, \dots, q^n, p_1, \dots, p_n)\big]_{\mathrm{P}} = 0\,, \qquad \forall j = 1, \dots, m\,. \tag{3.19}$$

Furthermore, we require that $\big\{\phi_j(q^j, p_j)\big\}$'s are in *mutual* involution.

Upon canonical quantisation, the $H_\perp$ and $\big\{\phi_j\big\}$'s are promoted to (if necessary, *self-adjoint*, see section 4) operators [91, sec. 5.1], and the condition of mutual involution with respect to $[\cdot,\cdot]_{\mathrm{P}}$ is promoted to commuting $\frac{1}{\mathrm{i}\hbar}[\cdot,\cdot]_-$. Equation (3.17) are promoted to the simultaneous eigenvalue equations

$$\begin{aligned} \phi_1\Big(q^1, \frac{\hbar}{\mathrm{i}}\partial_1\Big)\psi = \alpha_1\psi\,, \qquad \phi_2\Big(q^2, \frac{\hbar}{\mathrm{i}}\partial_2; \alpha_1\Big)\psi = \alpha_2\psi\,, \\ \dots\,, \qquad \phi_n\Big(q^n, \frac{\hbar}{\mathrm{i}}\partial_m; \alpha_1, \dots, \alpha_{m-1}\Big)\psi = \alpha_m\psi\,, \end{aligned} \tag{3.20}$$

so that one can write $\psi = \psi_{\alpha_1 \dots \alpha_m}$. Applying a WKB test solution to eq. (3.20) results in the WKB wave function in eq. (3.2) with S given by eq. (3.18). This finishes our construction.

3.5 Narrow WKB Gaussian wave-packet

Having proved that the WKB phase S of a mode function can be a complete integral of the Hamilton–Jacobi equation, we show in this section 3.5 that a narrow Gaussian wave-packet peaks around a classical trajectory, with the integral constant set by the centre of the Gaussian amplitude.

A narrow Gaussian wave-packet of the stationary WKB wave functions con-

structed in section 3.4 can be worked out in an explicit form. We begin with the two-dimensional case, so that the WKB wave function reads

$$\psi(q^1, q^2; \alpha) \approx \sqrt{D} \exp\left[\frac{\mathrm{i}}{\hbar}(S(q^1, q^2; \alpha) - \alpha\beta)\right], \tag{3.21}$$

where the additional phase $\alpha\beta$ will become clear soon. The Gaussian wave-packet is the result of

$$\Psi(q^1, q^2; \alpha, \sigma) = \int \mathrm{d}A\, \psi(q^1, q^2; A) \mathrm{GD}_1(\alpha, \sigma^2; A)^{1/2}, \tag{3.22a}$$

$$\mathrm{GD}_1(\alpha, \sigma^2; A) \coloneqq \frac{\exp\left(-\frac{1}{2}\sigma^{-2}(A-\alpha)^2\right)}{\sqrt{2\pi\sigma^2}}. \tag{3.22b}$$

Applying Taylor's theorem to the exponent of the integrand in eq. (3.22a) with respect to A at α gives

$$\begin{aligned} &\psi(q^1, q^2; A) \mathrm{GD}_1(\alpha, \sigma; A)^{1/2} \\ &= \exp\left[\mathrm{i}d_1^{(0)} + \mathrm{i}(A-\alpha)d_1^{(1)} - \frac{1}{2}(A-\alpha)^2 d_1^{(2)}\right] g(A), \end{aligned} \tag{3.23}$$

where

$$d_1^{(0)} \coloneqq \frac{1}{\hbar}(S(q^1, q^2; \alpha) - \alpha\beta), \tag{3.24a}$$

$$d_1^{(1)} \coloneqq \frac{1}{\hbar}(\partial_\alpha S - \beta), \tag{3.24b}$$

$$d_1^{(2)} \coloneqq \frac{1}{2}\sigma^{-2} - \frac{\mathrm{i}}{\hbar}\partial_\alpha^2 S; \tag{3.24c}$$

$$g(A) \coloneqq \sqrt{D} \exp\left(h(A)(A-\alpha)^2\right), \qquad h(\alpha) = 0. \tag{3.24d}$$

If $d_1^{(2)}$ dominates in eq. (3.23), i.e. $\left|d_1^{(2)}\right| \gg 1$, the integral in eq. (3.22a) can be estimated by the *stationary phase method* [5, 39]. This can be realised if $\sigma^{-2} \gg \hbar^{-1}\partial_\alpha^2 S$, which means that the wave-packet is constructed to be *narrow*. The result is

$$\Psi(q^1, q^2; \alpha, \sigma) \approx (2\pi)^{1/4} \left(\frac{D}{\sigma d_1^{(2)}}\right)^{1/2} \exp\left[\mathrm{i}d_1^{(0)} - \frac{\left(d_1^{(1)}\right)^2}{2d_1^{(2)}}\right], \tag{3.25}$$

and the corresponding Schrödinger density reads

$$\rho = \rho(q^1, q^2; \alpha, \sigma) = |\Psi|^2 = \sqrt{2\pi}\, \frac{D}{\sigma\left|d_1^{(2)}\right|} \exp\left[-\frac{\Re d_1^{(2)}}{\left|d_1^{(2)}\right|^2}\left(d_1^{(1)}\right)^2\right]. \tag{3.26}$$

(I, sv)	$\sqrt{2\pi}\frac{D}{\sigma\left\lvert d_1^{(2)}\right\rvert}\cdot\exp\left[-\frac{\Re d_1^{(2)}}{\left\lvert d_1^{(2)}\right\rvert}\left(d_1^{(1)}\right)^2\right]$
$(-,-)$	no solution
$(-,+)$	$\frac{2\sqrt{2\pi}\,\sigma}{\sqrt{+x^2-\nu^2+4\sigma^4}}\cdot\exp\left[-\frac{\sigma^2(+x^2-\nu^2)}{x^2-\nu^2+4\sigma^4}\left(\sqrt{\frac{3}{2\varkappa}}\,g(\gamma-\gamma_0)\mp\arccos\frac{\nu}{x}\right)^2\right]$
$(+,-)$	$\frac{2\sqrt{2\pi}\,\sigma}{\sqrt{+x^2+\nu^2+4\sigma^4}}\cdot\exp\left[-\frac{\sigma^2(+x^2+\nu^2)}{x^2+\nu^2+4\sigma^4}\left(\sqrt{\frac{3}{2\varkappa}}\,g(\gamma-\gamma_0)\mp\operatorname{arsinh}\frac{\nu}{x}\right)^2\right]$
$(+,+)$	$\frac{2\sqrt{2\pi}\,\sigma}{\sqrt{-x^2+\nu^2+4\sigma^4}}\cdot\exp\left[-\frac{\sigma^2(-x^2+\nu^2)}{x^2+\nu^2+4\sigma^4}\left(\sqrt{\frac{3}{2\varkappa}}\,g(\gamma-\gamma_0)\mp\operatorname{arcosh}\frac{\nu}{x}\right)^2\right]$

Table 4: Narrow Gaussian wave-packet of the WKB mode functions with $S_\pm$ by eq. (3.26), which are plotted in fig. 8.

Given that D, $d_1^{(2)}$ and $\Re\big(d_1^{(2)}\big)$ vary slowly with respect to (q^1, q^2), the peak of ρ dominates near $d_1^{(1)} = 0$, i.e. $\partial_\alpha S = \beta$ (c.f. eq. (3.16b)), which is just the classical trajectory. Narrow Gaussian wave-packets of $(-,+)$, $(+,-)$ and $(+,+)$ cases are calculated in table 4 and plotted in fig. 8.

The above result in two dimensions can easily be generalised to higher dimensions. Consider the WKB mode function

$$\psi(q^i;\alpha_k) \approx \sqrt{D}\exp\left[\frac{\mathsf{i}}{\hbar}\left(S(q^1\ldots q^n;\alpha_1\ldots\alpha_m)-\sum_{k=1}^{m}\alpha_k\beta_k\right)\right], \tag{3.27}$$

where $m = n-1$ is the number of integral constants.

Choosing a non-degenerate m-dimensional Gaussian amplitude leads to the Gaussian wave-packet

$$\Psi\big(q^i;\alpha_j,\Sigma_{jk}\big) = \int \mathbb{d}A_1\ldots\mathbb{d}A_m\,\psi(q^i;A_k)\mathrm{GD}_m(\alpha_k,\Sigma_{kl};A_k)^{1/2}\,, \tag{3.28a}$$

where

$$\mathrm{GD}_m(\alpha_k,\Sigma_{kl};A_k) := \frac{\exp\left[-\frac{1}{2}\sum_{k,l=1}^{m}\left(\Sigma^{-1}\right)_{kl}(A-\alpha)_k(A-\alpha)_l\right]}{\sqrt{(2\pi)^m\det\Sigma}} \tag{3.28b}$$

is the probability density function of the multivariate Gaussian distribution [72, ch. 5], $m = n-1$, and Σ is the non-degenerate, positive definite covariance matrix. The integral in eq. (3.28a) can also be estimated by the stationary phase method

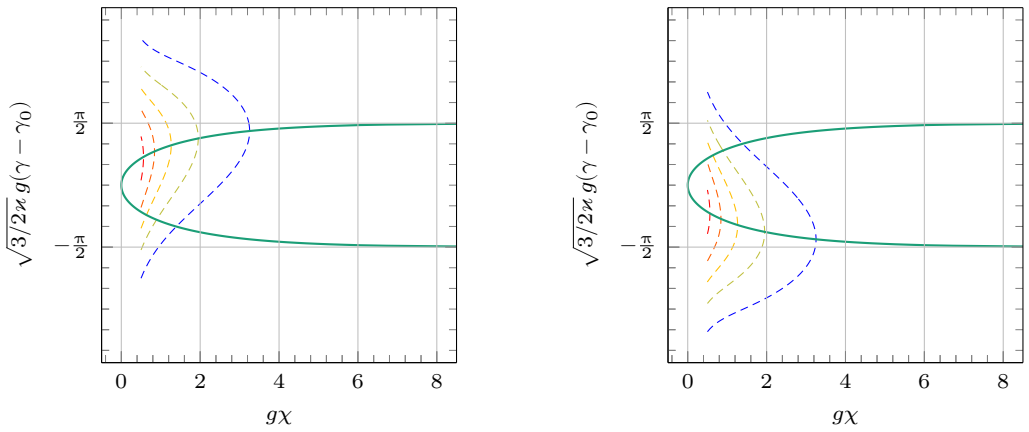

(a) $(-,+)$ with S_+

(b) $(-,+)$ with S_-

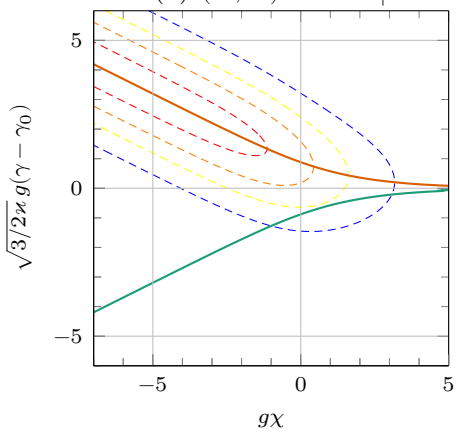

(c) $(+,-)$ with S_+

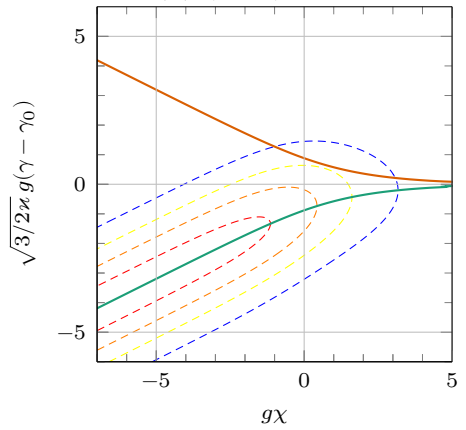

(d) $(+,-)$ with S_-

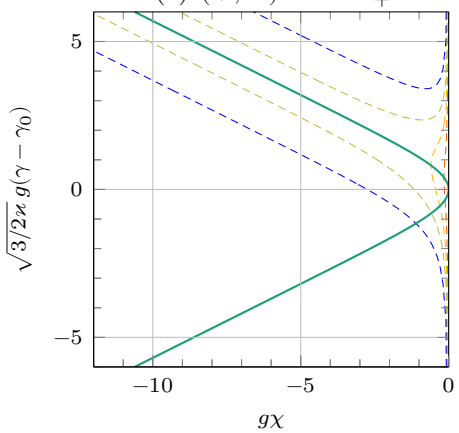

(e) $(+,+)$ with S_+

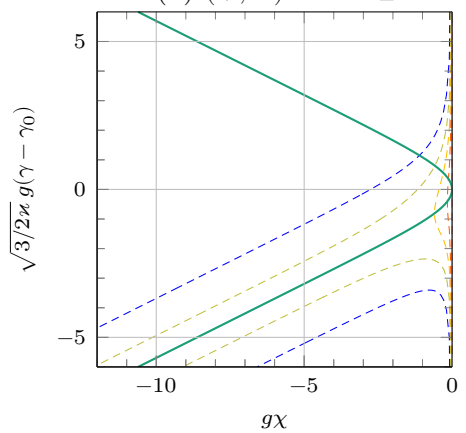

(f) $(+,+)$ with S_-

Figure 8: Narrow Gaussian wave-packets of the WKB mode functions with $S_\pm$ by eq. (3.26) as dashed contours, the expressions of which are listed in table 4. One sees that for each $S_\pm$, the wave-packet peaks around one asymptotic branch of the classical trajectory, which fails to hold near the turning point. Moreover, for the $(+,-)$- and $(+,+)$-cases, where $g\chi \to -\infty$ is a region that the corresponding Bessel functions are sinusoidal, the wave-packets form uniform tubes near the classical trajectory. For the $(-,+)$- and $(+,-)$-cases, where $g\chi \to +\infty$ is a region that the corresponding Bessel functions decay exponentially in amplitude, the wave-packets also decay. See also fig. 3.

as

$$\begin{aligned}\Psi(q^i;\alpha_k,\Sigma_{kl}) \approx \left(\frac{(2\pi)^m}{\det\Sigma}\right)^{1/4}\left(\frac{D}{\det d_m^{(2)}}\right)^{1/2} \\ \cdot\exp\left(\mathrm{i}d_m^{(0)} - \frac{1}{2}\sum_{k,l}\left(d_m^{(2)}\right)_{kl}\left(d_m^{(1)}\right)_k\left(d_m^{(1)}\right)_l\right),\end{aligned} \tag{3.29}$$

where

$$d_m^{(0)} := \frac{1}{\hbar}\left(S(q^i;\alpha^k) - \sum_{k=1}^m \alpha_k\beta_k\right), \tag{3.30a}$$

$$\left(d_m^{(1)}\right)_k := \frac{1}{\hbar}\left(\partial_{\alpha_k}S - \beta_k\right), \tag{3.30b}$$

$$\left(d_m^{(2)}\right)_{kl} := \left(\frac{1}{2}\Sigma^{-1} - \frac{\mathrm{i}}{\hbar}\mathrm{Hess}_\alpha\, S\right)_{kl}; \tag{3.30c}$$

$$\left(\mathrm{Hess}_\alpha\, S\right)_{kl} := \partial_{\alpha_k}\,\partial_{\alpha_l}S\,. \tag{3.30d}$$

The Schrödinger density of the wave-packet reads

$$\begin{aligned}\rho &= \rho(q^i,\alpha_k,\Sigma_{kl}) = |\Psi|^2 \\ &= \sqrt{\frac{(2\pi)^m}{\det\Sigma}}\frac{D}{\det d_m^{(2)}}\exp\left[-\Re\left(\sum_{k,l}\left(d_m^{(2)}\right)_{kl}\left(d_m^{(1)}\right)_k\left(d_m^{(1)}\right)_l\right)\right].\end{aligned} \tag{3.31}$$

The corresponding classical trajectory is $\left(d_m^{(1)}\right)_k = 0$, or $\beta_k = \partial_{\alpha_k}S$, which is identical to eq. (3.16a).

3.6 Summary

In this section 3 we have studied the WKB mode functions and the WKB wave-packets both for generic models and specifically for our prototype model. With the results established in section 3.5, we can be confident that a classical universe is likely to emerge from a quantum wave-packet constructed by a narrow Gaussian amplitude, and in regions where the WKB approximation is good. The amplitudes near the peak also seem to be constant. Departure from classicality is expected where these conditions are violated, for example when the wave-packet spreads (and becomes wider), is damped (and the amplitude becomes smaller), or near the classical turning point (and the WKB approximation fails).

The idea of the "peak" of a wave-packet, that was used in eqs. (3.26) and (3.31), is heuristic. If a wave-packet does not have a form as in eqs. (3.26) and (3.31), the heuristic idea does not easily apply, which has already happened in eq. (2.31). One needs a mathematical description for this idea, which will be studied in sec-

tion 6. One will see that in the contour approach of ridge-lines, as well as in the simple first-derivative test, the classical trajectories in eqs. (3.26) and (3.31) can be confirmed.

4 Self-adjoint extensions

In conventional quantum mechanics, the kinematic space of physical states is a Hilbert space, which the physicists usually perceive as a *finite*-dimensional Hilbert space as in linear algebra, and the physical observables are delegated by Hermitian operators. When generalising these statements to the *unbounded* operators in *infinite*-dimensional Hilbert spaces, it turns out that they need to be refined in the sense of general topology, namely the *convergence* of vectors becomes complicated compared to the finite-dimensional cases, which is usually not emphasised in physics. As a result, the Hermiticity of observables is to be understood not only in their *actions* on physical states, but also in their *domains*, which may have an impact on the spectra of the operators, leading to observable consequences.

In our prototype minisuperspace model, consider the case $(I, sv) = (-, +)$, where the mode functions are proportional to the unmodified Bessel functions $J_\nu(x)$, which is a result from eqs. (2.25a) and (2.25b). If the differential operator in those equations were naively Hermitian, these Bessel functions would be expected to be orthogonal upon $\int_{-\infty}^{+\infty} J_{\nu_1} J_{\nu_2} \,\mathrm{d}\chi \propto \int_0^{+\infty} J_{\nu_1} J_{\nu_2} \frac{\mathrm{d}x}{x}$. Surprisingly, calculation shows that [45, eq. (10.22.57)]

$$\int_0^{+\infty} J_{\nu_1}(x) J_{\nu_2}(x) \frac{\mathrm{d}x}{x} = \frac{1}{\nu_1 + \nu_2} \frac{\sin \frac{\pi(\nu_1 - \nu_2)}{2}}{\frac{\pi(\nu_1 - \nu_2)}{2}}, \qquad \Re(\nu_1 + \nu_2) > 0\,, \tag{4.1}$$

which is *not* zero unless $\nu_1 - \nu_2 = 2n$, $n \in \mathbb{Z}$.

This simple calculation motivated us to look into details of the self-adjointness of unbounded operators, which turns out to have already been extensively studied by von Neumann [126, sec. II.9] in the context of conventional quantum mechanics, and later summarised in e.g. [142, ch. VIII, 141, sec. X.1], which are easier to access. In the 2000s, there was a revival of interest in this problem in physics pedagogy, e.g. [7, 26, 36, 53].

In quantum gravitation, the technique of self-adjoint extensions was already applied in [173], in which the self-adjoint extension of the Wheeler–DeWitt operator is not unique, and was fixed by imposing simultaneous self-adjointness of other operators. [55] discussed the self-adjointness of another Wheeler–DeWitt operator, which is related to the *scale factor* in the Friedmann–Lemaître model, which is defined only on the *positive* real axis. In [35], the self-adjointness of the kinetic term of a scalar field was studied in a naked Reissner–Nordström spacetime. Furthermore, in [128–130], the self-adjoint extension was used to resolve the unitarity problem in anisotropic models with respect to an internal time parameter. Finally, [2] studied the self-adjointness of the Hamiltonian derived from a Brans–Dicke theory.

In this section 4, we first review the mathematical construction of a Hilbert space in section 4.1, and then give an elementary physical example in section 4.2, where the self-adjointness of operators has a non-trivial physical effect. Next, in section 4.3 we give a practical set of thumb-rules to check whether a self-adjoint extension exists. Finally, in section 4.4 we go back to our prototype model, and derive the consequences of imposing its Hamiltonian constraint to be self-adjoint, which are to be used in section 4.5, so that we can construct wave-packets from the eigenfunctions of the self-adjoint version of the Hamiltonian constraint.

Throughout this section 4, an operator A will be stressed with a hat like $\widehat{A}$.

4.1 Mathematical preliminaries

In this section 4.1 we introduce the mathematical concept of self-adjointness and describe the conditions, under which the concept can become alerting.

Let the Hilbert space in which the physical states live be $\mathbf{H}$, which is equipped with a Hermitian form as the inner product

$$(\psi, \phi) = \sum_i \psi_i^* \phi_i = (\phi, \psi)^* , \qquad \phi, \psi \in \mathbf{H} , \tag{4.2}$$

where $\{\phi_i\}$ are the components of ϕ under a standard basis. The *norm* of $\phi \in \mathbf{H}$ is then defined as

$$\|\phi\| = \sqrt{(\phi, \phi)} . \tag{4.3}$$

In such a linear space, one can pick up a linear operator $\widehat{A}$ and defines its *adjoint* $\widehat{A}^\dagger$ by imposing

$$\left(\widehat{A}^\dagger \phi, \psi\right) := \left(\phi, \widehat{A}\psi\right) , \qquad \forall \phi, \psi \in \mathbf{H} . \tag{4.4}$$

$\widehat{A}$ is called *Hermitian* if $\widehat{A}\psi = \widehat{A}^\dagger \phi$, $\forall \phi \in \mathbf{H}$, which is usually abbreviated as $\widehat{A} = \widehat{A}^\dagger$. Here, only the *action* of operator is described; the domain of $\widehat{A}$ is just $\mathbf{H}$.

A Hermitian operator has the following merits:

1. it has real eigenvalues;
2. its eigenvectors are orthogonal; and
3. it is the generator of a unitary operator.

These nice properties, especially the first and the third ones, make it a good candidate to delegate a physical observable. This is the reason why the Hermitian operators are important to quantum mechanics.

Finite-dimensional Hilbert spaces do have applications in physics, such as in the Stern–Gerlach experiment,[5] where the two-dimensional space of non-relativistic spins is essential. For most other applications, however, physical states often live in (separable [73, Def. A.32]) Hilbert spaces of infinite dimensions, which is a vector space equipped with an inner product, and is topologically *complete* in the corresponding norm.

The concepts in finite-dimensional spaces need to be refined here; in particular, the *domain* $\operatorname{Dom}\widehat{A}$ of the operator is to be specified, in addition to its *action*. To begin with, we define the *operator norm* as

$$\left\|\widehat{A}\right\| \coloneqq \sup_{\phi\in\mathbf{H}\setminus\{0\}} \frac{\left\|\widehat{A}\phi\right\|}{\|\phi\|} \equiv \sup_{\|\phi\|=1} \left\|\widehat{A}\phi\right\|, \tag{4.5}$$

namely the maximum norm of the result given by the operator acting on a unit vector. If the norm is finite, the operator is called *bounded*. In this case, $\widehat{A}$ is defined on the whole $\mathbf{H}$, and the merits mentioned above are essentially kept [73, sec. 7]. For a bounded "Hermitian" operator, the spectrum is also bounded [73, prop. 7.5]. Examples include the spin operator in the Stern–Gerlach experiment, and the density operator of a canonical ensemble $\hat{\rho} \coloneqq Z^{-1}\exp\bigl(-\beta\widehat{H}\bigr)$, where $Z \coloneqq \operatorname{Tr}\exp\bigl(-\beta\widehat{H}\bigr)$ is the partition function, $0 < \beta = 1/(k_{\mathrm{B}}T)$ is the inverse temperature, k_{B} the Boltzmann constant, and $\widehat{H}$ is a Hamiltonian operator which is bounded below [108, eq. (31.4), 151, eq. (2.6.6)].

If $\|A\|$ is not finite, the operator is *unbounded*. In this case, the operator can only be defined in a dense subset of $\mathbf{H}$, and the notion of "Hermiticity" is to be split into symmetricity and self-adjointness. On the one hand, an operator $\widehat{A}$ is called *symmetric* if $\widehat{A}\phi = \widehat{A}^{\dagger}\phi$, or

$$\bigl(\widehat{A}\phi, \psi\bigr) - \bigl(\phi, \widehat{A}\psi\bigr) = 0\,, \tag{4.6}$$

$\forall\phi \in \operatorname{Dom}\widehat{A}$; the definition includes the case in which $\operatorname{Dom}\widehat{A} \subsetneq \operatorname{Dom}\widehat{A}^{\dagger}$. On the other hand, $\widehat{A}$ is called *self-adjoint* if in addition to symmetric, $\operatorname{Dom}\widehat{A} = \operatorname{Dom}\widehat{A}^{\dagger}$ also holds.

In conventional quantum mechanics, unbounded "Hermitian" operators are very common. Consider a free particle moving in one dimension, then unbounded operators include the position and momentum operators, as well as the Hamiltonian. To explain in more detail, take the position operator $\hat{x}\phi(x) \coloneqq x\cdot\phi(x)$ as the example. The Hilbert space is the (Lebesgue) square-integrable functions $L^2(\mathbb{R})$, but $\operatorname{Dom}\hat{x} = \{x\phi(x) \in L^2(\mathbb{R})\} \subsetneq L^2(\mathbb{R})$; in words, for $\phi \in L^2(\mathbb{R})$, $\hat{x}\phi(x)$ may fail to be

[5] For a summary by the conductors of the experiments, see [62]; for a historical discussion, see [57]; for a pedagogical introduction, see [149, ch. 1].

in $L^2(\mathbb{R})$, for instance $\phi(x) \sim O(x^{-1})$ as $x \to \pm\infty$, so that $\phi(x) \sim O(x^0)$ and the integral of $|\phi|^2$ on $\mathbb{R}$ does not converge.

Compared to the introduction above, the mathematical details behind unbounded operators are more challenging, in which physicists may not be interested. There are, however, possible physical consequences, which cannot be ignored.

4.2 Particle in an infinite square well: an example

In this section 4.2 we give a simple example in which the self-adjointness of a physical operator is not trivial and has a physical consequence.

Consider the classic example of an infinite square well, in which a scalar particle of mass m moves non-relativistically in an infinite square potential wall between $[0, L]$ in one dimension. The common practice is to choose the Dirichlet boundary condition

$$\phi(0) = \phi(L) = 0 \tag{4.7}$$

for the stationary wave functions, yielding heuristically the space [105, eq. (22.5), 69, eq. (2), 73, sec. 9.6]

$$\left\{\phi \in L^2([0,L]) \cap C^1([0,L]) \;\middle|\; \phi(0) = \phi(L) = 0\right\}. \tag{4.8}$$

The condition in eq. (4.8) sounds physically plausible, since one can understand the infinite wall as the limiting case of a finite wall, in which the potential reads

$$\mathcal{V}(x) = \begin{cases} U > 0 & x < 0\,, x \geq L \\ 0 & 0 \leq x < L\,. \end{cases} \tag{4.9}$$

In this case, the stationary wave functions take the form

$$\phi_n(x) = \begin{cases} c_1 \mathsf{e}^{\kappa_n x} & x < 0 \\ c_2 \sin(k_n x + \delta_n) & 0 \leq x < L \\ c_3 \mathsf{e}^{-\kappa_n x} & x \geq L\,, \end{cases} \tag{4.10}$$

where c_i's are normalisation factors, and ϕ_k'/ϕ_k is expected to be continuous. One can estimate that for the ground state,

$$\delta_0 \approx \frac{\pi\hbar}{\sqrt{2m\bar{U}}L} \qquad U \to +\infty\,, \tag{4.11}$$

so that $\phi_0(0) \to 0$ as $U \to +\infty$. In words, one expects that the stationary wave

functions vanish at the limit of an infinite wall.

In the following we will study the momentum operator $\hat{p}$,

$$\hat{p}\phi = -\mathsf{i}\hbar\partial_x\phi\,. \tag{4.12}$$

Taking it naively as "Hermitian", we will check the domain of its conjugate $\hat{p}^\dagger$. Let $\phi \in \operatorname{Dom}\hat{p}$ be given by eq. (4.8). If $\hat{p}$ is symmetric,

$$(\psi, \hat{p}\phi) - (\hat{p}\psi, \phi) = 0 \tag{4.13}$$

needs to hold, and the condition under which eq. (4.13) is true will give $\operatorname{Dom}\hat{p}^\dagger$.

Direct calculation shows that

$$(\psi, \hat{p}\phi) - (\hat{p}\psi, \phi) = -\mathsf{i}\hbar(\psi^*\phi)_{x=0}^{x=L} \equiv 0\,, \tag{4.14}$$

meaning that there is no further restraint for ψ, and $\operatorname{Dom}\hat{p}^\dagger = L^2([0,L]) \supsetneq \operatorname{Dom}\hat{p}$. Apparently, $\hat{p}$ *is symmetric but not self-adjoint!*

The problem is that the boundary conditions imposed to ϕ are too strong and can be relaxed. This process is called *self-adjoint extension*. We can go back to eq. (4.13) and set $\psi = \phi$, which gives $|\phi(0)|^2 = |\phi(L)|^2$, or

$$\phi(L) = \mathsf{e}^{-\mathsf{i}\alpha}\phi(0)\,, \qquad \alpha \in \mathbb{R}\,. \tag{4.15}$$

Inserting eq. (4.15) into eq. (4.13) yields

$$0 = -\mathsf{i}\hbar(\psi^*\phi)_{x=0}^{x=L} = -\mathsf{i}\hbar\phi(0)\big(\mathsf{e}^{-\mathsf{i}\alpha}\psi^*(L) - \psi^*(0)\big)\,, \tag{4.16}$$

$$\text{or } \psi(L) = \mathsf{e}^{-\mathsf{i}\alpha}\psi(0)\,, \tag{4.17}$$

which is the same condition as that for ϕ. In other words, roughly speaking, we now have

$$\begin{aligned}\operatorname{Dom}\hat{p}_\alpha &:= \{\phi \in L^2([0,L]) | -\mathsf{i}\hbar\partial_x\phi \in L^2([0,L]), \phi(L) = \mathsf{e}^{-\mathsf{i}\alpha}\phi(0)\} \\ &= \operatorname{Dom}\hat{p}_\alpha^\dagger\,,\end{aligned} \tag{4.18}$$

making $\hat{p}_\alpha$ self-adjoint.

Note that each α gives a different self-adjoint domain and therefore a different operator $\hat{p}_\alpha$. If there were no such freedom to choose, the operator would be called *essentially self-adjoint*. In this example, $\hat{p}$ is not essentially self-adjoint, and has a family of *self-adjoint extensions*, labelled by α.

More exact mathematical details of this specific example can be found in [142, sec. VIII.2, 141, sec. X.1, 66, sec. 6.1.3]. We now turn to the physical implica-

tions. Fixing an α, the eigenvalues and eigenfunctions of $\hat{p}_\alpha$ are $\left(k_\alpha, \mathsf{e}^{\frac{\mathsf{i}}{\hbar}k_\alpha x}\right)$, where $k_\alpha := \frac{L}{\hbar}(\alpha + 2\pi n)$, $n \in \mathbb{Z}$. One sees that a different α (mod 2π) corresponds to a different momentum spectrum; in other words, distinct extensions potentially have an experimental effect.

Is self-adjointness a common problem in quantum mechanics? Having seen the problem of self-adjointness in the elementary example of a square well, one may wonder whether such a problem would also occur in other basic cases in quantum mechanics. If this were true, things could become nasty because the study of self-adjointness is in general a difficult task.

Fortunately, in quantum mechanics, we mostly deal with operators that are formally polynomial with respect to differentiation (*differential operations*), say $\sum_{i=0}^{n} c_i \frac{\mathrm{d}^i}{\mathrm{d}x^i}$, where x represents a position variable. This fact greatly simplifies the task, and the self-adjointness can be established for quite generic situations. For example, consider a non-relativistic particle moving in one dimension in a potential $\mathcal{V}(x)$. Then the Hamiltonian is essentially self-adjoint if $\mathcal{V}(x)$ is square-integrable, or bounded below by some $-Kx^2$, $K > 0$ [64, ch. 7.1]. This condition is even more relaxed than bounded below by a constant, and therefore guarantees the self-adjointness of most Hamiltonians that describe a physical system.

The Dirac notation In conventional quantum mechanics, the Dirac notion is often introduced [41], such that the matrix element of an operator $\widehat{A}$ reads

$$\left\langle \psi \,\middle|\, \widehat{A} \,\middle|\, \phi \right\rangle := \left(\psi, \widehat{A}\phi\right). \tag{4.19}$$

One readily sees that the calculation in eq. (4.14) is impossible under such a notion, because it can only express two types of matrix elements, $\left\langle \psi \,\middle|\, \widehat{A} \,\middle|\, \phi \right\rangle$ and $\left\langle \psi \,\middle|\, \widehat{A}^\dagger \,\middle|\, \phi \right\rangle$, whilst there are four possibilities $\left(\psi, \widehat{A}\phi\right)$, $\left(\psi, \widehat{A}^\dagger\phi\right)$, $\left(\widehat{A}\psi, \phi\right)$ and $\left(\widehat{A}^\dagger\psi, \phi\right)$. We see that the Dirac notion as in eq. (4.19) is inadequate in the context of studying the self-adjointness.

4.3 Criterion of the existence of self-adjoint extensions

The generic theory of self-adjoint extensions is technically complicated, and an outline is given in appendix D. A set of thumb-rules, however, can be described in short. In this section 4.3, we give a *criterion* for the existence of self-adjoint extensions.

Define the *deficiency subspaces* $\mathbf{H}_{\widehat{A},\pm}$ as the kernel of $\pm\mathsf{i}\lambda\hat{\mathbb{1}} - \widehat{A}^\dagger$, where $\widehat{A}$ ia symmetric, λ is introduced only for dimensional reason. Roughly speaking, $\mathbf{H}_{\widehat{A},\pm}$

is spanned by the solutions ϕ in

$$\widehat{A}^\dagger \phi = \pm \mathsf{i}\lambda\phi \,. \tag{4.20}$$

The *deficiency indices* are defined by

$$\mathcal{N}_{\widehat{A},\pm} := \dim \mathbf{H}_{\widehat{A},\pm}. \tag{4.21}$$

There are three cases:

1. $\mathcal{N}_{\widehat{A},+} = 0 = \mathcal{N}_{\widehat{A},-}$: $\widehat{A}$ is essentially self-adjoint.
2. $\mathcal{N}_{\widehat{A},+} = \mathcal{N}_{\widehat{A},-} = \mathcal{N}$: $\widehat{A}$ has self-adjoint extensions, which correspond one-to-one to the unitary maps

$$\widehat{U} : \mathbf{H}_{\widehat{A},+} \to \mathbf{H}_{\widehat{A},-} \,, \qquad \dim \widehat{U} = \mathcal{N}^2 \,. \tag{4.22}$$

3. Otherwise, $\widehat{A}$ has no self-adjoint extension.

Use the momentum operator for the infinite-well model in section 4.2 as an example. Equation (4.20) now reads

$$-\mathsf{i}\hbar\partial_x \phi = \pm \mathsf{i}\lambda\phi \,. \tag{4.23}$$

The solutions are

$$\phi_\pm \propto \mathsf{e}^{\mp \frac{\lambda}{\hbar} x} \,, \tag{4.24}$$

so that $\mathcal{N}_{-\mathsf{i}\hbar\partial_x,+} = 1 = \mathcal{N}_{-\mathsf{i}\hbar\partial_x,+}$, and $\hat{p} = -\mathsf{i}\hbar\partial_x$ has a one-parameter family of self-adjoint extensions, which fits the conclusion in eq. (4.18).

In practice, however, it is possible that the symmetricity condition in eq. (4.6) alone can determine the self-adjoint domain(s) of the operator, see section 4.4.

4.4 Self-adjointness of the exponential potential

Now in this section 4.4 we go back to the specific case in our prototype model in eq. (2.1a). After separation of variables in eq. (2.24), the non-trivial part of the model can be abstracted as the following non-relativistic particle with an exponential potential, described by the Hamiltonian

$$H(y,p) = \frac{p^2}{2M} + U\mathsf{e}^{ky} \,, \tag{4.25}$$

where M has the dimension of mass, $U \in \mathbb{R} \setminus \{0\}$.

(e,u)	$\mathrm{Bessel}_\nu(x)$
$(-,-)$	$c_1 J_\nu(x)$
$(-,+)$	no solution
$(+,-)$	$c_1 F_{\mathrm{i}\nu}(x) + c_2 G_{\mathrm{i}\nu}(x)$
$(+,+)$	$c_1 K_{\mathrm{i}\nu}(x)$

Table 5: Physical solutions to eq. (4.26b), which are adapted from table 2 with $\mathsf{e} = \mathsf{l}$, $\mathsf{u} = \mathsf{lsv}$.

Upon the usual canonical quantisation, the stationary Schrödinger equation reads

$$0 = \left[H\left(y, \frac{\hbar}{\mathsf{i}}\frac{\mathbb{d}}{\mathbb{d}y}\right) - \mathcal{E}\right]\phi(y) = \left[-\frac{\hbar^2}{2M}\frac{\mathbb{d}^2}{\mathbb{d}y^2} + U\mathsf{e}^{ky} - \mathcal{E}\right]\phi(y) \tag{4.26a}$$

$$= -\frac{\hbar^2 k^2}{8M}\left[x^2\frac{\mathbb{d}^2}{\mathbb{d}x^2} + x\frac{\mathbb{d}}{\mathbb{d}x} + (\mathsf{e}\nu^2 - \mathsf{u}x^2)\right]\phi(x)\,, \tag{4.26b}$$

where the dimensionless parameters $x \coloneqq \frac{2\sqrt{2M|U|}}{\hbar k}\mathsf{e}^{ky/2}$, the energy $\mathcal{E} =: \mathsf{e}\frac{\hbar^2 k^2}{8M}\nu^2$; $\mathsf{e} \coloneqq \operatorname{sgn}\mathcal{E}$, $\mathsf{u} \coloneqq \operatorname{sgn} U$. Equations (4.26a) and (4.26b) take the same form as eqs. (2.25a) and (2.25b), respectively. The solutions to eq. (4.26a) are therefore also Bessel functions, see table 5.

One could use the criterion with deficiency indices in section 4.3, and would see that for $\mathsf{u} = +$, the deficiency indices are both 0, and the Hamiltonian is essentially self-adjoint. For $\mathsf{u} = -$, in contrast, there is one *bounded* solution for each of $\pm\mathrm{i}\lambda$, respectively, so that the deficiency indices are both 1, meaning that there is a one-parameter family of self-adjoint extensions.

In the case of an exponential potential, however, it turns out that the symmetricity condition in eq. (4.6) alone already fixs the self-adjoint domains of the Hamiltonian. The symmetricity of $\widehat{H}$ requires the vanishing of

$$\begin{aligned}&\left(\psi, \widehat{H}\phi\right) - \left(\widehat{H}\psi, \phi\right)\\ &= -\frac{\hbar^2}{2M}\int_{-\infty}^{+\infty}\mathbb{d}y\left[\psi^*\frac{\mathbb{d}^2\phi}{\mathbb{d}y^2} - \frac{\mathbb{d}^2\psi^*}{\mathbb{d}y^2}\phi\right] &(4.27a)\\ &= -\frac{\hbar^2 k^2}{8M}\int_0^{+\infty}\frac{\mathbb{d}x}{x}\left\{\psi^*\left[x\frac{\mathbb{d}}{\mathbb{d}x}\left(x\frac{\mathbb{d}\phi}{\mathbb{d}x}\right)\right] - \left[x\frac{\mathbb{d}}{\mathbb{d}x}\left(x\frac{\mathbb{d}\psi}{\mathbb{d}x}\right)\right]^*\phi\right\}. &(4.27b)\end{aligned}$$

For stationary states, one sets $\psi = \mathrm{Bessel}_{\nu_1}$, $\phi = \mathrm{Bessel}_{\nu_2}$, inserts eq. (4.26b) into eq. (4.27b) and obtains

$$-\frac{\hbar^2 k^2}{8M}(\nu_1^2 - \nu_2^2)\mathsf{e}\int_0^{+\infty}\frac{\mathbb{d}x}{x}\,\mathrm{Bessel}_{\nu_1}(x)\mathrm{Bessel}_{\nu_2}(x)\,. \tag{4.27c}$$

This integral can be evaluated by the method in appendix C; here we only summarise the results.

The simpler case is $u = +$, in which the potential is bounded below by 0, and the Hamiltonian is essentially self-adjoint, which has a continuous positive spectrum ($e = +$) and no negative spectrum. Therefore the generalised eigenvalues and eigenfunctions are proportional to $(\nu^2, K_{\mathrm{i}\nu}(x))$. From [174, 131, 157]

$$\int_0^{+\infty} K_{\mathrm{i}\nu_1}(x) K_{\mathrm{i}\nu_2}(x) \frac{\mathbb{d}x}{x} = \frac{\pi^2}{2\nu_1 \sinh(\pi\nu_1)} \delta(\nu_1 - \nu_2)\,, \qquad \nu_1, \nu_2 > 0 \tag{4.28a}$$

one sees that the δ-normalisation factor for $K_{\mathrm{i}\nu}\Big(x = \frac{2\sqrt{2M|U|}}{\hbar k} \mathsf{e}^{ky/2}\Big)$ is

$$N_{K,\nu}^{-2} = \frac{\pi^2}{k\nu \sinh(\pi\nu)}\,. \tag{4.28b}$$

The more complicated cases are where $u = -$, for which the Hamiltonian is *not* essentially self-adjoint [5]; a family of self-adjoint extensions is characterised by a number $a \in [0, 2)$. For its positive part $e = +$, the spectrum is continuous, and the orthonormal eigenfunction corresponding to ν is

$$\Xi_\nu^{(a)}(y) = N_{\Xi,\nu}^{(a)} \Big(F_{\mathrm{i}\nu}(x) \cos\frac{\pi a}{2} + G_{\mathrm{i}\nu}(x) \sin\frac{\pi a}{2} \Big)\,, \tag{4.29}$$

where $N_{\Xi,\nu}$ is the δ-normalisation factor for the original variable y. Adapting the method in [157], one can derive

$$\int_0^{+\infty} F_{\mathrm{i}\nu_1}(x) F_{\mathrm{i}\nu_2}(x) \frac{\mathbb{d}x}{x} = \frac{\tanh\frac{\pi\nu_1}{2}}{\nu_1} \delta(\nu_1 - \nu_2)\,, \tag{4.30a}$$

$$\int_0^{+\infty} G_{\mathrm{i}\nu_1}(x) G_{\mathrm{i}\nu_2}(x) \frac{\mathbb{d}x}{x} = \frac{\coth\frac{\pi\nu_1}{2}}{\nu_1} \delta(\nu_1 - \nu_2)\,, \tag{4.30b}$$

$$\int_0^{+\infty} \Big[F_{\mathrm{i}\nu_1}(x) G_{\mathrm{i}\nu_2}(x) + F_{\mathrm{i}\nu_2}(x) G_{\mathrm{i}\nu_1}(x) \Big] \frac{\mathbb{d}x}{x} = 0\,; \tag{4.30c}$$

therefore

$$\Big(N_{\Xi,\nu}^{(a)}\Big)^{-2} = \frac{2}{k\nu} \Big(\tanh\frac{\pi\nu}{2} \cos^2\frac{\pi a}{2} + \coth\frac{\pi\nu}{2} \sin^2\frac{\pi a}{2} \Big)\,. \tag{4.30d}$$

For its negative part $e = -$, the spectrum is *discrete* with

$$\nu = 2n + a\,, \qquad n \in \mathbb{N}\,, \tag{4.31a}$$

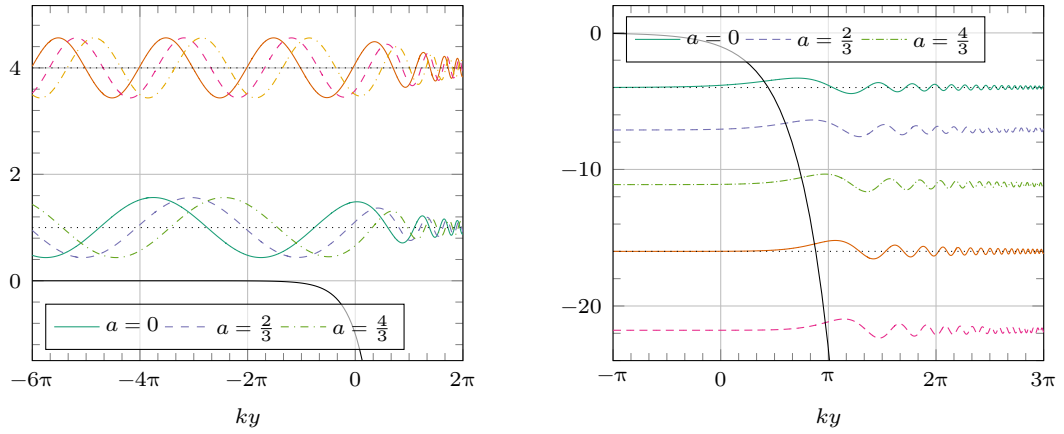

(a) $\mathsf{e} = +$ with $\Xi_\nu^{(a)}$

(b) $\mathsf{e} = -$ with J_{2n+a}

Figure 9: Normalised eigenfunctions of the Hamiltonian with negative exponential potential in eq. (4.25). Solid, dashed and dash-dotted lines denote different families of eigenfunctions in distinct self-adjoint domains. The functions are shifted with the corresponding energy level, plotted as black, dotted lines. One sees that in fig. 9a, different extensions correspond to phase shifts in the asymptotically sinusoidal region $ky \to -\infty$. In fig. 9b, different domains give rise also to different families of energy levels, in addition to "phase shifts".

and the corresponding orthonormal eigenfunctions read

$$\Phi_n^{(a)}(y) = N_{J,n}^{(a)} J_{2n+a}(x)\,, \tag{4.31b}$$

$$\left(N_{J,n}^{(a)}\right)^{-2} = \frac{1}{k(2n+a)}\,. \tag{4.31c}$$

These eigenfunctions are plotted in fig. 9.

The exponential potential in eq. (4.25) is also a special case of the so-called Morse potential [120]

$$g_1 \mathrm{e}^{-2cy} + g_2 \mathrm{e}^{-cy}\,, \qquad g_1, g_2 \in \mathbb{R}, \quad c > 0\,, \tag{4.32}$$

which belongs to the exact solvable potentials of the one-dimensional stationary Schrödinger equation. Lists and comprehensive results of such potentials can be found in e.g. [11, appx. I]. The self-adjointness of the exponential potential has been studied in [64, sec. 8.5.3] as well, which confirms our results.

4.5 Wave-packets of the minisuperspace model

Having fixed the self-adjoint domains of the Hamiltonian constraint, we can now construct wave-packets for our minisuperspace model that are more physically

relevant.

For the $(+,-)$ and $(+,+)$-cases, the quantum number p_γ or ν ranges in $\mathbb{R}$, so that we can use Gaussian amplitudes for them, as in eq. (3.22a). For the $(-,+)$-case, where the quantum number n takes non-negative integral values, we choose the *Poisson distribution*, the probability mass function reads

$$\mathrm{PD}(\mu;k) := \frac{\mu^k \mathsf{e}^{-\mu}}{k!}\,, \tag{4.33a}$$

$$\mu > 0, \qquad k = 0, 1, 2, \ldots\,, \tag{4.33b}$$

where μ is the mean value. The reason for the choices will be given in section 5.3.

None of the wave-packets can be worked out analytically; the numerical constructions are shown in fig. 10, which should also be compared to fig. 8. One sees that the classical trajectories, in which the integral constants are proportional to the corresponding quantum numbers, lie near the ridge of the wave-packets. This will be studied in detail in section 6.

4.6 Summary

Non-trivial results of self-adjoint extensions can appear in those quantum mechanical systems, with degrees of freedom taking values in a *subinterval* of $\mathbb{R}$, or with a potential $\mathcal{V}(x)$ that cannot be bounded below by $-Kx^2$, $K > 0$. These conditions can be satisfied in certain cosmological models, for example when one uses the scale factor a that ranges in $(0, +\infty)$. Alternatively, as shown by the prototype model, they also arise in a Friedmann–Lemaître–Liouville model where the Liouville field is *phantom*. In this case, there is an one-parameter family of self-adjoint domains, that leads to a phase-shift for the mode functions, or the discretisation of a quantum number that are also subject to the shift.

In the early development of quantum theory, people recognised discrete observable values in e.g. the atomic emission or the Stern–Gerlach experiment, which were distinguishing phenomena that told them apart from the continuous classical world. It has been known since the advent of quantum mechanics that these discretisations root in the spectra of self-adjoint operators acting on the physical Hilbert space. Now that different discrete spectra also appear with the requirement of operators being self-adjoint, we expect this is a chance for experimentalists to realise such an ambiguous system, and a challenge for theorists to work out rules that select a privileged spectrum over the others.

In the phantom Friedmann–Lemaître–Liouville model with parameters that lead to the discrete spectrum, the Poisson amplitude gives many wave-packets that overlap and interfere in the long-tailed region. Heuristically, one can argue

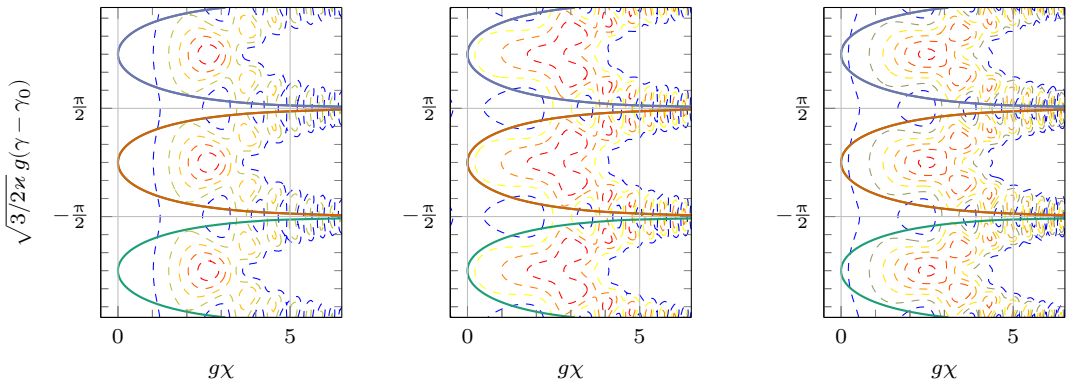

(a) $(-,+)$, $a=\frac{0}{3}$ (b) $(-,+)$, $a=\frac{1}{3}$ (c) $(-,+)$, $a=\frac{2}{3}$

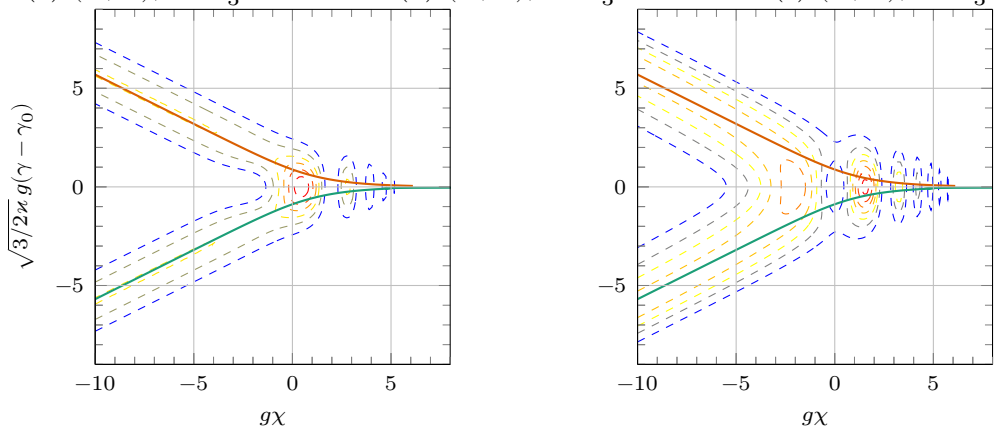

(d) $(+,-)$, $a=\frac{0}{3}$ (e) $(+,-)$, $a=\frac{1}{3}$

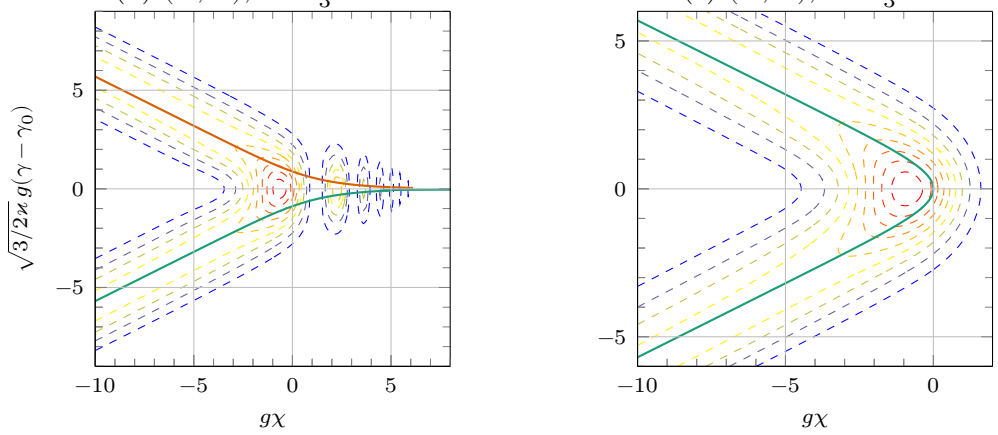

(f) $(+,-)$, $a=\frac{2}{3}$ (g) $(+,+)$

Figure 10: Wave-packets of the minisuperspace model. In figs. 10a to 10c, a *Poisson amplitude* with mean value $\mu = 1$ is chosen, whereas in figs. 10d to 10g, a *Gaussian amplitude* with mean value $\mu = 1$, standard distribution $\sigma = 1/2$ is chosen; see section 5.3 for arguments. In figs. 10a to 10f, the $(-,+)$- and $(+,-)$-cases with different self-adjoint extensions are plotted; One sees that they produce different interference patterns. The classical trajectories, where the integral constant is the same as the quantum number, lie near the ridge of the wave-packets.

from the experience in quantum mechanics that these could lead to tunnelling between the adjacent multiverses and a departure from the classical universe, that meets singularities at the end of the tail. More discussion will be given in section 6.

5 Stationary wave-packets

In quantum cosmology, the usual way of constructing a wave-packet is linearly superposing the complete integrals ψ_ν, containing constants ν, of the Wheeler–DeWitt equation,

$$0 = H_\perp \psi_\nu = \left(-\frac{\hbar^2}{2} \mathcal{G}^{IJ} \frac{\partial}{\partial q_I} \frac{\partial}{\partial q_J} + \mathcal{V} \right) \psi_\nu , \qquad \text{(2.22a revisited)}$$

$$\Psi = \int \mathbb{d}\nu \, \mathcal{A}(\nu) \psi_\nu \, . \qquad \text{(2.29 revisited)}$$

In quantum mechanics, eq. (2.22a) is comparable to the stationary Schrödinger equation

$$H\psi_\nu = E\psi_\nu \, , \tag{5.1}$$

the solution ψ_ν to which is called the wave function of a *stationary state*, where ν is another quantum number that marks different states in a degenerate level. If one writes $H_\perp = H - E$ and fixes the energy level E, eq. (5.1) becomes $H_\perp \psi_\nu = 0$, which looks identical to eq. (2.22a). In this resemblance, constructing a wave-packet corresponds to the superposition of degenerate stationary states in the same energy level, the result of which is also an energy eigenstate of the same level.

We will call such a quantum wave-packet a *stationary wave-packet*, that encompasses both conventional quantum mechanics and the Wheeler–DeWitt quantum cosmology. Relating a tentative theory of quantum gravitation to quantum mechanics can lead to analogue models, which has been realised in the study of black holes [13, 156, 158, 167] and quantum field theory in curved space-time [24, 166]. For a review of analogue gravitation, see [14].

On the one hand, we did not find suggestions that relate the superposition of degenerate energy eigenstates and quantum cosmology in the literature. On the other hand, we noticed that the Rydberg or highly excited atom, has indeed a description of such a superposition as a wave-packet [58, 111, 153]. Independent of this experimental aspect, in section 5.1 we introduce the two-dimensional hydrogen atom as a toy model, and then construct stationary wave-packets in section 5.2. Meanwhile, in section 5.3 we discuss the choice of superposition amplitudes, arguing in favour of Gaussian, binomial and Poisson amplitudes, etc., which maximises the entropy. In the end, we turn to the study of the classical limit, and verify the correspondence principles in section 5.4.

5.1 Two-dimensional hydrogen atom

Consider a spinless non-relativistic two-dimensional hydrogen atom, described by the action

$$S = \int \mathrm{d}t \left[\frac{m}{2}(\dot{\varrho}^2 + \varrho^2 \dot{\varphi}^2) + \frac{\alpha}{\varrho} \right], \qquad \alpha > 0 \tag{5.2}$$

in polar coordinates (ϱ, φ). The classical trajectory can be solved in terms of the conserved energy and angular momentum (E, L) as

$$\varrho = \frac{L^2}{m\alpha + \sqrt{m(2EL^2 + m\alpha^2)}\cos(\varphi - \varphi_0)} \,. \tag{5.3}$$

For $E < 0$, the system is bounded, and the trajectory is an ellipse. Fixing $\varphi_0 = 0$, the trajectory passing through $(\varrho, \varphi) = (\varrho_0, 0)$ and (ϱ_π, π) can be worked out in terms of

$$E = -\frac{\alpha}{\varrho_0 + \varrho_\pi} < 0 \,, \qquad L = \pm\sqrt{\frac{2m\alpha}{\varrho_0^{-1} + \varrho_\pi^{-1}}} \,. \tag{5.4}$$

Upon canonical quantisation, the stationary Schrödinger equation reads

$$\left(-\frac{\hbar^2}{2m}\nabla^2 - \frac{\alpha}{\varrho} \right) \psi(\varrho, \varphi) = E\psi(\varrho, \varphi) \,, \tag{5.5}$$

where the Laplace–Beltrami operator

$$\nabla^2 \coloneqq \partial_\varrho^2 + \varrho^{-1}\partial_\varrho - \frac{1}{\hbar^2 \varrho^2} L^2 \,, \qquad L \coloneqq -\mathrm{i}\hbar\, \partial_\varphi \tag{5.6}$$

is chosen. In appendix E we show that the stationary wave functions, with definite main and angular quantum numbers, are

$$\psi_{nl}(\xi, \varphi) = P_{nl}(\xi)\Phi_l(\varphi) \,, \tag{5.7a}$$

$$P_{nl}(\xi) = N_{nl}\xi^{|l|}\mathrm{e}^{-\xi/2}G_{nl}(\xi) \,, \tag{5.7b}$$

$$N_{nl} = \frac{1}{(2|l|)!}\left(\frac{(n + |l|)!}{(2n+1)(n - |l|)!} \right)^{1/2} , \tag{5.7c}$$

$$\Phi_l(\varphi) = (2\pi)^{-1/2}\mathrm{e}^{\mathrm{i}l\varphi}, \qquad l = 0, \pm 1, \pm 2, \dots \,, \tag{5.7d}$$

where

$$\xi \coloneqq \beta_n \varrho \,, \qquad \beta_n \coloneqq \frac{2m\alpha}{\hbar^2}\left(n + \frac{1}{2} \right)^{-1} \tag{5.7e}$$

are the *dimensionless radial coordinate*, and G_{nl} is a special function given in eqs. (E.5a) to (E.5c). Note that eq. (5.7c) is chosen such that eq. (5.7a) is normalised with respect to ξ, rather than ϱ. The energy levels for the bounded states are

$$E_n := -\frac{m\alpha^2}{2\hbar^2}\left(n+\frac{1}{2}\right)^{-2}. \tag{5.8}$$

The normalisation condition for scattering states $E \geq 0$ does not lead to a closed-form expression for the normalisation factor, see e.g. [175, eq. (2.28)]. For simplicity, we focus on the case $E < 0$ in the following.

5.2 Stationary wave-packets for the hydrogen atom

For bounded states of the two-dimensional hydrogen atom in eq. (5.2), one fixes E or n and chooses a probability amplitude for different l's to construct a stationary wave-packet,

$$\Psi_{nq} := \sum_{k=-n}^{n} A_{nk;q}\psi_{nk}\,. \tag{5.9}$$

We would like to find a choice for the $A_{nk;q}$'s, such that the expectation value of angular momentum

$$\left(\Psi_{nq}, L\,\Psi_{nq}\right) = q\hbar\,, \tag{5.10}$$

where $q \in [-n,n]$, $q \in \mathbb{R}$. Since $k \in [-n,n]\cap\mathbb{Z}$, a "natural" choice for the probability masses seems to be the *binomial distribution*, where the probability mass function is

$$\mathrm{BD}(k;u,s) := \binom{u}{k} s^k (1-s)^{u-k}, \tag{5.11a}$$

$$\binom{u}{k} := \frac{u!}{k!(u-k)!}\,, \tag{5.11b}$$

$$k = 0,1,\ldots,u, \qquad s \in [0,1]\,. \tag{5.11c}$$

In our case, the amplitude satisfies

$$\begin{aligned}\left|A_{nk;q}\right|^2 &= \mathrm{BD}\left(n+k; 2n, \frac{n+q}{2n}\right)\\ &= (2n)^{-2n}(n-q)^{n-k}(n+q)^{n+k}\binom{2n}{n+k}.\end{aligned} \tag{5.12a}$$

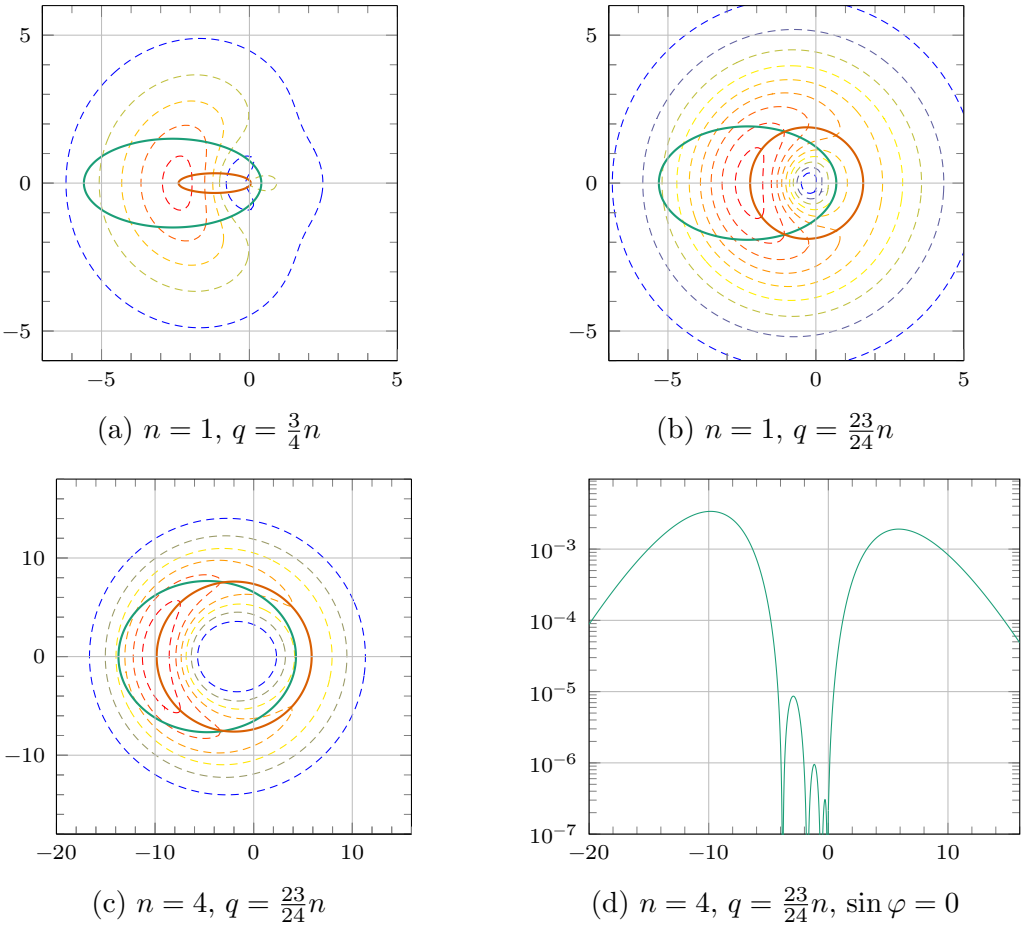

(a) $n = 1$, $q = \frac{3}{4}n$ (b) $n = 1$, $q = \frac{23}{24}n$

(c) $n = 4$, $q = \frac{23}{24}n$ (d) $n = 4$, $q = \frac{23}{24}n$, $\sin\varphi = 0$

Figure 11: Stationary wave-packets $\left|\Psi_{nq}(\xi,\varphi)\right|^2$ of the two-dimensional hydrogen atom. The green lines denote a classical trajectory in eq. (5.3) with $\varphi_0 = 0$, $E = E_n$ and $L = q\hbar$. The orange lines are the classical trajectories passing through the two highest peaks of the wave-packet, with the integral constants (E, L) given by eq. (5.4). Apparently, the green line in fig. 11b fits the orange line better than in fig. 11a, but worse than in fig. 11c. In fig. 11d we show the normal projection of fig. 11c on the $\sin\varphi = 0$ line (in logarithm scale). One sees that there are multiple maxima; the highest two were chosen for plotting fig. 11c.

The most naive choice

$$A_{nk;q} = \sqrt{\mathrm{BD}\left(n+k, 2n, \frac{n+q}{2n}\right)} \tag{5.12b}$$

leads to stationary wave-packets that "peak around" a classical trajectory for $|q| \lesssim n$, see fig. 11.

5.3 Wave-packets and the choice of amplitudes

In the previous sections, we have studied *Gaussian* wave-packets for the quantum numbers that take values in $\mathbb{R}$, and a binomial amplitude for the quantum number that takes finite integral values. In this section, we try to justify the usage of

wave-packets and discuss the choice of amplitudes.

In reality, a physical system interacts with the environment, which contains a vast number of degrees of freedom. At the quantum level, describing the system plus the environment as an entirety, and then eliminating the latter, is not equivalent to beginning with separate descriptions of the system and the environment. To be more specific, if one begins with a wave function of the entirety, and then eliminating the environment by tracing out the corresponding degrees of freedom, one necessarily arrives at a *density operator* of the system. In other words, an open quantum system is usually in a mixed state, even though the entirety may be described by a pure state.

During evolution, the open quantum system loses coherence with the environment and becomes a mixed state. Such a process is called *decoherence*, and the evolution cannot be simply described by, say, the Schrödinger equation for conventional quantum mechanics, with respect to the Hamiltonian of the system. Instead, the Hamiltonian of the environment and that of the interaction also play a role. Now in quantum cosmology, we also study a reduced number of degrees of freedom, with e.g. the inhomogeneities suppressed at the beginning, serving effectively as the environment. Therefore, it should be the density operator of the universe, rather than the wave-packet, that we are talking about [90].

Nevertheless, we have been sticking to wave-packets throughout this work. From a practical point of view, on the one hand, wave-packets are much easier to handle, that obey the familiar Schrödinger equation or the Wheeler–DeWitt equation. On the other hand, it has been shown that local interactions lead to a density operator that is narrowly diagonal with respect to the position eigenstates, which can be described as an incoherent superposition of narrow wave-packets [178], each of which is called an Everett branch.

Having decoherence in mind, which serves as a dynamical mechanism that results in (an incoherent superposition of) wave-packets, the choice of an amplitude is no longer arbitrary and has a physical priority. We note that decoherence increases the *entropy* of the open quantum system, and the Everett branches have Gaussian amplitudes [82]. From a statistical point of view, maximisation of the entropy is also the most probable result [139]. Incidentally, the Gaussian distribution

$$\mathrm{GD}_1(\alpha,\sigma^2;A) := \frac{\exp\bigl(-\frac{1}{2}\sigma^{-2}(A-\alpha)^2\bigr)}{\sqrt{2\pi\sigma^2}}\,. \qquad \text{(3.22b revisited)}$$

is also a *maximum entropy distribution* [37, ch. 12]. Taking the maximality of entropy seriously, we propose that *this property should also hold in cases where the quantum number is discrete.*

Following this proposal, for the two-dimensional hydrogen atom, we chose bi-

nomial amplitude, that squares to be eq. (5.11a). For quantum numbers taking values in $\mathbb{N}$, as in the case of our minisuperspace model $(-,+)$ in section 3.5, we chose the Poisson distribution

$$\mathrm{PD}(\mu;k) := \frac{\mu^k \mathsf{e}^{-\mu}}{k!}\,, \qquad \text{(4.33a revisited)}$$

These are both maximum entropy distributions for their corresponding discrete random variables [77].

5.4 Ridge-line of a wave-packet and the correspondence principles

In quantum cosmology, people argue that the ridge-line of a wave-packet peaks along a classical trajectory [75]. This would be more convincing if the statement also holds for the stationary wave-packets in conventional quantum mechanics.

For the binomial wave-packets here, defined by eqs. (5.9), (5.7a), (5.7d) and (5.12b), we approximate the ridge by finding the two highest peaks of the wave-packet, and find the elliptic classical trajectory passing them, see fig. 11. The approximate ridge-line is described by the integral constants $(E_{\mathrm{ar}}, L_{\mathrm{ar}})$ given by eq. (5.4).

One sees that this approximation is good as n increases, which fits Bohr's correspondence principle [25], stating that the quantum system reproduces its classical behaviour in the limit of large *main* quantum number n. This can be seen in fig. 12a, where one fixes q/n and observes the relative difference between $(E_{\mathrm{ar}}, L_{\mathrm{ar}})$ and (E_n, L) vanishes polynomially as $n \to +\infty$.

In our application, on the other hand, we are more concerned with fixed n or E_n, and varying q. In this case, the ridge-line gets closer to the classical trajectory as the effective *angular* quantum number $q \to n^-$, in the sense that the relative differences between $(E_{\mathrm{ar}}, L_{\mathrm{ar}})$ and $(E_n, q\hbar)$ become smaller in the aforementioned limit, see fig. 12b. The differences, however, will not vanish. This correspondence phenomenon is relevant in quantum cosmology, where the "main quantum number" is to be fixed, and only the other quantum numbers in the degenerate "energy eigenspace" can change.

5.5 Summary

The stationary wave-packets are realised in quantum mechanics with the superposition of degenerate energy eigenstates. Such cases are illustrated by the toy model of a two-dimensional hydrogen atom. In reality, the Rydberg atom can also be described by such a superposition, providing a chance to verify the theoretical statements.

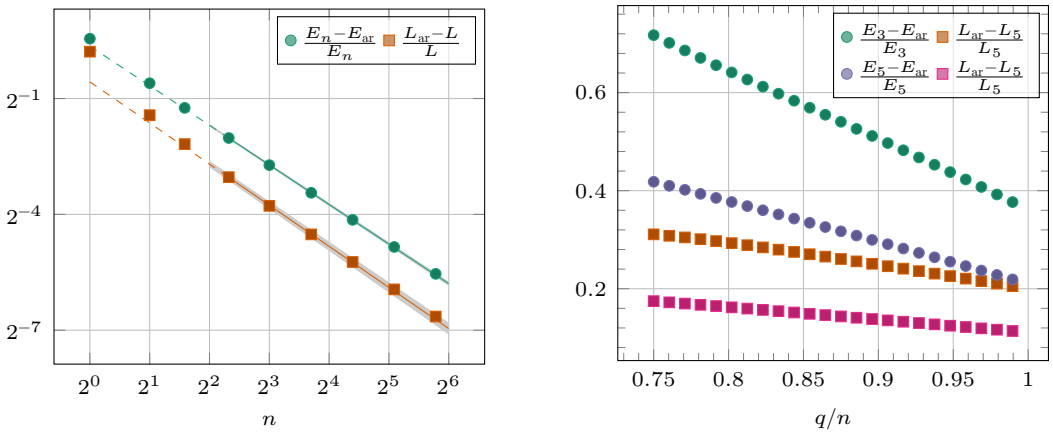

(a) Bohr's, $\frac{l}{n} \equiv \frac{23}{24}$.

(b) Ours, $n = 3$ and 5.

Figure 12: Correspondence principles shown in terms of the difference between $(E_{\mathrm{ar}}, L_{\mathrm{ar}})$ and $(E_n, q\hbar)$, where the former with subscript $_{\mathrm{ar}}$ denotes the integral constants that give a trajectory passing through the two highest peaks of the binomial wave-packet (fig. 11). In fig. 12a, the difference vanishes as $n \to +\infty$, which is accordance with Bohr. The solid line is the best fit with the generalised linear model [124] $y = g^{-1}(\beta_0 + \beta_1 \ln n)$ with $g(y) = \ln y$. In fig. 12b, the difference becomes smaller as $q \to n^-$, but will not vanish; this correspondence phenomenon is relevant in quantum cosmology.

Wave-packets constructed by superposing solutions of the Wheeler–DeWitt are also formally stationary. It is imaginable to make use of this fact and use quantum systems in laboratory to simulate a quantum universe or a quantum black hole.

However, one crucial difference between common quantum mechanical systems and quantum cosmology is that, the latter usually has a *Lorentzian* "kinetic energy term" in the Hamiltonian constraint, whereas the former mostly have a *Euclidean* kinetic energy term. One needs to be very creative to set up a simulated quantum cosmology system in laboratory.

6 Ridge-lines of wave-packets

In the Wheeler–DeWitt approach of quantum gravitation, due to the absence of a Hilbert space, one cannot use the usual way to make predictions as in conventional quantum mechanics. This includes, on the one hand, interpreting the inner product as a probability amplitude; on the other hand, analysing self-adjoint operators and studying their spectra. In particular, when the wave-packet of the universe (c.f. section 5.3) needs a semi-classical interpretation, there is no quantitative way to calculate the emerged classical trajectory from the quantum wave function.

In section 3.5, we have studied a special case, in which the wave-packet is constructed by superposing the WKB mode functions with a narrow Gaussian amplitude. The mathematical result confirms the heuristic idea, that such a wave-packet peaks near the classical trajectory, which shares the same integral constant as the centre of the Gaussian amplitude. In section 5.3, we have also discussed the reason to study wave-packets and a maximum-entropy criterion of amplitudes.

In this section 6, we try to quantify the qualitative arguments in the literature, that a classical trajectory can be read off from wave-packets in specific forms. Intuitively, one may imagine the profile of a wave-packet as a terrain in its configuration space, where the hills and valleys are the most and least probable places to "find" the system. In physical geography, chains of mountains or hills stretch a distance, where the "highest points" form the *ridge-lines*; conversely, one can define the valleys or the *dale-lines* by the "lowest points".

The ridge- and dale-lines are in some sense the generalisation of local maxima and minima, which are isolated points. The latter are also easier to be solved in terms of local extrema as $\nabla\rho = 0$ as necessary but not sufficient conditions, and distinguishing them is more involved. One may give a sufficient condition when the Hessian is non-singular, but when it is, more works need to be done. For simplicity and clearance, we will study the ridge- and dale-lines on the equal foot.

The ridge- and dale-lines have been studied by the computer scientists working on imaging and vision [48, 97, 98], where the ridge- and dale-lines have rich applications, especially in two-dimensional *Euclidean geometry*. In physical configuration spaces having a higher-dimensional *(pseudo-)Riemannian geometry*, the ridge- and dale-lines have not been much used, to our knowledge. In addition, the Euclidean experience from computer science also needs to be thought twice.

From now on, we will not use the analogy with terrain any further, which we argue as follows. For terrain, the altitude has the dimension of length, which is comparable to the dimension of the geographic coordinates. For a wave-packet, in contrast, the dimension of its profile is *not* comparable to the dimensions of the configuration space coordinates; the former might be the inverse of the configura-

tion volume if one has the Schrödinger normalisation condition in mind,

$$\int \mathbb{d}\mathrm{Vol}\,|\Psi|^2 = 1\,, \tag{6.1}$$

which is *dependent* on the configuration space coordinates. Based on these considerations, we shall find an *intrinsic* description of the ridge-lines of a wave-packet, where the wave-packet is *not* to be plotted in an additional dimension.

Heuristically, one can simply use the first partial derivative to find the ridge- and dale-lines, see section 6.1. We mainly introduce two distinct intrinsic approaches, in terms of *contours* and *stream-lines*, which will be explained in sections 6.2 and 6.3, respectively. Details of these approaches are discussed in the subsequent sections 6.4 to 6.6.

6.1 First-derivative test

One can easily come up with a simple first-derivative test for a ridge-line, which we also describe here in section 6.1. In two dimensions with Cartesian coordinates (x, y), it reads

$$\rho_{,x} = 0 \qquad \text{or} \qquad \rho_{,y} = 0\,, \tag{6.2}$$

which is weaker than the extremum condition $\rho_{,x} = 0$ *and* $\rho_{,y} = 0$.

Geometrically, eq. (6.2) can be interpreted as a directional extremum test, namely to find the extremum with respect to only the x- or y-direction.

Take the "linear" wave-packet in eq. (2.31) as an example. With $\rho_{\mathrm{lin}} = |\Psi_{\mathrm{lin}}|^2$, the condition $\partial_\chi \rho_{\mathrm{lin}} = 0$ gives

$$\mathsf{e}^{g\chi}\cosh\Big[\sqrt{\tfrac{3}{2\varkappa}}\,g(\gamma-\gamma_0)\Big]^2 = \frac{g^2\hbar^2}{8\mathrm{Vol}_3^2|V|}\,. \tag{6.3}$$

Compared with eq. (2.14) and table 1, eq. (6.3) has exactly the form of a classical trajectory, with

$$p_\gamma^2 = \frac{3g^2\hbar^2}{2\varkappa}\,. \tag{6.4}$$

On the other hand, the condition $\partial_\gamma \rho_{\mathrm{lin}} = 0$ gives

$$\mathsf{e}^{g\chi}\cosh\Big[\sqrt{\tfrac{3}{2\varkappa}}\,g(\gamma-\gamma_0)\Big]^2 = \frac{g^2\hbar^2}{8\mathrm{Vol}_3^2|V|}\coth\Big[\sqrt{\tfrac{3}{2\varkappa}}\,g(\gamma-\gamma_0)\Big]^4\,. \tag{6.5}$$

Since $\coth\Big[\sqrt{\frac{3}{2\varkappa}}\,g(\gamma-\gamma_0)\Big] \to 1$ as $\sqrt{\frac{3}{2\varkappa}}\,g(\gamma-\gamma_0) \to \pm\infty$, eq. (6.5) also coincides

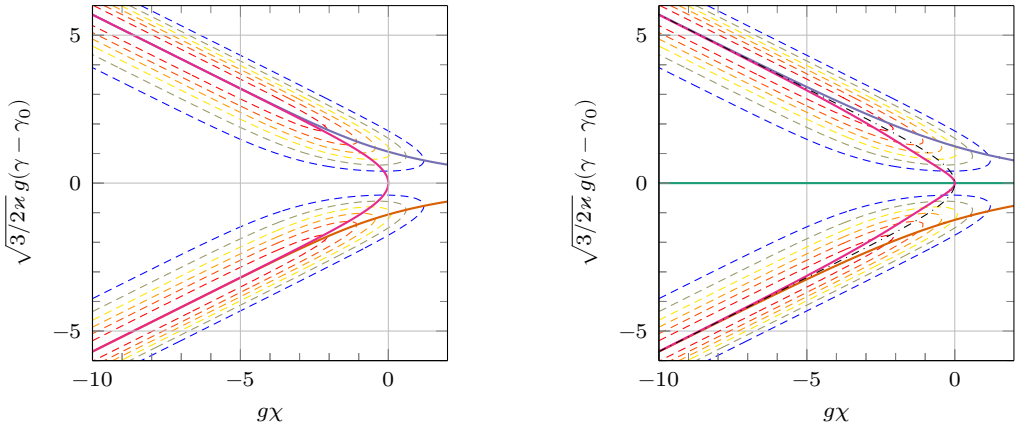

(a) First-derivative test

(b) Contour approach

Figure 13: Two ridge-line approaches shown with the "linear" wave-packet in eq. (2.31). In fig. 13a where the first-derivative test is used, the orange and purple lines are the results from eq. (6.5), whereas the pink line is from eq. (6.3). In fig. 13b, we have used the *Lorentzian* minisuperspace metric in eq. (2.1b). The solid lines in color dash-dotted line are derived by the contour approach in eq. (6.18). Unfortunately, we failed to solve the problem in the stream approach.

asymptotically with a classical trajectory, with the same p_γ as in eq. (6.4). In contrast to eq. (6.3), one has two distinct trajectories, which approach the same classical trajectory in the above-mentioned asymptotic region, while they depart from the trajectory near the classical turning point. The two results are plotted in fig. 13a.

Now consider a classical trajectory that is implicitly given by an equation $f(x,y) = 0$. This works only in two dimensions; for d-dimensions, $d > 2$, one needs $d-1 > 1$ equations to specify an implicit curve. One can intuitively imagine a wave-packet that "peaks around" this trajectory, the density of which is given by [75, eq. (6.3)]

$$\rho = \mathsf{e}^{-f^2}\,, \tag{6.6}$$

so that the density ρ peaks to 1 at $f = 0$, and is less than 1 for $f \neq 0$.

Using the first-derivative test with an arbitrary variable x, one has

$$0 = \partial_x \rho = -2\rho f\, \partial_x f\,, \tag{6.7}$$

and therefore

$$f = 0\,, \qquad \text{or} \qquad \partial_x f = 0\,. \tag{6.8}$$

Hence the trajectory $f = 0$ is *included* in the result of the first-derivative test.

The first-derivative test is intuitive and easy to implement. However, it is not covariant under coordinate transformation; moreover, one can construct examples where the test does not give sensible results, see fig. 14b. One may imagine using the eigenvector field of the Hessian $\partial_i \partial_j \rho$ as the "principle directions" and perform a directional derivative test with respect to them. This is the approach in [48].

Unfortunately, the directional derivative test is not practical in higher dimensions, where no generic expression for roots of the algebraic eigenvalue equation exists. In addition, the smoothness of the eigenvector field is difficult to establish. Moreover, upon moving to (pseudo-)Riemannian geometry, one needs to deal with the $(1,1)$-Hessian tensor, which is not symmetric as a matrix, and the analysis is lost in challenging calculations. We now move forward to the other two approaches of ridge-lines.

6.2 Contour ridge-lines

In this section 6.2 we describe the ridge-lines in terms of a certain character of the contour lines. One can imagine finding the *locally most curved neighbourhoods* on the contour lines, the trajectory of which forms a ridge- or dale-line. The defining equation of this approach was first written down by Barré de Saint-Venant in 1852 [148] without derivation. We refer to [48] for a comprehensive explanation.

We will begin with the two-dimensional Euclidean case, where there are two equivalent definitions of the contour ridge-lines, both of which can be generalised to higher dimensions, as well as to (pseudo-)Riemannian geometry. For the "linear" wave-packet in eq. (2.31), the contour approach can directly be applied.

First definition In topography, contour lines give the altitude intrinsically. One can formulate the ridge- and dale-lines in terms of the contour lines as follows [116, sec. 4.1]:

> When representing ridges, contour lines are elongated towards ridge stretch and they are convex as they are turned towards the fall of the ridge or the ground ...

Mathematically, one considers a C^2 real function $\rho(x,y)$, the contour lines γ_c of which are given by the implicit equation $\rho \equiv c$.

Having the idea of "locally most curved neighbourhoods" in the introduction in mind, now let $\kappa(x,y)$ be a *characteristic function*, such that the crossing of a ridge and the contour γ_c is an extremum of κ on γ_c. This gives the first definition of a contour ridge-line, namely *the ridge-line is regarded as the locus of extrema of* κ *under the constraint* $\rho = c$.

The statement can be formulated by the method of Lagrange multipliers,

$$\mathbb{d}\rho = \lambda_c \, \mathbb{d}\kappa \,, \tag{6.9a}$$

$$\rho = c \,, \tag{6.9b}$$

where λ_c is the Lagrange multiplier. Equation (6.9a) can be separated into a system of equations in the bases $\mathbb{d}x$ and $\mathbb{d}y$. Then eliminating λ_c gives

$$0 = \rho_{,x}\kappa_{,y} - \rho_{,y}\kappa_{,x} \,, \tag{6.10}$$

where "," denotes partial derivative [118, eq. (2.25)].

In practice, one can use the squared norm of $\mathbb{d}\rho$ as the characteristic function

$$\kappa = \kappa_{\text{sqr}}(x, y) = \rho_{,x}^2 + \rho_{,y}^2 \,. \tag{6.11}$$

Substituting eq. (6.11) in eq. (6.10) results in the *de Saint-Venant equation for ridges* (dSVr) [97, 148]

$$0 = \rho_{,x}\rho_{,y}\big(\rho_{,x,x} - \rho_{,y,y}\big) - \big(\rho_{,x}^2 - \rho_{,y}^2\big)\rho_{,x,y} \,. \tag{6.12}$$

Second definition To see the mathematical structure more clearly, we use the generalisation of eq. (6.11) in eq. (6.15). Substituting the latter in eq. (6.9a) gives the tensorial equation

$$\rho_{;i} = 2\lambda_c \rho_{;i}{}^{;j} \rho_{;j} \,. \tag{6.13}$$

In other words, $\rho^{;i}$ is an eigenvector of its Hessian $\rho^{;i}{}_{;j}$. This gives the second characteristic of a contour ridge-line: it is *the locus of points where the gradient is an eigenvector of the Hessian.*

Generalisations The results above in two dimensions can easily be generalised to higher dimensional (pseudo-)Riemannian spaces. From eq. (6.9a) one can derive

$$0 = \mathbb{d}\rho \wedge \mathbb{d}\kappa \,, \tag{6.14}$$

which takes the place of eq. (6.10). For eq. (6.11), the generic version reads

$$\kappa_{\text{sqr}} = \star^{-1}(\mathbb{d}\rho \wedge \star\mathbb{d}\rho) = \mathbb{d}\rho^\sharp \lrcorner \, \mathbb{d}\rho = g^{ij}\rho_{;i}\rho_{;j} \,, \tag{6.15}$$

where $\star$ is the Hodge star operator [29, sec. 28], $^\sharp$ is a musical isomorphism, $\lrcorner$ is the interior product or contraction [29, sec. 23], g^{ij} is the inverse metric, and the

symbol ; denotes the covariant derivative with respect to an affine connection [107, sec. 85].

Inserting eq. (6.15) in eq. (6.14) gives the *covariant dSVr equation*

$$0 = \mathbb{d}\rho \wedge \mathbb{d}\big(\mathbb{d}\rho^\sharp \lrcorner \mathbb{d}\rho\big)\,. \tag{6.16}$$

This equation is to be understood as imposing all its components to be zero, and therefore defining an *implicit* curve.

Application to the "linear" wave-packet The contour approach can immediately be applied to the "linear" wave-packet in eq. (2.31). Using the DeWitt metric in eq. (2.1b), the de Saint-Venant equations for ridges (6.16) can be factorised such that

$$0 = y\,, \qquad \text{or} \tag{6.17a}$$
$$0 = x^3\sinh(y)^4 - x^2\cosh(y)\sinh(y)^2 - x\cosh(y)^2 + \cosh(y)\,, \tag{6.17b}$$

where $x > 0$ is given in eq. (2.26b), $y = \sqrt{\frac{3}{2\varkappa}}\, g(\gamma - \gamma_0)$. One can solve x from eq. (6.17b) in terms of y,

$$\begin{aligned} 3x_k &= 1 + 4\cos\frac{2k\pi + \arctan\big[19 - 8\cosh(2y), 3\sqrt{48\cosh(2y) - 33}\big]}{3}\,, \\ k &= 0, 1, 2\,, \end{aligned} \tag{6.18}$$

where $\arctan(x, y)$ gives $\varphi \in [0, 2\pi)$ such that $\cos\varphi = \frac{x}{\sqrt{x^2+y^2}}$, $\sin\varphi = \frac{y}{\sqrt{x^2+y^2}}$.

In eq. (6.18), since

$$\lim_{y\to\infty} \arctan\big[19 - 8\cosh(2y), 3\sqrt{48\cosh(2y) - 33}\big] = \pi\,, \tag{6.19}$$

one obtains

$$\lim_{y\to\infty} x_k = (-)^{k+1}3\,. \tag{6.20}$$

Therefore, the cases $k = 0$ and 2 give positive x and real χ as $\chi \to \infty$, whereas $k = 1$ does not. Exact calculation shows that $x_2 < 0$ for all $y \in \mathbb{R}$, and is to be excluded.

These results are plotted in fig. 13b. One sees a redundant line $y = 0$ that is a dale, a pink line that resembles a classical trajectory, and two further solid lines that converge to the same classical trajectory as $\gamma \to \pm\infty$.

Curvature as the characteristic function In two dimensions, it is tempting and intuitive to use the curvature of the contours as the characteristic function. We argue that this choice will not fit our purpose. Upon generalising to higher dimensions, the curvature of an $(n-1)$-dimensional contour becomes the scalar-valued second fundamental form (see appendix B.1), which is a symmetric tensor. One may want to further analyse this tensor, and study its orthonormal eigenvectors [48].

Unfortunately, for the cases where the (DeWitt) metric is indefinite (e.g. Lorentzian), the second fundamental form is defined differently for the time- and space-like patches [3, sec. 1.2.4], which discontinues at the null edge, where the second fundamental form is again defined differently [101]. The reason is that, for time- and space-like hypersurfaces, the second fundamental form depends on the choice of a unit normal vector, which of course discontinues going from a time-like patch to a space-like patch. Moreover, the eigenvectors of the second fundamental form may also not exist ([3, sec. 2.5.(2)]).

The contour ridge-line is based on first- and second-derivatives of ρ and always give equations for an algebraic curve. However, aside from sensible ridge-lines, this approach also gives counter-intuitive curves. Examples, further properties and comments about the contour approach will be given in sections 6.4 and 6.5.

6.3 Stream ridge-lines

Now we consider the ridges in terms of *singular* stream-lines of the gradient vector field, which dates back to Rudolf Rothe in 1915 [145]. Heuristically, one imagines that water slowly flows from the top of a hill along the stream-lines of the gradient vector field. The water stream diverges from a ridge and converges to a dale. This is the intuitive notion of the singularity of the stream-lines along ridge- and dale-lines.

The stream approach is also adapted by modern computer scientists in image processing and computer vision [97, 98]. The mathematics behind this approach is the inverse integral factor and inverse Jacobi multiplier, which work for two- and higher-dimensional cases, respectively [19, 59]. We will focus on the two-dimensional case.

Inverse integral factor In $\mathbb{R}^2$ with Cartesian coordinates (x, y), the contours of ρ are defined by $\mathbb{d}\rho = 0$, or $\rho = c$; dual to them are the stream-lines, characterised by $\mathbb{d}w = 0$ or $w = c$, where

$$\theta\, \mathbb{d}w = \star \mathbb{d}\rho = -\rho_{,y}\, \mathbb{d}x + \rho_{,x}\, \mathbb{d}y\,, \tag{6.21}$$

in which θ compensates the non-integrability of the right-hand side and is therefore called an *inverse integral factor*. One also has

$$0 = \rho_{,x} w_{,x} + \rho_{,y} w_{,y} = \star^{-1}(\mathrm{d}\rho \wedge \star \mathrm{d}w)\,. \tag{6.22}$$

(θ, w) is unique up to

$$\theta \to \theta / F'(w)\,, \qquad w \to F(w)\,, \tag{6.23}$$

where $F(w)$ is an arbitrary function. One may worry that this arbitrariness renders the stream approach not giving definite results, which fortunately does not seem to be the case, see section 6.4.

One sees that if $\theta = 0$ and $\rho_{,x} \neq 0 \neq \rho_{,y}$ at (x_0, y_0), w cannot be expanded by the Taylor theorem at (x_0, y_0), since the linear term blows up by eq. (6.21) [145, sec. 7]. (x_0, y_0) is said to be on a *singular stream-line*.

One can imagine that if the ridge- and dale-lines are required also to be stream-lines themselves, then the neighbouring stream-lines converge to the former, and diverge from the latter along the direction of the gradient vector field. In other words, *stream ridge- and dale-lines are singular stream-lines*. It has been shown that along these stream-lines, one has [59]

$$\theta(x, y) = 0\,. \tag{6.24a}$$

The integrability condition $\mathrm{d} \wedge \mathrm{d}w = 0$, or $w_{,x,y} = w_{,y,x}$, gives the differential equation for θ,

$$\rho_{,x}\theta_{,x} + \rho_{,y}\theta_{,y} = \big(\rho_{,x,x} + \rho_{,y,y}\big)\theta\,. \tag{6.24b}$$

Equations (6.24a) and (6.24b) define the stream ridge- and dale-lines.

Generalisations The results above in two dimensions can readily be generalised to n-dimensional curved spaces. Consider local coordinates $(x^1, \ldots, x^n)$, $n \geq 2$. The gradient vector field v of ρ is given by

$$v^i\, \partial_i \equiv v = \mathrm{d}\rho^\sharp := g^{ij} f_{,j} \partial_i\,. \tag{6.25}$$

One has $(n-1)$ linearly independent w's for the stream-lines, satisfying

$$0 = v^i\, \partial_i w = v(w)\,, \tag{6.26}$$

which is the generalisation of eq. (6.22). They are nothing else but the $(n-1)$ first integrals [8], that require $(n-1)$ inverse integral factors θ.

Similar to eq. (6.21), one has for instance

$$\theta \, \mathbb{d}w = v^1 \, \mathbb{d}x^j - v^j \, \mathbb{d}x^1 \,, \qquad 2 \leq j \leq n \,, \tag{6.27}$$

given $v^i \neq 0, 1 \leq i \leq n$. All of the θ's satisfying the linear, first-order partial differential equation

$$v^i \theta_{,i} = \theta v^i{}_{;i} \,, \qquad \text{or} \qquad v \lrcorner \, \mathbb{d}\theta = \theta \, \mathbb{d}^\dagger v^\flat \,, \tag{6.28}$$

where $\mathbb{d}^\dagger$ is the codifferential or the adjoint [29, sec. 29]. The solutions to eq. (6.28) are called *inverse Jacobi multipliers* [19], first appeared in [81].

For Riemannian geometry, the stream approach seems to always give sensible results, in contrast with the contour approach and the simple first-derivative test. However, the approach involves giving the *general integral* [54, sec. 3.1.2] of the partial differential equation (6.26) or (6.28), which is only possible in very limited cases. Moreover, Lorentzian geometry gives rise to counter-intuitive configurations of gradient *vector* fields, where the time-like component of the gradient one-form fields is flipped. This leaves us problems that are yet to be solved. See sections 6.4 and 6.6.

6.4 Relations of the contour and stream approaches

In this section 6.4 we compare the contour and stream approaches, as well as argue against the first-derivative test. Much of the material is adapted from [97, 145].

The contour and stream ridge-lines can be derived on the same footing. In $\mathbb{R}^2$, from $\mathbb{d}\rho = \rho_{,x} \, \mathbb{d}x + \rho_{,y} \, \mathbb{d}y$, eqs. (6.11) and (6.21), one deduces that [145, sec. 5]

$$\frac{1}{2} \, \mathbb{d}\kappa_{\text{sqr}} = R \, \mathbb{d}\rho + \theta S \, \mathbb{d}w \,, \tag{6.29}$$

where

$$R := \frac{\rho_{,x}^2 \rho_{,x,x} + 2\rho_{,x}\rho_{,y}\rho_{,x,y} + \rho_{,x}^2 \rho_{,y,y}}{\kappa_{\text{sqr}}^2} \,, \tag{6.30a}$$

$$S := \frac{\rho_{,x}\rho_{,y}\big(\rho_{,x,x} - \rho_{,y,y}\big) - \big(\rho_{,x}^2 - \rho_{,y}^2\big)\rho_{,x,y}}{\kappa_{\text{sqr}}^2} \,. \tag{6.30b}$$

Imposing κ_{sqr} to be stationary in the direction of w gives

$$0 = \frac{1}{2} \frac{\partial \kappa_{\text{sqr}}}{\partial w} = \theta S \,, \tag{6.31}$$

which gives either $\theta = 0$ or $S = 0$; they corresponds to the contour and stream ridge-lines defined in eqs. (6.12) and (6.24a), respectively.

The contour and stream ridge-lines are distinct, except for two special cases. Breton de Champ (see [145, sec. 2]) has shown that, *stream-lines* satisfying $S = 0$ are *necessarily straight lines*; otherwise, contour ridge-lines should not be stream-lines, and they are therefore no stream ridge-line. However, it seems to us that points satisfying $\rho_{,x} = \rho_{,y} = 0$ also lie on both the contour and stream ridge-lines, see sections 6.5 and 6.6 for an example.

The differences, of the contour and stream ridge-lines, as well as the simple first-derivative test, can be shown with a so-called two-dimensional *helicoidal gutter* [97, sec. 6]; in polar coordinates (ϱ, φ) the metric and the gutter are

$$\begin{aligned} \mathbb{d}s^2 = g_{ij}\,\mathbb{d}x^i\,\mathbb{d}x^j = \mathbb{d}\varrho^2 + \varrho^2\,\mathbb{d}\varphi^2\,, \\ \varrho > 0\,, \quad 0 \leq \varphi < 2\pi\,; \end{aligned} \tag{6.32a}$$

$$\rho(\varrho, \varphi) = \varphi - \frac{1}{2}\left(\frac{\varrho}{\varrho_0} - 1\right)^2\,, \tag{6.32b}$$

see fig. 14.

The contour ridge-lines of eq. (6.32b) are given by the dSVr equation, or $S = 0$ in eq. (6.30b). From the covariant expression in eq. (6.16), one derives

$$0 = \left(\frac{\varrho}{\varrho_0}\right)^4 - \left(\frac{\varrho}{\varrho_0}\right)^3 - 1\,. \tag{6.33}$$

The only positive root reads

$$\frac{\varrho}{\varrho_0} \approx 1.380\,28\,. \tag{6.34}$$

See fig. 14a. Roughly speaking, it crosses the contours where the latter are curved more.

As for the stream ridge-lines, using eq. (6.26) yields the equation for w

$$\mathbb{d}\rho^\sharp \lrcorner\, \mathbb{d}w = 0\,, \qquad \text{or} \qquad 0 = \rho_{,i} g^{ij} w_{,j} = \left(\frac{\varrho}{\varrho_0} - 1\right)\frac{w_{,\varrho}}{\varrho_0} + \frac{w_{,\varphi}}{\varrho^2}\,. \tag{6.35}$$

The general integral to eq. (6.35) reads

$$w = F\left(-\frac{\varrho_0}{u} + \varphi - \ln\left(1 - \frac{\varrho_0}{\varrho}\right)\right)\,, \tag{6.36}$$

where F is an arbitrary function, see eq. (6.23). In order to obtain θ, one applies

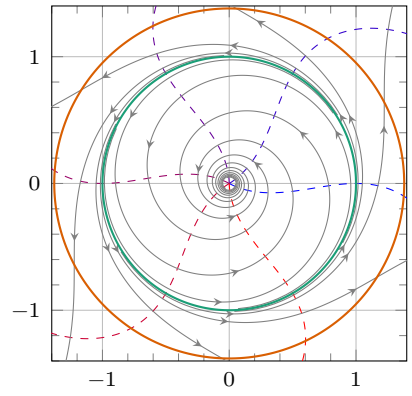

(a) Contour and stream ridge-lines

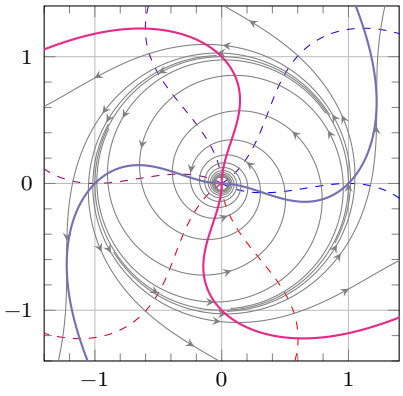

(b) First-derivative lines

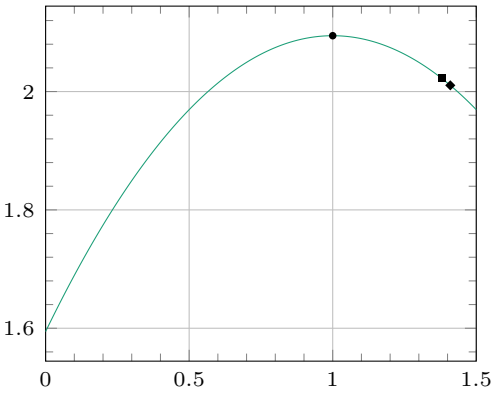

(c) Section at $\varphi = 2\pi/3$

Figure 14: The so-called helicoidal gutter in eq. (6.32b), its contours (dashed lines) and gradient vector field (represented by the grey stream-lines with arrows), and its ridge-lines. In fig. 14a, the green line is the stream ridge-line given by $\theta = 0$, and the orange line is the contour ridge-line predicted by the dSVr equation. In fig. 14b, the pink and the purple lines are $\rho_{,x} = 0$ and $\rho_{,y} = 0$, respectively. In fig. 14c, the section at $\varphi = 2\pi/3$ is plotted, where the round, square and diamond points are the stream and contour ridge-lines, as well as the first-derivative line. One sees that it is the *stream ridge-line* that picks the highest point in the sense of constant φ-section.

eq. (6.21)

$$\theta \, \mathbb{d}w = \star \mathbb{d}\rho = -\frac{\rho_{,\varphi}}{\varrho} \, \mathbb{d}\varrho + \varrho \rho_{,\varrho} \, \mathbb{d}\varphi \, . \tag{6.37}$$

The result is

$$\theta = \frac{\varrho}{\varrho_0} \left(\frac{\varrho}{\varrho_0} - 1 \right) \left\{ F' \left(-\frac{\varrho_0}{\varrho} + \varphi - \ln\left(1 - \frac{\varrho_0}{\varrho} \right) \right) \right\}^{-1} . \tag{6.38}$$

The stream ridge-lines are then given by $\theta = 0$, or

$$\varrho = \varrho_0 \, . \tag{6.39}$$

See fig. 14a. One sees that the arbitrariness of w encoded in F does *not* affect the effectiveness of the stream approach. Furthermore, the stream ridge-line really marks the highest point for a constant φ-section. As a stream-line by itself, the stream ridge-line is also a limit cycle [8, sec. 1.6.3] of the gradient vector field, and is also a watershed for two distinct families of stream-lines, one spirals inwards and another outwards. The contour ridge-line, on the other hand, is close to the highest point, see fig. 14b.

Finally, the curves given by the first-derivative test with respect to (x, y) can also be easily worked out, see fig. 14b. They do not respect the rotational symmetry of ρ and is therefore not very sensible. One may argue for an alternative test with respect to (ϱ, φ), but the choice itself cannot be arbitrary and needs a mathematical description, which renders the method losing its simpleness.

6.5 Aspects of the contour approach

In this section 6.5 we first establish a scenario with an exponential wave-packet, in which the contour approach gives intuitive results. We then generalise this scenario with a slowly varying amplitude and show that an intuitive result is still contained in the result. We show how the redundant results can be identified with a toy example.

Invariance under regular transformation and applications For a transformation $\rho \to F \circ \rho$, the dSVr equation (6.16) transforms to

$$0 = \left(\frac{\mathbb{d}F}{\mathbb{d}\rho} \right)^3 \mathbb{d}\rho \wedge \mathbb{d}\big(\mathbb{d}\rho^\sharp \lrcorner \, \mathbb{d}\rho \big) \, . \tag{6.40}$$

If F is strictly monotonic, i.e. $\mathbb{d}F/\mathbb{d}\rho \neq 0$, the extra factor is non-zero, and eq. (6.40) gives the same ridge-line as eq. (6.16).

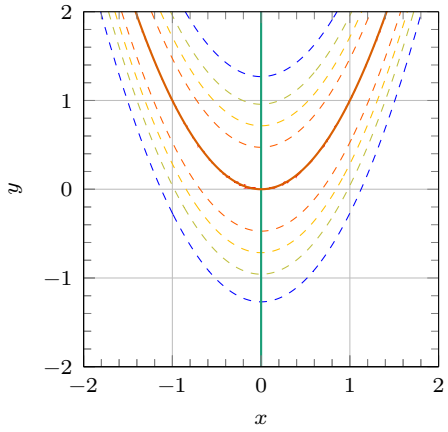

Figure 15: Density function $\rho = \mathsf{e}^{-(y-x^2)^2}$ and the contour ridge-lines, which are $x = 0$ (green, ridge-line for $y < 0$ and dale-line for $y > 0$) and $y = x^2$ (orange). Incidentally, these lines are also given by the first-derivative test $\rho_{,x} = 0$, $\rho_{,y} = 0$.

Now we move back to the two-dimensional wave-packet

$$\rho = \mathsf{e}^{-f^2} \,. \tag{6.6 revisited}$$

Since e^x increases monotonically with respect to x, applying the above-mentioned property gives the ridge-line

$$\begin{aligned} 0 &= \mathrm{d}(f^2) \wedge \mathrm{d}\Big(\mathrm{d}(f^2)^\sharp \lrcorner\, \mathrm{d}(f^2)\Big) \\ &= 8f^3\, \mathrm{d}f \wedge \mathrm{d}\big(\mathrm{d}f^\sharp \lrcorner\, \mathrm{d}f\big)\,, \end{aligned} \tag{6.41}$$

which means

$$0 = f \qquad \text{or} \tag{6.42a}$$

$$0 = \mathrm{d}f \wedge \mathrm{d}\big(\mathrm{d}f^\sharp \lrcorner\, \mathrm{d}f\big)\,. \tag{6.42b}$$

Equation (6.42a) gives what we wanted to set up, whereas eq. (6.42b) gives the ridge- (or dale-)line of f itself.

This is easier to see with the toy example

$$f(x, y) = y - x^2\,, \tag{6.43}$$

so that $f = 0$ gives the parabola $y = x^2$. There is an additional solution to the dSVr equation, $x = 0$, satisfying eq. (6.42b). See fig. 15.

The parabola $y = x^2$ is what we wanted. However, we also get $x = 0$, which is a dale-line for the density function $f = y - x^2$; as for $\rho = \mathsf{e}^{-f^2}$, it is a ridge-line for $y < 0$, and a dale line for $y > 0$. This line is a concrete mathematical result,

although it does not fit our expectation.

Modulation and redundant lines The results for the wave-packet in eq. (6.6) can be generalised to the narrow wave-packet with varying amplitude

$$\rho(x,y) = g(x,y)\mathsf{e}^{-\frac{f(x,y)^2}{2\sigma^2}}\,, \tag{6.44}$$

where σ is a constant, $\sigma \ll |\nabla g|$ characterising the narrowness, and g is a modulation. Substituting eq. (6.44) into eq. (6.12) gives

$$0 = g^3 f^3\big(p_f q_f(r_f - t_f) - \big(p_f^2 - q_f^2\big)s_f\big) + O(\sigma^2)\,, \tag{6.45}$$

where $\big(p_f, \dots, t_f\big)$ are the symbols with respect to f.

As $\sigma \to 0^+$, the wave-packet becomes sharper and sharper; except for an additional factor g^3, the leading-order dSVr equation recovers the case without modulation. At the limit $\sigma = 0^+$, the wave-packet becomes a wall with zero width, and extends along the classical trajectory $f = 0$. Equation (6.45) shows that a slow modulation does not drastically change the ridge-lines.

The narrow WKB Gaussian wave-packets in section 3.5 is an instance of this model. The heuristic arguments we used in that section can now be replaced with the derivation in eq. (6.45).

Exact calculation reveals that the approximation we used to derive eq. (6.45) loses details. To see this, we also modulate eq. (6.43) by

$$g = \mathsf{e}^{-2\epsilon y}\,, \qquad \epsilon = \frac{1}{2}, \frac{1}{10}\,. \tag{6.46}$$

The dSVr equation for $\rho = g\,\mathsf{e}^{-(y-x^2)^2}$ with g given in eq. (6.46) reads

$$\begin{aligned} 0 = 16x[&-2y^3 + 2y^2(3x^2 - \epsilon) + y(-6x^4 + 8\epsilon x^2 + \epsilon) \\ &+ 2x^6 - 6\epsilon x^4 - \epsilon x^2 + \epsilon^2]\,, \end{aligned} \tag{6.47}$$

which has been factorised into $x = 0$, and a term cubic in y. One can solve y in terms of x from the factor in a square bracket, where the three roots $y = y(x)$ are all real. See fig. 16.

Only one of the three roots approaches $y = x^2$ as $x \to \infty$. This can be seen by expanding $y(x) - x^2$ at $\epsilon = 0^+$, which yields

$$y_{1,2}(x) - x^2 = \mp\sqrt{\frac{1+4x^2}{2}}\epsilon^{1/2} + \left(-1 + \frac{1}{1+4x^2}\right)\frac{\epsilon}{2} + O\big(\epsilon^{3/2}\big)\,, \tag{6.48a}$$

$$y_3(x) - x^2 = -\epsilon\frac{1}{1+4x^2} + O(\epsilon^2)\,. \tag{6.48b}$$

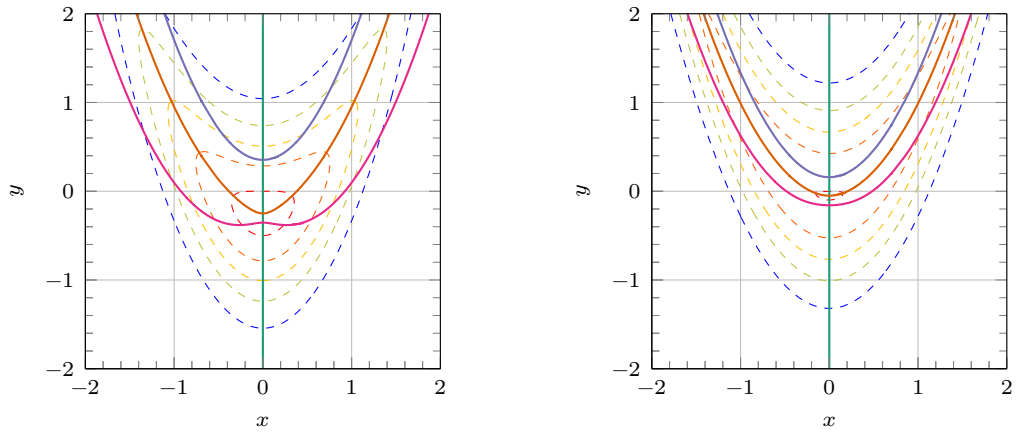

(a) $\rho = \mathsf{e}^{-(y-x^2)^2-y/2}$ (b) $\rho = \mathsf{e}^{-(y-x^2)^2-y/10}$

Figure 16: Density function $\rho = g\,\mathsf{e}^{-(y-x^2)^2}$ and the contour ridge-lines for $g = \mathsf{e}^{-y/2}$ and $g = \mathsf{e}^{-y/10}$ with a Euclidean metric. The green line $x = 0$ and the orange line are (qualitatively) the same as in fig. 15; however, the dSVr equation (6.16) also gives the purple and the pink lines, which are apparently neither ridge- nor dale-lines.

As $x \to \pm\infty$, $y_3 - x^2$ converges to 0, whereas $y_{1,2} - x^2$ diverge, and can be interpreted as the locus of the "locally flattest places on the contour", resembling $x = 0$ for $y = x^3$.

The extra curves in eq. (6.48a) seem to be a common feature of the dSVr equation. Here we have managed to remove them by asymptotic analysis at infinity, recovering the intuitive result y_3. The extra line $x = 0$ has been discussed at the end of the last part.

Two-dimensional hydrogen atom revisited The binomial stationary wave-packets of two-dimensional hydrogen atom, described in section 5.2, can also be studied by the contour approach. For $n = 1$, the dSVr equation is a sextic equation with respect to the dimensionless radial coordinate ξ, which has a quadratic and

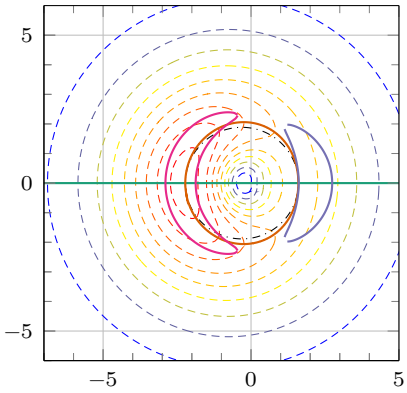

Figure 17: Stationary wave-packet $\left|\Psi_{1,\frac{23}{24}}(\xi,\varphi)\right|^2$ of the two-dimensional hydrogen atom with $n=1$, $q=\frac{23}{24}$. See section 5.2 for details. The thick lines with colour are solutions of the dSVr equation, whereas the dash-dotted line is the "best-fit trajectory" that crosses the maxima, adapted from the orange line in fig. 11b. The discontinuities within the same color are a numerical artefact.

a quartic factor

$$
\begin{aligned}
0 = {} & -x^2\left(\sqrt{\dots}\cos\varphi - 1\right)^2 \\
& + x\left(\sqrt{\dots}^2\cos(2\varphi) + 3\sqrt{\dots}^2 - 6\sqrt{\dots}\cos\varphi + 2\right) \qquad (6.49a) \\
& + \sqrt{\dots}\left(2\cos\varphi - 3\sqrt{\dots}\right), \qquad \text{or} \\
0 = {} & +4x^4\left(\sqrt{\dots}\cos\varphi - 1\right)^3 \\
& + x^3\Big[-4\sqrt{\dots}^3\cos(3\varphi) + 30\sqrt{\dots}^2\cos(2\varphi) \\
& \qquad - 4\left(5\sqrt{\dots}^2 + 16\right)\sqrt{\dots}\cos\varphi + 38\sqrt{\dots}^2 + 20\Big] \\
& + x^2\Big\{6\sqrt{\dots}\Big[+2\left(3\sqrt{\dots}^2 + 8\right)\cos\varphi \qquad (6.49b) \\
& \qquad\qquad - 5\sqrt{\dots}\cos(2\varphi)\Big] - 74\sqrt{\dots}^2 - 28\Big\} \\
& + 4x\left[-2\left(3\sqrt{\dots}^2 + 4\right)\sqrt{\dots}\cos\varphi + 13\sqrt{\dots}^2 + 2\right] \\
& - 12\sqrt{\dots}^2,
\end{aligned}
$$

where $\sqrt{\dots} := \sqrt{1-q^2}$. We are therefore able to obtain solutions in terms of roots. Aside from $\sin\varphi = 0$, there are six solution $\xi = \xi(\varphi)$, three in which are real and positive near $\varphi = 0$ and $\varphi = \pi$; one is from the quadratic factor and has a simple form, while the other two are very complicated. We managed to plot them in fig. 17.

One sees that the orange ridge given by the dSVr equation is very close to the "best-fit trajectory" that passes through the maxima of the wave-packet. Like in the case $\rho = g\,\mathrm{e}^{-f^2}$, there are two additional lines, which might be the locally flattest points of the contours.

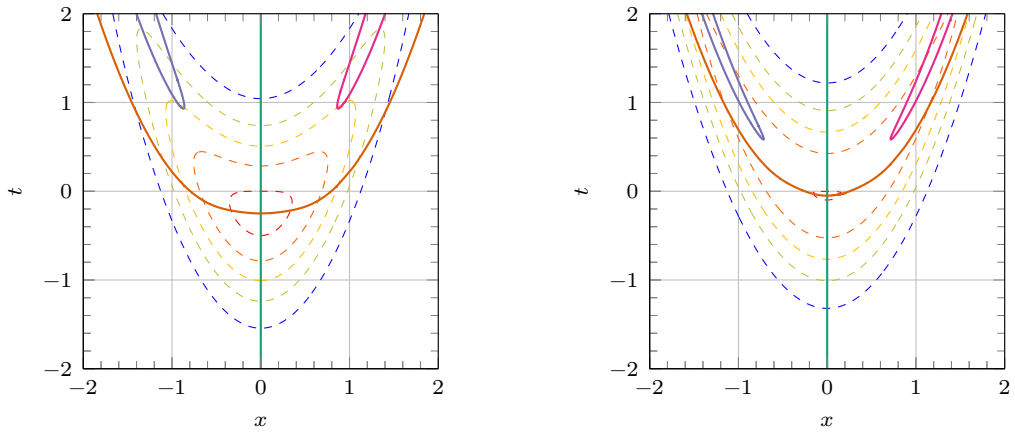

(a) $\rho = \mathsf{e}^{-(t-x^2)^2-t/2}$ (b) $\rho = \mathsf{e}^{-(t-x^2)^2-t/10}$

Figure 18: Density function $\rho = g\,\mathsf{e}^{-(t-x^2)^2}$ and the contour ridge-lines for $g = \mathsf{e}^{-t/2}$ and $g = \mathsf{e}^{-t/10}$ with an Lorentzian metric (6.50). The green line $x = 0$ is the same as in figs. 15 and 16. The orange line fits intuition better near $x = 0$, whereas the other two lines both have a sharp turning point, and one of the branches fits the intuitive ridge in the asymptotic region.

Lorentzian signature In quantum cosmology, the minisuperspace DeWitt metric usually has a Lorentzian signature. For the Lorentzian metric

$$\mathbb{d}s^2 = -\mathbb{d}t^2 + \mathbb{d}x^2\,, \tag{6.50}$$

the Lorentzian dSVr, according to eq. (6.16), reads

$$0 = -\rho_{,x}\rho_{,t}\big(\rho_{,x,x} + \rho_{,t,t}\big) + \big(\rho_{,x}^2 + \rho_{,t}^2\big)\rho_{,x,t}\,. \tag{6.51}$$

In fig. 13b, we have already shown a sensible result with contour ridge-lines in a Lorentzian signature.

For the $\rho = g\,\mathsf{e}^{-f^2}$ model, we can also mimic the scenario by replacing $y \to t$ in eqs. (6.43) and (6.46), and using the metric in eq. (6.50). The result can still be factorised to $x = 0$ and a cubic algebraic equation with respect to t, see fig. 18.

Intriguingly, *none* of the three curves given by the latter factor lies on the intuitive ridge globally; instead, for the turning and asymptotic regions, there is one branch for each case that fits well with intuition.

Summary The contour approach to ridge-lines, which dates back to Barré de Saint-Venant in 1852, gives us an implicit equation (6.16) that can readily be plotted. It may not give results that are directionally minimal, but the difference can be small, see fig. 14c.

The curves given by the dSVr equations are typically higher-order algebraic

equations, which can at least be numerically solved. For the "linear" wave-packet, as well as for narrow Gaussian WKB wave-packets, this approach gives sensible results, as discussed in section 6.2 and earlier in this section.

With a Euclidean signature, redundant curves can appear, as we have seen in this section with the modulated toy model $\rho = g\,\mathsf{e}^{-f^2}$, as well as with the two-dimensional hydrogen atom, that may arise from the fact that the dSVr equations collect not only the most convex and concave neighbourhoods, but also the flattest points. For the toy model, the redundant lines can be removed by careful asymptotic analysis, leaving results that also fit intuition.

As for the Lorentzian signature, however, it can happen that no result fully agrees with intuition, as we have seen in the modulated toy model. We have to decide whether to believe in mathematics and abandon our intuition, or stick to the intuition and find a better mathematical description.

Finally, an algorithm is needed to find the contour ridge-lines for numerically constructed wave-packets, like in section 4.5. This is to be investigated in the future.

6.6 Aspects of the stream approach

In this section 6.6 we first examine two families of density function, for which the stream ridge-lines can be exactly solved. We then show that the toy model $\rho = \mathsf{e}^{-(y-x^2)^2}$ introduced in section 6.5 belongs to one of the families. In the end we investigate the cases with a Lorentzian metric signature.

Stream ridge-lines of two function families For density functions of the following two forms

$$\rho(u,v) = f(f^u(u) + f^v(v))\,, \tag{6.52a}$$

$$\rho(u,v) = f(f^u(u) f^v(v)) \tag{6.52b}$$

with the metric

$$\begin{aligned} \mathbb{d}s_1^2 &= h(u,v)^2(g\,\mathbb{d}u^2 + \mathbb{d}v^2)\,, \\ g &= \pm\,, \qquad h(u,v) > 0 \end{aligned} \tag{6.53}$$

the stream-lines of the gradient vector field can be exactly solved. Note that for the Euclidean signature $g = +$, eq. (6.53) includes the bipolar, Cartesian, elliptic and planar parabolic coordinates for the flat geometry, and the stereographic coordinates for the spherical geometry, so that it is quite comprehensive. The

Hodge-stars of the coordinate differentials read

$$\star \mathbb{d}u = g\, \mathbb{d}v\,, \qquad \star \mathbb{d}v = -\mathbb{d}u\,; \tag{6.54}$$

one therefore gets

$$\theta\, \mathbb{d}w = \star \mathbb{d}\rho = -\rho_{,v}\, \mathbb{d}u + g\rho_{,u}\, \mathbb{d}v\,. \tag{6.55}$$

By using eqs. (6.22), (6.53) and (6.54), one obtains for eq. (6.52a)

$$w = F\bigg(-g\int^u \frac{\mathbb{d}\mu}{f^{u\prime}(\mu)} + \int^v \frac{\mathbb{d}\nu}{f^{v\prime}(\nu)}\bigg) \tag{6.56a}$$

$$\theta = -\frac{1}{F'} f' f^{u\prime}(u) f^{v\prime}(v)\,, \tag{6.56b}$$

and for eq. (6.52b)

$$w = F\left(-g\int^u \frac{\mathbb{d}\mu}{\big(\ln f^u(\mu)\big)'} + \int^v \frac{\mathbb{d}\nu}{\big(\ln f^v(\nu)\big)'}\right) \tag{6.57a}$$

$$\theta = -\frac{1}{F'} f' f^{u\prime}(u) f^{v\prime}(v) \tag{6.57b}$$

Curiously, both eqs. (6.56b) and (6.57b) includes the result from the first-derivative test, $\rho_{,u} = 0$ or $\rho_{,v} = 0$.

Application to the toy model The toy model $\rho = \mathsf{e}^{-(y-x^2)^2}$ in section 6.5 has the form of eq. (6.52a). One can adapt the results in eqs. (6.56a) and (6.56b) and get

$$w = F\Big(gy + \frac{1}{2}\ln x\Big)\,, \tag{6.58a}$$

$$\theta = 4g\mathsf{e}^{-(y-x^2)^2}\frac{x(y-x^2)}{F'\big(gy + \frac{1}{2}\ln x\big)}\,. \tag{6.58b}$$

See fig. 19. The Lorentzian results are to be understood with y having the negative signature in the Minkowski metric. Equation (6.58b) gives the same ridge-lines as in the contour approach, as well as in the first-derivative test, $y = x^2$ and $x = 0$.

Now we move to the modulated toy model $\rho = g(x,y)\,\mathsf{e}^{-(y-x^2)^2}$. Using $g_\epsilon = \mathsf{e}^{-2\epsilon y}$, eq. (6.35) becomes

$$g(-x^2 + y + \epsilon)w_{,y} + 2x(x^2 - y)w_{,x} = 0. \tag{6.59}$$

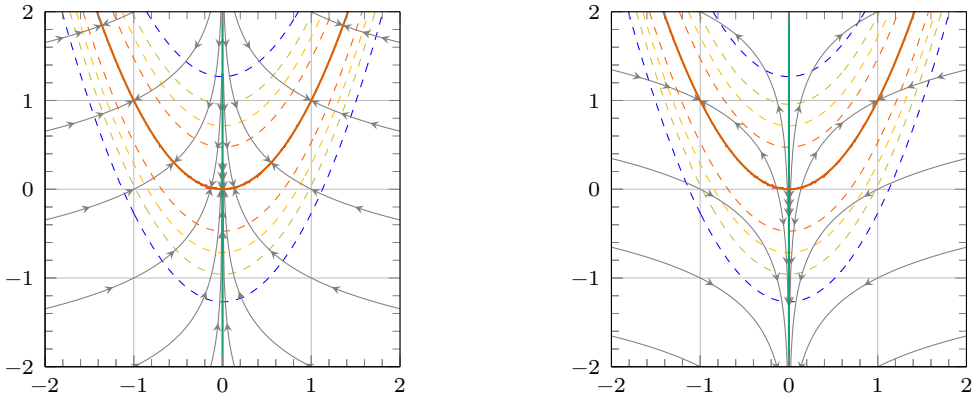

(a) Euclidean signature $g = +$ (b) Lorentzian signature $g = -$

Figure 19: Density function $\rho = \mathsf{e}^{-(y-x^2)^2}$, the stream-lines of the gradient vector field in both Euclidean and Lorentzian geometry, and the stream ridge-lines which are $x = 0$ (green) and $y = x^2$ (orange). The Lorentzian results are to be understood with y having the negative signature in the Minkowski metric.

For $\epsilon \ll 1$, one uses the series test solution

$$w = \sum_{n=0}^{\infty} w_n \epsilon^n \qquad \text{with} \qquad w_0 = F\Big(gy + \frac{1}{2}\ln x\Big)\,, \tag{6.60}$$

and for $n \geq 0$,

$$(y - x^2)\big(2gx\partial_x w_{n+1} - \partial_y w_{n+1}\big) = \partial_y w_n\,. \tag{6.61}$$

On the other hand,

$$\theta = g\frac{\rho_{,x}}{w_{,y}} = -\frac{\rho_{,y}}{w_{,x}}, \tag{6.62}$$

where ρ can also be expanded with respect to ϵ, i.e.

$$\rho = \rho_0 \sum_{n=0}^{+\infty} \left(1 + \frac{\epsilon^n}{n!}\,\frac{\partial^n \mathsf{e}^{-2\epsilon y}}{\partial \epsilon^n}\bigg|_{\epsilon=0}\right), \qquad \rho_0 = \mathsf{e}^{-(y-x^2)^2}. \tag{6.63}$$

This implies that $\theta \propto \partial_x \rho_0 \propto x(y - x^2)$.

We failed to obtain a general integral w for the modulated toy model $\rho = g\,\mathsf{e}^{-(y-x^2)^2}$. Numerically integrated stream-lines of the gradient vector field are plotted in fig. 20. One sees that for the Euclidean signature, the stream-lines indicate the fastest up-hill direction, in which the singular stream-lines are ridge- or dale-lines that fit the intuition. Moreover, the dash-dotted orange line $y = x^2$ is a good approximation of the actual ridge-line for small ϵ (fig. 20b), but fails for larger ϵ (fig. 20a); in other words, there are non-perturbative effects that cannot

be revealed by the perturbative analysis above.

With the Lorentzian signature shown in figs. 20c and 20d, things become more complicated. The above-mentioned property, that the gradient vector field points to the up-hill direction, is lost. Furthermore, the apparent ridge in the plot is no longer accompanied by a possible singular stream-line; instead, on the plot one sees a series of turning points that could play the role of indicating a ridge-line that also fits human cognition.

Numerical applications to other models As mentioned before, the stream approach is difficult to obtain analytic results. For the two-dimensional hydrogen atom and the "linear" wave-packet that were studied before, we make numeric plots of the stream-lines of the gradient vector fields, see fig. 21.

One sees again the good quality in the case with a Euclidean signature in fig. 21a, that no counter-intuitive lines are present. There seems to be a singular stream-line that is very close to the "best-fit" classical trajectory. For the Lorentzian geometry, the "best-fit" classical trajectory lies again near the "turning points" of the stream-lines, instead of being near a singular stream-line.

Summary The stream approach to ridge-lines, which dates back to Rudolf Rothe in 1915, tells us to solve for a generic first integral w of the gradient vector field from eq. (6.22), so that an inverse integral factor θ can be calculated, and $\theta = 0$ gives the singular stream-lines, that define the stream ridge-lines. As has been shown with fig. 14c, it can give results that are also directionally minimal.

With the Euclidean signature, the directions of the gradient vector field give the fastest ascent. The stream approach here gives results that agree with intuitive expectations, and no redundant lines appear except for those given by symmetries. We have shown this with the helicoidal gutter, as well as the toy model $\rho = \mathsf{e}^{-f^2}$ analytically; numerically, the modulated toy model $\rho = g\,\mathsf{e}^{-f^2}$ as well as the two-dimensional hydrogen atom also seem to perform pretty well under this approach.

As for the Lorentzian signature, the singular stream-lines of the gradient vector field do not seem to agree with the intuitive ridge-lines, as we have seen in the numeric results of the "linear" wave-packet in fig. 21b. The reason is that, for Lorentzian geometry, the directions of the gradient vector field differ from those of the gradient one-form field, and the former field no longer points to the direction of the fastest ascent. One can either discard intuition and embrace what mathematical generalisation gives, or invent a novel notion of ridge-lines, keeping in mind that this new notion is also to work with the Euclidean case.

Finally, an algorithm is needed to find the singular ridge-lines for an analytically given gradient vector field, since the generic first integral is difficult to solve.

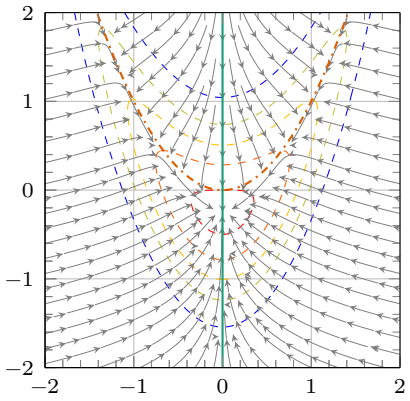

(a) $\rho = \mathsf{e}^{-(y-x^2)^2 - y/2}$

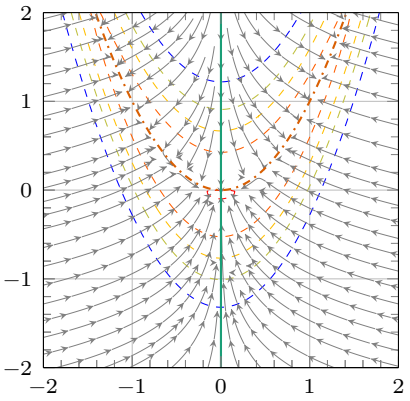

(b) $\rho = \mathsf{e}^{-(y-x^2)^2 - y/10}$

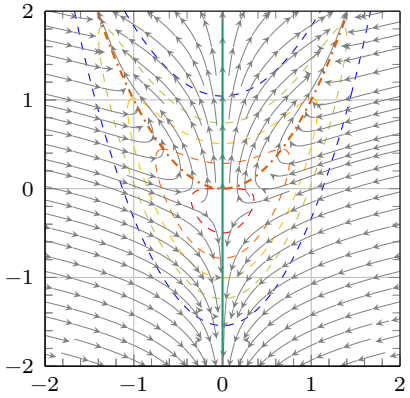

(c) $\rho = \mathsf{e}^{-(t-x^2)^2 - t/2}$

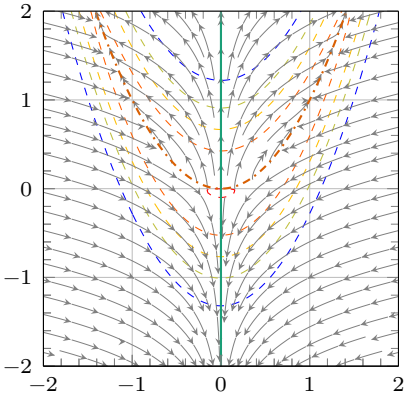

(d) $\rho = \mathsf{e}^{-(t-x^2)^2 - t/10}$

Figure 20: Density function $\rho = g\,\mathsf{e}^{-(y-x^2)^2}$ and the contour ridge-lines for $g = \mathsf{e}^{-y/2}$ and $g = \mathsf{e}^{-y/10}$ with the Euclidean and Lorentzian metrics. The green solid line $x = 0$ remains a ridge-dale-line, whereas the orange dash-dotted line is merely an approximation in the Euclidean case; the actual singular stream-lines seem to be under the orange lines. The stream ridge-line in the Lorentzian signature is apparently more intriguing.

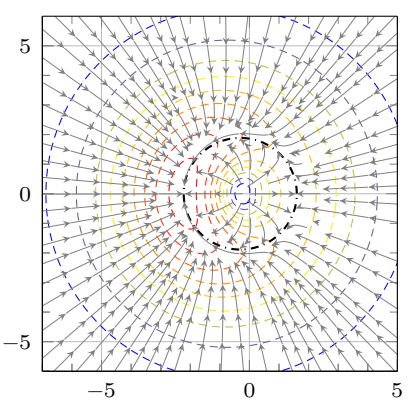

(a) 2d hydrogen atom $\Psi_{1,\frac{23}{24}}$

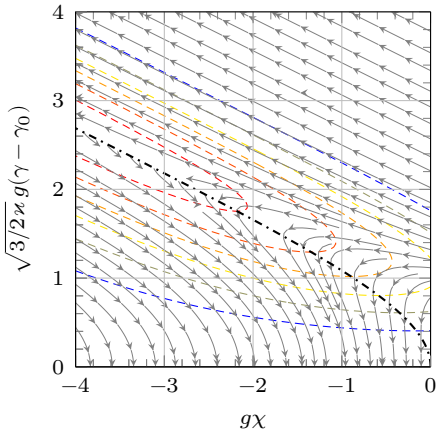

(b) "Linear" wave-packet

Figure 21: Numerical results of stream ridge-lines for the two-dimensional hydrogen atom 21a and the "linear" wave-packet 21b. In fig. 21a, the geometry is Euclidean, and the dash-dotted line is the "best-fit" classical elliptic trajectory, passing through the maxima of the stationary wave-packet. In fig. 21b, the geometry is Lorentzian, and the dash-dotted line is the "best-fit" trajectory used before.

Moreover, for the cases where wave-packets are already constructed numerically, another algorithm is needed to find the singular ridge-lines from the numerically given gradient vector field.

6.7 Prospective applications

The systematics of ridge-lines enables us to *calculate* the classical trajectories that emerge from a quantum wave-packet.

In fig. 13, for example, one sees three trajectories, one of which coincides or is close to a classical trajectory; with the profile of the wave-packet considered, one may understand it as predicting a *tunnelling* between two branches of the wave-packet, in that the wave-packet describes a semi-classical universe evolving from one classical trajectory in the asymptotic region to *another* classical trajectory, tunnelling near the origin of the plot. In contrast, the other two trajectories depart from classical trajectories near the classical turning point, giving a semi-classical behaviour that essentially differs from the classical one.

The tunnelling picture can be useful for the singularity avoidance, which also tells a semi-classical fate. In figs. 10a to 10f, one can understand γ as an exponential scale factor, so that $g\gamma \to +\infty$ is a classical singularity. If one could equip with numerical tools to find ridge-lines, it is plausible from the plots that in figs. 10a to 10c, a classical trajectory that is wavy and remains near the vertical axis can be found, whereas in figs. 10d to 10f, an orbit that comes from the bottom-left corner goes back to the upper-left, so that the $g\gamma \to +\infty$ singularities are avoided

in both cases.

7 Conclusion and outlook

In this dissertation, we summarised our work on various aspects that link quantum geometrodynamics of Wheeler–DeWitt with the conventional quantum theory, which can be shown by the prototype model in a two-dimensional minisuperspace, that was introduced in section 2. As we have seen, this solvable model not only has its practical value, but is also related to several realistic physical models. After the Dirac quantisation that leads to "cosmological" wave functions. We were also able to construct an exact "linear" wave function, where we would like to ask about its corresponding classical trajectory, which cannot be read off directly, as people would usually do. This question would be explored later in section 6.

It would be of interest to look into higher-dimensional minisuperspace models, and see if one could use them for the same purposes below.

Then in section 3, we performed the standard WKB approximation to the prototype model at the beginning, which is one of the usual ways to connect the Wheeler–DeWitt approach to classical gravitational system. Seeing that the obtained WKB mode functions happened to contain a quantum number, we then established a theory, showing that such WKB mode functions *generally* exist, in which the quantum numbers correspond to classical first integrals. Using the theory, we showed that a narrow Gaussian wave-packet necessarily peaks near the classical trajectory, which has the same classical first integral as the centre of the Gaussian amplitude. Within the WKB approximation, the matching of a wave-packet and a classical trajectory seems to be a mathematical fact.

By set-up, this theory was restricted to Liouville integrable systems that can be solved by separation of variables in the Hamilton–Jacobi formulation. Since there are also non-integrable cases in the Bianchi models [113], one might want to study how to make sense of a wave-packet there.

Next, in section 4 we first introduced the mathematical concept of self-adjointness, showing with an example that such operators can have different domains, which may have a physical effect. We then argued that a boundary condition is needed for the "cosmological" wave functions, that led to a Hilbert space for the quantum states of the universe. The self-adjoint analysis of the Hamiltonian constraint gave non-essential extensions in certain cases, which lead to different phases of the mode functions, and can discretise the spectrum. The wave-packets, constructed by different mode functions, also differ in their profiles. These results can become predictions in suitable experiments.

So far, no guiding principle is known for choosing a preferred self-adjoint domain in quantum geometrodynamics, and the issue is open for further investigation.

In section 5 we constructed a parallel between the minisuperspace Wheeler–DeWitt equation and the stationary Schrödinger equation, particularly a parallel between wave-packets in both cases, which were called *stationary wave-packets*. This concept was illustrated by the minimal example of a two-dimensional hydrogen atom, for which we constructed a wave-packet by superposing with a binomial amplitude. From the results we could recover Bohr's correspondence principle that is related to large *main* quantum numbers, as well as establish a new correspondence phenomenon, in which the main quantum number remains fixed, while the average *angular* quantum number is close to its maximal allowed value. Meanwhile, we also argued for the importance of wave-packets for the observed classical universe, and proposed a criterion for the superposition amplitude for a given set of quantum states, labelled with a quantum number.

Although there has been much interest in simulating black holes and quantum field theory in curved space-time, a simulation of quantum cosmology has not yet been proposed. Stationary wave-packets could help to establish such an analogue, provided the Lorentzian kinetic term could be realised.

Finally, in section 6, we discussed possible mathematical descriptions of ridge-lines of a wave-packet, that are the only way to make sense of a semi-classical wave-packet in the literature, as well as in our derivation before. We gave three ways to calculate the ridge-lines. First of all, the simple first-derivative test is easy to calculate, but is not invariant under coordinate transform, and may give results that do not even respect the symmetry of the wave function. If the wave-packet is numerically given, it is relatively easy to work out a result by using an existing algorithm. Second, the contour approach of Barré de Saint-Venant gives implicit equations of ridge-lines, but in most cases the results contain redundant lines. This approach performs similarly in Euclidean and Lorentzian geometries. Finally, the stream approach of Rudolf Rothe outperforms the other two approaches in Euclidean geometry, but solving the ridge-lines is difficult even when the wave-packet is given analytically. In Lorentzian geometry, this approach loses its advantage and the results are difficult to make sense of.

These approaches gave ridge-lines that could be interpreted as semi-classical trajectories that emerge from the wave-packets. One could identify behaviours such as tunnelling or singularity avoiding, and perform further analysis on them.

For both the latter two approaches, an algorithm for numerically given wave-packets is yet to be looked for.

A Hamiltonian formulation of singular systems

Singular systems are those whose dynamics cannot simply be determined by imposing an arbitrary initial condition in terms of generalised positions and velocities, as is demanded by the Newton's principle of determinacy [9, sec. 1.1]. Important field-theoretical examples in fundamental physics include electrodynamics [135], general relativity (appendix B below), the Dirac spinor, Proca theory,[6] Yang–Mills theory, and the bosonic string theory; even a point particle in special relativity, described in the covariant formulation, is a singular system.

In appendix A.1, we give the Hamiltonian kinematics of a singular system. Then in appendix A.2, we sketch the way towards solving the dynamics of a singular system. Appendix A.3 contains an example. Our treatment basically follows [65, 144].

Nomenclature Singular systems are also called *constrained systems*, the latter of which contains more generic cases. Here we will stick to the former, more precise term.

A.1 The Hamiltonian

Consider a conserved system with several degrees of freedom, described by the Lagrangian action that does not depend on time explicitly,

$$S[q] = \int \mathbb{d}t\, L(q^a, \dot{q}^a)\,. \tag{A.1}$$

Define the matrix

$$M_{ab} \coloneqq \frac{\partial^2 L}{\partial q^a\, \partial q^b}\,. \tag{A.2}$$

The system is called *singular* if M_{ab} is a singular matrix. This could also be understood within the Lagrangian formulation, but we will go directly to the Hamiltonian approach, which fits our purpose.

Failure in constructing the canonical Hamiltonian One way to understand the singularity of the system is to recognise that the momenta

$$p_a = p_a(q, \dot{q}) \coloneqq \frac{\partial L}{\partial \dot{q}^a} \tag{A.3}$$

[6] For a bibliographic account of Alexandru Proca, see [137].

need to be *partially inverted* to get the velocities in terms of q and p,

$$\dot{q}^a = w^a(q,p)\,, \tag{A.4}$$

so that one can perform the Legendre transformation and derive the canonical Hamiltonian of the system

$$H^{\mathrm{c}} \coloneqq (p_a\dot{q}^a - L)|_{\dot{q}^a = w^a(q,p)}\,. \tag{A.5}$$

If M_{ab} is singular, eq. (A.3) cannot be inverted to get eq. (A.4) by the implicit function theorem, and the canonical Hamiltonian approach fails to be constructed.

Extended action and Hamiltonian A viable work-around is to use the *extended action*

$$S^{\mathrm{e}}[q,p,v] \coloneqq \int \mathbb{d}t\,\{L(q,v) + p_a(\dot{q}^a - v^a)\}\,, \tag{A.6}$$

where $\{q^a, p^a, v^a\}$ are independent variables. Variation of S^{e} with respect to $\{q^a, p^a, v^a\}$ gives

$$\frac{\partial L(q,v)}{\partial q^a} - \dot{p}_a = 0\,, \tag{A.7a}$$

$$\dot{q}^a - v^a = 0\,, \tag{A.7b}$$

$$\frac{\partial L(q,v)}{\partial v^a} - p_a = 0\,. \tag{A.7c}$$

Inserting eqs. (A.7b) and (A.7c) into S^{e} gives

$$S^{\mathrm{e}}\left[q, p^a = \frac{\partial L(q,\dot{q})}{\partial \dot{q}^a}, v^a = \dot{q}^a\right] = \int \mathbb{d}t\, L(q,\dot{q}) = S[q]\,; \tag{A.8}$$

In words, *S^e is equivalent to S on-shell.* One can then define the *extended Hamiltonian* and rewrite S^{e}

$$H^{\mathrm{e}}(q,p,v) \coloneqq p_a v^a - L(q,v)\,, \tag{A.9a}$$

$$S^{\mathrm{e}}[q,p,v] = \int \mathbb{d}t\,\{p_a\dot{q}^a - H^{\mathrm{e}}\}\,. \tag{A.9b}$$

H^{e} contains *all* the velocities $\{v^a\}$.

Inexpressible velocities Now that not all the velocities can be given in terms of eq. (A.4), one chooses instead a maximal subset $\{v^i\}$ that can, which are called *expressible velocities*; the rest, $\{v^\alpha\}$, are called *inexpressible velocities*. Note that

the overall indices for degrees of freedom $a, b, ...$ are divided into the expressible ones $i, j, ...$ and the inexpressible ones $\alpha, \beta, ...$

Primary constraints More explicitly, one derives from eq. (A.7c) that

$$v^i = w^i\big(q, p_j\big)\,, \tag{A.10a}$$

$$\Phi_\alpha\big(p_\beta, q\big) \coloneqq p_\alpha - \left.\frac{\partial L(q,v)}{\partial v^\alpha}\right|_{v^i = w^i(q,p_j)} = 0\,. \tag{A.10b}$$

Note that w^i does not depend on p_α. Φ_α in eq. (A.10b) are called *primary constraints*. The condition $\Phi_\alpha = 0$ is to be considered as a part of the equations of motion. They cannot be directly imposed in the action; $\Phi_\alpha = 0$ only holds on-shell.

Hamiltonian and action with primary constraints Inverting eq. (A.10a) and inserting the results into H^e gives the *Hamiltonian with primary constraints* and the corresponding action

$$\begin{aligned} H^\mathrm{p}(q,p,v^i) &\coloneqq H^\mathrm{e}\big|_{v^i = w^i(q,p_j)} \\ &= p_i w^i\big(q,p_j\big) - L(q,v)\big|_{v^i = w^i(q,p_j)} + p_\alpha v^\alpha \\ &=: H^\mathrm{s}(q,p) + v^\alpha \Phi_\alpha\,, \end{aligned} \tag{A.11a}$$

$$H^\mathrm{s}(q,p) \coloneqq \left[p_i w^i(q,p) + v^\alpha \frac{\partial L(q,v)}{\partial v^\alpha} - L(q,v)\right]_{v^i = w^i(q,p_i)}\,; \tag{A.11b}$$

$$S^\mathrm{p}\big[q,p,v^i\big] \coloneqq \int \mathrm{d}t\, \{p_a \dot{q}^a - H^\mathrm{s}(q,p) - v^\alpha \Phi_\alpha\}\,. \tag{A.11c}$$

H^s does not contain any velocities, since one can easily verify from eq. (A.11b) that $\partial H^\mathrm{s}/\partial v^\alpha = 0$. Some authors see v^α as merely Lagrangian multipliers, and according to them, these as well as the Φ_α can somewhat be manually *imposed*; in the formulation here, in contrast, they originate from the description of the system and are *derived*.

Breakdown of the Newton's principle of determinacy The constraints are also to be obeyed by the initial condition. From this perspective, the Newton's principle of determinacy is already broken by the primary constraints.

A.2 Classical dynamics

Poisson bracket The Poisson bracket is defined as usual,

$$[A, B]_{\mathrm{P}} := \frac{\partial A}{\partial q^a}\frac{\partial B}{\partial p_a} - \frac{\partial A}{\partial p_a}\frac{\partial B}{\partial q^a}\,. \tag{A.12}$$

By varying eq. (A.9b) or eq. (A.11c), one can show that the evolution of phase-space functions is still given by $[\cdot, H^*]_{\mathrm{P}}$, $* = \mathrm{e}$ or p, with the corresponding constraints considered. For example,

$$\begin{cases} \dot{A}(q,p) = [A, H^{\mathrm{p}}]_{\mathrm{P}}\,, \\ \quad \Phi_\alpha = 0 \end{cases} \tag{A.13}$$

determines the evolution of A.

Secondary constraints Now, we consider Φ_α, which are to be constrained to zero throughout the evolution of the system. This *persistency condition* requires

$$0 = [\Phi_\alpha, H^{\mathrm{p}}]_{\mathrm{P}}\,. \tag{A.14}$$

which may lead to new generations of constraints, collectively called *secondary constraints*.

Second-class constraints We *suppose* that

$$H^{\mathrm{p}} = H^{\mathrm{c}} + \lambda^\mu \Phi_\mu\,, \tag{A.15}$$

where Φ^μ are *all* primary and secondary constraints, and H^{c} does not contain any constraint. In this case, the persistency condition reads

$$0 = [\Phi_\nu, H^{\mathrm{c}}]_{\mathrm{P}} + \lambda^\mu \big[\Phi_\nu, \Phi_\mu\big]_{\mathrm{P}}\,. \tag{A.16}$$

If the anti-symmetric matrix $\big[\Phi_\mu, \Phi_\nu\big]_{\mathrm{P}}$ is invertible, one can choose

$$\lambda^\mu = [\Phi_\nu, H^{\mathrm{c}}]_{\mathrm{P}} \Big[\big([\Phi, \Phi]_{\mathrm{P}}\big)^{-1}\Big]^{\nu\mu} \tag{A.17}$$

and then only deal with the q's and p's. One way to solve the dynamics of a second-class system is to keep all the phase-space variables and use the Dirac bracket, instead of the Poisson one. Another way is to find a canonical transformation that reduces the constraints to conjugate pairs of phase-space variables, which are constrained to zero, and study the rest of the phase-space variables, which

constitute a regular system.

In fundamental physics, the Dirac spinor and the Proca theory are examples of second-class systems. Apart from the literature mentioned at the beginning of this appendix A, the Hamiltonian formulation of Dirac spinor ψ has also been studied in popular textbooks on quantum field theory, e.g. [133, sec. 3.5], where the momentum conjugate to the spinor field ψ was mentioned to be $\mathrm{i}\psi^\dagger$, so that the phase space has the *same* dimension as the configuration space, rather than *doubling* the size; in other words, the authors took a short-cut of the second way mentioned above, and only studied the reduced physical phase space.

Although we could not find a proof, in all examples we know, eq. (A.15) holds without the need of adding the secondary constraints by hand.

First-class constraints When $\left[\Phi_\mu, \Phi_\nu\right]_{\mathrm{P}}$ in eq. (A.16) is not invertible, these constraints are called *first-class*, which generate "gauge" or redundancy transformations in the phase space, that can shift the phase-space trajectory while keeping the initial values intact. The algorithm to construct gauge transformations is given in e.g. [32].

In fundamental physics, electrodynamics, general relativity, Yang–Mills theory and the bosonic string theory are all first-class systems.

In practice, it has been proven that $\left[\Phi_\mu, \Phi_\nu\right]_{\mathrm{P}}$ can always be blockwise diagonalised into $\begin{pmatrix} \mathrm{I} & \mathbb{0} \\ \mathbb{0} & \mathrm{II} \end{pmatrix}$, such that II contains all the second-class constraints, whereas no further constraint of such can be separated from I, which is therefore purely first-class.

A.3 Example: relativistic point particle

Consider the quadratic action of a free point particle in special relativity [23, eq. (2.7)]

$$S[x, N] := \frac{1}{2} \int \mathrm{d}\lambda \left\{ \eta_{\mu\nu} \frac{\dot{x}^\mu \dot{x}^\nu}{N} - N m^2 \right\}, \qquad \mu, \nu = 0, 1, \dots, d\,, \tag{A.18}$$

where $m \geq 0$ is the mass; $N = N(t)$ is an auxiliary variable, the equation of motion of which reads

$$0 = \eta_{\mu\nu} \dot{x}^\mu \dot{x}^\nu + m^2 N^2\,. \tag{A.19}$$

For $m > 0$, substituting eq. (A.19) into eq. (A.18) gives the usual action for a point particle

$$S\Big[x, N = m^{-1}\sqrt{-\eta_{\mu\nu}\dot{x}^\mu\dot{x}^\nu}\Big] = -m\int \mathrm{d}\lambda\,\sqrt{-\eta_{\mu\nu}\dot{x}^\mu\dot{x}^\nu}\,. \tag{A.20}$$

Let the configuration-space variables be ordered as $(x^0, x^1, \dots, x^d, N)$. The $(d+2)\times(d+2)$ matrix

$$M_{ab} = \frac{\partial^2 L}{\partial q^a\,\partial q^b} = \frac{1}{N}\begin{pmatrix} \eta_{\mu\nu} & -\eta_{\mu\nu}\frac{\dot{x}^\nu}{N} \\ -\eta_{\mu\nu}\frac{\dot{x}^\mu}{N} & \eta_{\mu\nu}\frac{\dot{x}^\mu\dot{x}^\nu}{N^2}\end{pmatrix} \tag{A.21}$$

has a matrix rank of $(d+1)$, and is therefore singular.

Using the formulation above, we choose v^N to be the inexpressible velocity, and the action with primary constraints reads

$$S^{\mathrm{p}}[x, N, p, P_N, V^N] = \frac{1}{2}\int \mathrm{d}\lambda\,\big\{p_\mu\dot{x}^\mu - H^{\mathrm{p}}(x, N, p, P_N, V^N)\big\}\,, \tag{A.22a}$$

$$H^{\mathrm{p}} = NH_\perp + V^N P_N\,, \tag{A.22b}$$

$$H_\perp \coloneqq \eta^{\mu\nu}p_\mu p_\nu + m^2\,. \tag{A.22c}$$

where P_N is the only primary constraint. The Poisson bracket of P_N and H^{p} is

$$[P_N, H^{\mathrm{p}}]_{\mathrm{P}} = H_\perp\,. \tag{A.23}$$

For this reason, $H_\perp$ is often called *Hamiltonian constraint*, although it is unfortunately not a Hamiltonian itself. There is no further constraint, and the system is first-class, since $[P_N, H_\perp]_{\mathrm{P}} \equiv 0$.

Note that H^{p} consists of constraints only. Using the Dirac quantisation scheme for such second-class systems, equations for the quantum wave function reads

$$0 = \frac{\hbar}{\mathrm{i}}\partial_N\psi\,, \tag{A.24a}$$

$$0 = \big(-\hbar^2\eta^{\mu\nu}\partial_\mu\partial_\nu + m^2\big)\psi\,. \tag{A.24b}$$

Equation (A.24a) eliminates the dependence of ψ on N, and eq. (A.24b) is nothing else but the Klein–Gordon equation.

Instead of the quadratic action (A.18), one could have begun with the usual action (A.20) instead. The system is still singular; choosing $v^0 > 0$ to be the

inexpressible velocity, the action with primary constraints reads

$$S^{\mathrm{p}}[x,p,v^0] = \int \mathrm{d}\lambda \left\{ p_\mu \dot{x}^\mu - H^{\mathrm{p}}(x,p,v^0) \right\}, \tag{A.25}$$

$$H^{\mathrm{p}} = v^0 \Phi_0 \,, \tag{A.26}$$

$$\Phi_0 \coloneqq p_0 + \sqrt{m^2 + \delta^{ij} p_i p_j} \,, \tag{A.27}$$

where Φ_0 is the primary and the only constraint. Equations (A.25) and (A.26) are different from eqs. (A.22a) and (A.22b). The quantum equation read

$$\left\{ \frac{\hbar}{\mathrm{i}} \partial_0 + \sqrt{m^2 - \hbar^2 \nabla^2} \right\} \psi = 0 \,, \tag{A.28}$$

so that we arrive at the same equation as the one found by Paul Dirac in the development of his equation for electrons [42, sec. 74].

B Canonical quantum gravitation à la Wheeler–DeWitt

In this appendix B we briefly review the Wheeler–DeWitt approach of canonical quantum gravitation. In appendix B.1 we give general relativity in terms of the Einstein–Hilbert Lagrangian action plus the boundary term. Then in appendix B.2 we give a Hamiltonian formulation of general relativity that was developed by Richard Arnowitt, Stanley Deser and Charles Misner. In the end, we give the quantum equations of the Arnowitt–Deser–Misner formulation, which dates back to John Wheeler and Bryce DeWitt, using the quantisation scheme of Paul Dirac.

B.1 General relativity

The most popular theory of gravitation is the general theory of relativity, or briefly general relativity, originally developed by Albert Einstein [49]. At the moment, there are many alternative theories that are indistinguishable from general relativity by observations and experiments, including the gauge approaches [22], the scalar–tensor–vector theories [119], etc.

In general relativity, gravitation is a geometric effect of the pseudo-Riemannian metric $g_{\mu\nu}$ of space-time manifold $\mathcal{M}$; the dynamics of the metric is governed by the Einstein field equations

$$R_{\mu\nu} - \frac{1}{2} R g_{\mu\nu} = \varkappa T_{\mu\nu} - \Lambda g_{\mu\nu} \,, \tag{B.1}$$

where $R_{\mu\nu}$ is the Ricci tensor, R the Ricci scalar, $\varkappa := 8\pi G$, $T_{\mu\nu}$ the energy-momentum tensor of matter, and Λ the cosmological constant.

These field equations can be derived from the Einstein–Hilbert action [79]

$$S_{\mathrm{EH}} := \frac{1}{2\varkappa} \int_{\mathcal{M}} \mathrm{d}^4 x \, \sqrt{-\tilde{\tilde{g}}} \, (R - 2\Lambda) \,, \tag{B.2}$$

where $\tilde{\tilde{g}} := \det g_{\mu\nu}$, which is a scalar density of weight 2, hence the double tilde above. S_{EH} contains second derivatives of $g_{\mu\nu}$ as well, which are to be eliminated in order to be in accordance with the Newton's principle of determinacy [9, sec. 1.1], see also the endnote of section 2.2. This can be realised by adding a boundary term that was given credit to York, Gibbons and Hawking as

$$S_{\mathrm{GHY}} := -\frac{1}{2\varkappa} \int_{\partial\mathcal{M}} \mathrm{d}^3 y \, t \sqrt{-\tilde{\tilde{h}}} \, K \,, \tag{B.3}$$

where $\partial\mathcal{M}$ is the boundary of $\mathcal{M}$, which is supposed to be a time- or space-

like hypersurface; $t = \pm$ for time- and space-like cases of $\partial\mathcal{M}$, respectively; $\tilde{\tilde{h}}$ is the determinant of the induced metric on $\partial\mathcal{M}$, and K is the trace of the scalar-valued second fundamental form of $\partial\mathcal{M}$ [91, sec. 4.2.1, 3, sec. 1.2.4]. A different boundary term has already been used by Einstein in [50]. The total action of general relativity can now be written as sum of the bulk term and the boundary term

$$S_{\text{gr}} = S_{\text{EH}} + S_{\text{GHY}}\,. \tag{B.4}$$

For a detailed derivation of the Lagrangian formulation, see [138, sec. 4.1]

Ambiguity of the action The quantisation schemes depend on the action of the system. Unfortunately, not only does the boundary term have ambiguities (see e.g. [34]); the bulk Lagrangian of the system also contains arbitrariness [140, sec. 1.1.2].

Generic form of the boundary term One can use the method of moving frames to study the boundary term, treating the null boundary within the same framework, and dealing with the possible contribution from the non-smooth junction, or *corner*, of a piece-wise-defined boundary [83].

B.2 The Arnowitt–Deser–Misner formulation of geometrodynamics

The Arnowitt–Deser–Misner (ADM) formulation [10] is the most popular Hamiltonian formulation of general relativity, that uses the $(3+1)$-*decomposed* metric as the configuration-space variables. For detailed derivations, see [91, ch. 4, 138, sec. 4.2]. One can also use the *original* space-time metric as the variable, which traces back to [43]; see [96] for a comparison.

When the space-time manifold can be decomposed $\mathcal{M} = \mathbb{R} \times \Sigma$, where Σ is space-like, one can adapt the coordinates (t, y^a) such that the metric has the components

$$g_{\mu\nu}\,\mathbb{d}x^\mu\,\mathbb{d}x^\nu = -N^2\,\mathbb{d}t^2 + h_{ab}(N^a\,\mathbb{d}t + \mathbb{d}y^a)(N^b\,\mathbb{d}t + \mathbb{d}y^b)\,, \tag{B.5}$$

where $h_{ab}\,\mathbb{d}y^a\,\mathbb{d}y^b$ is the induced metric on Σ, (N, N^a) are the lapse and shift functions, respectively.

Eliminating S_{GHY} on the time-like boundaries from S_{gr} yields the ADM action

$$S_{\mathrm{ADM}} = \frac{1}{2\varkappa}\int_{\mathbb{R}\times\Sigma} \mathbb{d}t\,\mathbb{d}^3y\, N\sqrt{\tilde{\tilde{h}}}\left\{K_{ab}K^{ab} - K^2 + R[h] - 2\Lambda\right\} \tag{B.6a}$$

$$= \frac{1}{2\varkappa}\int_{\mathbb{R}\times\Sigma} \mathbb{d}t\,\mathbb{d}^3y\, N\left\{\tilde{\underset{\sim}{G}}^{abcd}K_{ab}K_{cd} + \sqrt{\tilde{\tilde{h}}}\,(R[h] - 2\Lambda)\right\}, \tag{B.6b}$$

$$\tilde{\underset{\sim}{G}}^{abcd} := \frac{\sqrt{\tilde{\tilde{h}}}}{2}(h^{ac}h^{bd} + h^{ad}h^{bc} - 2h^{ab}h^{cd}), \tag{B.6c}$$

where $\tilde{\underset{\sim}{G}}^{abcd}$ is the DeWitt metric [40], K_{ab} are components of the scalar-valued second fundamental form, and $R[h]$ is the Ricci scalar of h_{ab}.

Equation (B.6b) describes a singular system. Using the formulation in appendix A, one finds the ADM action with constraints

$$S^{\mathrm{p}}_{\mathrm{ADM}} = \frac{1}{2\varkappa}\int_{\mathcal{M}} \mathbb{d}t\,\mathbb{d}^3y\left\{\tilde{\underset{\sim}{p}}^{ab}\dot{h}_{ab} + \tilde{P}\dot{N} + \tilde{P}_a\dot{N}^a - \tilde{\mathcal{H}}^{\mathrm{p}}\right\}, \tag{B.7a}$$

$$\tilde{\mathcal{H}}^{\mathrm{p}} := N\tilde{H}^{\mathrm{gr}}_{\perp} + N^a\tilde{H}^{\mathrm{gr}}_a + V\tilde{P} + V^a\tilde{P}_a, \tag{B.7b}$$

$$\tilde{\mathcal{H}}^{\mathrm{gr}}_{\perp} := 2\varkappa G_{\underset{\sim}{abcd}}\tilde{\underset{\sim}{p}}^{ab}\tilde{\underset{\sim}{p}}^{cd} - \frac{\sqrt{\tilde{\tilde{h}}}}{2\varkappa}(R[h] - 2\Lambda), \tag{B.7c}$$

$$\tilde{\mathcal{H}}^{\mathrm{gr}}_a := -2\tilde{\underset{\sim}{p}}_a{}^b{}_{|b}, \tag{B.7d}$$

$$G_{\underset{\sim}{abcd}} := \frac{1}{2\sqrt{\tilde{\tilde{h}}}}(h_{ac}h_{bd} + h_{ad}h_{bc} - h_{ab}h_{cd}), \tag{B.7e}$$

where $\left(\tilde{\underset{\sim}{p}}^{ab}, \tilde{P}, \tilde{P}_a\right)$ are momenta conjugate to (h_{ab}, N, N^a), respectively; $G_{\underset{\sim}{abcd}}$ is the inverse DeWitt metric, and $_{|}$ denotes the induced covariant derivative on Σ.

One can read off that $\tilde{P}$ and $\tilde{P}_a$ are the primary constraints, and $\tilde{\mathcal{H}}^{\mathrm{gr}}_{\perp}$, $\tilde{\mathcal{H}}^{\mathrm{gr}}_a$ are the corresponding secondary constraints, which are called the Hamiltonian and momentum (also diffeomorphism) constraints, respectively. Altogether, the four of them generate the gauge transformations of the ADM action, see [96].

The classical Hamiltonian dynamics is discussed in e.g. [138, sec. 4.2, 162, appx. E.2], which is not needed here.

B.3 The Wheeler–DeWitt approach

Applying the Dirac quantisation scheme to the ADM action gives the Wheeler–DeWitt approach of quantum gravitation [40]. In this scheme, the generalised positions and momenta are promoted to operators, as in the usual canonical quantisation procedure in quantum mechanics. It gives rise to a functional Schrödinger formulation, in which the kinetics of the system is described by a wave functional, the arguments of which are the configuration space variables, or the field configurations, see e.g. [80]. This is in contrast to the usual practice in quantum field

theories in special relativity, the kinetics of which is mostly written with the help of a Fock space.

Since the ADM action describes a first-class system, the Hamiltonian of which is constrained to zero, so that the equations that govern the wave function are just the constraint equations. One can promote the conditions, that the classical constraints are constrained to zero, to the quantum level, that the quantised constraints acting on the wave functional also give zero. For the gravitational part of the system, this gives

$$0 = \frac{\hbar}{\mathrm{i}} \frac{\delta}{\delta N} \psi \,, \tag{B.8a}$$

$$0 = \frac{\hbar}{\mathrm{i}} \frac{\delta}{\delta N^a} \psi \,, \tag{B.8b}$$

$$\begin{aligned} 0 &= \tilde{\mathcal{H}}_{\perp}^{\mathrm{gr}} \left(h_{ab}, \frac{\hbar}{\mathrm{i}} \frac{\delta}{\delta h_{ab}} \right) \psi \\ &= \left\{ -2\varkappa\hbar^2 \underset{\sim}{G}_{abcd} \frac{\delta^2}{\delta h_{ab}\, \delta h_{cd}} - \frac{\sqrt{\tilde{\tilde{h}}}}{2\varkappa} (R[h] - 2\Lambda) \right\} \psi \,, \end{aligned} \tag{B.8c}$$

$$0 = \tilde{\mathcal{H}}_{a}^{\mathrm{gr}} \left(h_{ab}, \frac{\hbar}{\mathrm{i}} \frac{\delta}{\delta h_{ab}} \right) \psi \,. \tag{B.8d}$$

Equations (B.8a) and (B.8b) just eliminate the lapse- and shift-dependence of the wave functional. Equations (B.8c) and (B.8d) are called the Wheeler–DeWitt equations.

C Normalisation integral of the Bessel functions

Bessel functions are common transcendental functions in theoretical physics, dating back to Friedrich Bessel [47]. Unfortunately, undergraduate students nowadays have decreasingly less lecture time on the special functions. We recommend [164, ch. 7] for an introduction to these practical functions.

The integral of Bessel functions

$$\int_0^{+\infty} \frac{\mathrm{d}x}{x} W_{\nu_1}(x) W_{\nu_2}(x)\,, \qquad \text{(4.27c revisited)}$$

where $W_\nu(x)$ is a Bessel function of order ν, can be evaluated by a method that has been given in [157, sec. 3]. Here we outline the calculation that is not available in standard references, e.g. [45, ch. 10].

The Bessel equation (4.26b) can be rewritten as

$$x\frac{\mathrm{d}}{\mathrm{d}x}\left(x\frac{\mathrm{d}W_\nu}{\mathrm{d}x}\right) + (\epsilon\nu^2 - \upsilon x^2) W_\nu(x) = 0\,, \qquad \text{(C.1)}$$

where $\epsilon, \upsilon = \pm 1$, and the correspondence of $W_\nu(x)$ to $J_\nu(x)$, $F_{\mathrm{i}\nu}(x)$, $G_{\mathrm{i}\nu}(x)$ and $K_{\mathrm{i}\nu}(x)$ can be found in table 5. Moving the second term to the right-hand side and multiplying by W_{ν_2} gives

$$\frac{\mathrm{d}}{\mathrm{d}x}\left(x\frac{\mathrm{d}W_{\nu_1}}{\mathrm{d}x}\right) W_{\nu_2} = \left(\upsilon x - \epsilon\frac{\nu_1^2}{x}\right) W_{\nu_1} W_{\nu_2}\,, \qquad \text{(C.2a)}$$

$$\frac{\mathrm{d}}{\mathrm{d}x}\left(x\frac{\mathrm{d}W_{\nu_2}}{\mathrm{d}x}\right) W_{\nu_1} = \left(\upsilon x - \epsilon\frac{\nu_2^2}{x}\right) W_{\nu_2} W_{\nu_1}\,. \qquad \text{(C.2b)}$$

Subtracting eq. (C.2a) from eq. (C.2b) and integrate with x, one gets

$$\begin{aligned} &\epsilon(\nu_1^2 - \nu_2^2) \int_\xi^{+\infty} \frac{\mathrm{d}x}{x} W_{\nu_1} W_{\nu_2} \\ &= \int_{x=\xi}^{x\to+\infty} \left[\mathrm{d}\left(x\frac{\mathrm{d}W_{\nu_2}}{\mathrm{d}x}\right) W_{\nu_1} - \mathrm{d}\left(x\frac{\mathrm{d}W_{\nu_1}}{\mathrm{d}x}\right) W_{\nu_2}\right] \qquad \text{(C.3a)} \\ &= \left[x\left(\frac{\mathrm{d}W_{\nu_2}}{\mathrm{d}x} W_{\nu_1} - \frac{\mathrm{d}W_{\nu_1}}{\mathrm{d}x} W_{\nu_2}\right)\right]_{x=\xi}^{x\to+\infty}, \qquad \text{(C.3b)} \end{aligned}$$

where integrating by parts was used to derive eq. (C.3b). One can then substitute the asymptotic expressions of W_ν at $x = 0^+$ and $x \to +\infty$ (table 6) to evaluate the integral (4.27c). The δ-function is obtained by a more detailed discussion of the sin or cos functions of the divergent logarithm, see [157, sec. 3].

$W_\nu(x)$	$x = 0^+$	Source
$J_\nu(x)$	$\left(\frac{x}{2}\right)^\nu \left[\frac{1}{\Gamma(\nu+1)} + O(x^2)\right]$	[45, eq. (10.2.2)]
$F_{\mathrm{i}\nu}(x)$	$\sqrt{\frac{2\nu\tanh(\pi\nu/2)}{\pi}}\left[\frac{1}{\nu}\cos(\nu \ln \frac{x}{2} - \arg\Gamma(1+\mathrm{i}\nu)) + O(x^2\cos)\right]$	[46, eq. (3.8)]
$G_{\mathrm{i}\nu}(x)$	$\sqrt{\frac{2\nu\coth(\pi\nu/2)}{\pi}}\left[\frac{1}{\nu}\sin(\nu \ln \frac{x}{2} - \arg\Gamma(1+\mathrm{i}\nu)) + O(x^2\sin)\right]$	[46, eq. (3.9)]
$K_{\mathrm{i}\nu}(x)$	$\sqrt{\frac{\pi}{\nu\sinh(\pi\nu)}}\cos(-\nu \ln \frac{x}{2} + \arg\Gamma(\mathrm{i}\nu)) + O(x^2\sin)$	[157, eq. (2.7)]

(a) $x = 0^+$

$W_\nu(x)$	$x \to +\infty$	Source
$J_\nu(x)$	$\sqrt{\frac{2}{\pi x}}\left[\cos(x - \frac{\pi\nu}{2} - \frac{\pi}{4}) + O(x^{-1})\right]$	[45, eq. (10.17.3)]
$F_{\mathrm{i}\nu}(x)$	$\sqrt{\frac{2}{\pi x}}\left[\cos(x - \frac{\pi}{4}) + O(x^{-1})\right]$	[46, eq. (3.17)]
$G_{\mathrm{i}\nu}(x)$	$\sqrt{\frac{2}{\pi x}}\left[\sin(x - \frac{\pi}{4}) + O(x^{-1})\right]$	[46, eq. (3.18)]
$K_{\mathrm{i}\nu}(x)$	$\sqrt{\frac{\pi}{2x}}\mathrm{e}^{-x}\left[1 + O(x^{-1})\right]$	[157, eq. (2.5)]

(b) $x \to +\infty$

Table 6: Asymptotic expressions of the Bessel function $W_\nu(x)$. At $x = 0^+$ (table 6a), $J_\nu(x)$ can be expressed as a power series, whereas the other three cases have a logarithmic sinusoidal form. For $x \to +\infty$ (table 6b), $K_{\mathrm{i}\nu}(x)$ is exponentially suppressed, while the other three cases are sinusoidal with an amplitude $\sim x^{-1/2}$.

D Construction of a self-adjoint extension

The self-adjoint extension of a (closed) symmetric operator $\widehat{A}$ is best to be constructed by finding the extension of its *Cayley transform* [125]

$$\widehat{T}_{\widehat{A}} := \big(\widehat{A} - \mathsf{i}\hat{\mathbb{1}}\big)\big(\widehat{A} + \mathsf{i}\hat{\mathbb{1}}\big)^{-1}, \tag{D.1}$$

named after Arthur Cayley [33]. $\widehat{T}_{\widehat{A}}$ is a unitary operator [73, thm. 10.28], The inverse transform

$$\widehat{A} = \mathsf{i}\big(\widehat{T}_{\widehat{A}} + \hat{\mathbb{1}}\big)\big(\widehat{T}_{\widehat{A}} - \hat{\mathbb{1}}\big)^{-1} \tag{D.2}$$

gives back $\widehat{A}$. The logic of the construction is easier to be understood than to be proven, which is described below.

1. $\widehat{A}$ if self-adjoint, if and only if the spectrum of $\widehat{A}^\dagger$ is also real [141, thm. X.1]. Therefore we first study the *complex* spectrum of $\widehat{A}^\dagger$.

2. Let the *deficiency subspaces* be

$$\mathbf{H}_{\widehat{A},\lambda} := \ker\big(\lambda\hat{\mathbb{1}} - \widehat{A}^\dagger\big) \equiv \mathrm{range}\big(\lambda^*\hat{\mathbb{1}} + \widehat{A}\big)^\perp, \tag{D.3}$$

   where $^\perp$ denotes orthogonal complement [141, thm. X.1]. Their dimensions $\mathcal{N}_{\widehat{A},\lambda} := \dim \mathbf{H}_{\widehat{A},\lambda}$ are called the *deficiency indices*.

3. The deficiency indices are constants for $\Im\lambda > 0$ and < 0, respectively [141, thm. X.1]. Hence for simplicity and definiteness, we fix $\lambda = \pm\mathsf{i}$, and focus on $\mathbf{H}_{\widehat{A},\pm}$ as well as $\mathcal{N}_{\widehat{A},\pm}$, where $\pm$ is to be understood as $\pm\mathsf{i}$.

4. Now, it has been shown that $\mathrm{Dom}\,\widehat{A}^\dagger$ can be decomposed as [141, p. 138, 64, thm. 3.1]

$$\mathrm{Dom}\,\widehat{A}^\dagger = \mathrm{Dom}\,\widehat{A} \oplus \mathbf{H}_{\widehat{A},\lambda} \oplus \mathbf{H}_{\widehat{A},\lambda^*}, \tag{D.4}$$

   where $\oplus$ means direct sum. We will try to extend $\mathrm{Dom}\,\widehat{A}$ to, say, $\mathbf{H}_{\widehat{A},+}$, so that $\mathrm{Dom}\,\widehat{A}^\dagger$ is shortened.

5. Now go back to $\widehat{T}_{\widehat{A}}$. One has

$$\mathrm{Dom}\,\widehat{T}_{\widehat{A}} = \big(\widehat{A} + \mathsf{i}\hat{\mathbb{1}}\big)\,\mathrm{Dom}\,\widehat{A} \equiv \mathrm{range}\big(\widehat{A} + \mathsf{i}\hat{\mathbb{1}}\big) \equiv \big(\mathbf{H}_{\widehat{A},+}\big)^\perp. \tag{D.5}$$

6. One can extend $\mathrm{Dom}\,\widehat{T}_{\widehat{A}}$ to $\mathbf{H}_{\widehat{A},+}$ by assigning a unitary transformation

$\widehat{U} : \mathbf{H}_{\widehat{A},+} \to \mathbf{H}_{\widehat{A},-}$, so that $\operatorname{Dom} \widehat{A}$ is extended to

$$\operatorname{Dom} \widehat{A}_{\widehat{U}} \equiv \left\{ \phi + \left(\hat{\mathbb{1}} - \widehat{U}\right)\phi_+ \mid \phi \in \operatorname{Dom} \widehat{A}, \phi_+ \in \mathbf{H}_{\widehat{A},+} \right\}, \tag{D.6}$$

and the action of the extended operator

$$\widehat{A}_{\widehat{U}}\left(\phi + \left(\hat{\mathbb{1}} - \widehat{U}\right)\phi_+\right) := \widehat{A}\phi + \mathsf{i}\left(\hat{\mathbb{1}} + \widehat{U}\right)\phi_+ \,, \tag{D.7}$$

which is given by eq. (D.2) [141, thm. X.2].

For a technical note about the proofs, see [141, p. 318]

E Quantisation of the two-dimensional hydrogen atom

In this appendix E we describe the canonical quantisation of the two-dimensional hydrogen atom in more detail.

The system is described by the action

$$S = \int \mathbb{d}t \left[\frac{m}{2}(\dot{\varrho}^2 + \varrho^2\dot{\varphi}^2) + \frac{\alpha}{\varrho}\right]. \qquad \alpha > 0 \qquad \text{(5.2 revisited)}$$

Upon quantisation, the stationary Schrödinger equation reads

$$\left(-\frac{\hbar^2}{2m}\nabla^2 - \frac{\alpha}{\varrho}\right)\psi(\varrho,\varphi) = E\psi(\varrho,\varphi)\,. \qquad \text{(5.5 revisited)}$$

A separated test solution

$$\psi(\varrho,\varphi) = P(\varrho)\Phi(\varphi) \qquad \text{(E.1)}$$

gives the orthonormal angular eigenfunction

$$\Phi_l(\varphi) = (2\pi)^{-1/2}\mathsf{e}^{\mathsf{i}l\varphi}, \qquad l = 0, \pm1, \pm2, \ldots\,, \qquad \text{(5.7d revisited)}$$

and the corresponding angular momenta reads $l\hbar$, where l is called the *angular quantum number*. The remaining radial wave function satisfies

$$\left\{\frac{\mathbb{d}^2}{\mathbb{d}\varrho^2} + \frac{1}{\varrho}\frac{\mathbb{d}}{\mathbb{d}\varrho} + \left[\frac{2m}{\hbar}\left(E + \frac{\alpha}{\varrho}\right) - \frac{l^2}{\varrho^2}\right]\right\}P(\varrho) = 0\,. \qquad \text{(E.2)}$$

For bounded states $E < 0$, rewrite the energy levels as [177]

$$E_n := -\frac{m\alpha^2}{2\hbar^2}\left(n + \frac{1}{2}\right)^{-2}, \qquad \text{(5.8)}$$

where n is called the *main quantum number*. Introducing the *dimensionless radial coordinate*

$$\xi := \beta_n\varrho\,, \qquad \beta_n := \frac{2m\alpha}{\hbar^2}\left(n + \frac{1}{2}\right)^{-1}, \qquad \text{(5.7e revisited)}$$

the radial wave function can be factorised [105, sec. 32, 36]

$$P(x) =: \xi^{|l|}\mathsf{e}^{-\xi/2}G(\xi)\,, \qquad \text{(E.3)}$$

and eq. (E.2) becomes

$$\left\{\xi\frac{\mathrm{d}^2}{\mathrm{d}\xi^2}+[(2|l|+1)-\xi]\frac{\mathrm{d}}{\mathrm{d}\xi}-(|l|-n)\right\}G(\xi)=0\,. \tag{E.4}$$

The solutions that are regular at $\xi=0$ can be given in terms of a Kummer's [100] confluent hypergeometric function [45, sec. 13.2], Sonin's [155, sec. 40] associated Laguerre polynomial [45, eq. (18.11.2)], or a Whittaker function [45, eq. (13.14.4)] as

$$G(\xi)={}_1F_1(|l|-n,2|l|+1,\xi)\,N_{nl} \tag{E.5a}$$

$$=L_\mu^{(a)}(\xi)\frac{a!}{(\mu+1)_{2|l|}}N_{nl}\qquad a=2|l|\,,\quad \mu=n-|l|\,; \tag{E.5b}$$

$$=M_{\nu,|l|}(\xi)\xi^{-|l|}\mathrm{e}^{\xi/2}\,N_{nl}\qquad \nu=n+\frac{1}{2}\,, \tag{E.5c}$$

where $(a)_n \coloneqq a(a-1)\dots(a-n+1)$ is the Pochhammer's [136] symbol [45, sec. 5.2(iii)]. The usual orthonormal condition requires $n\in\mathbb{N}\cup\{0\}$; $l=0,\pm1,\dots,\pm n$, and

$$N_{nl}=\frac{1}{(2|l|)!}\left(\frac{(n+|l|)!}{(2n+1)(n-|l|)!}\right)^{1/2}. \tag{5.7c revisited}$$

Together with eqs. (5.7a) to (5.7d), these results complete the canonical quantisation of the two-dimensional hydrogen atom.

F Manipulation of differential forms

In this appendix F we establish an *inductive* framework, in which one can effectively manipulate differential forms used in section 6. In practice, we have found that the *closed-form* definitions and formulae are much less useful than the *inductive* ones. It is not intended to give a consistent introduction of the topic. We mostly follow [29, ch. 4, 122, sec. 7.9].

In (pseudo-)Riemannian geometry, the partial differentials ∂_i serve as bases for the tangent vector space, which we denote by $\mathbf{V}$, without specifying the point.

One- and zero-forms A(n) (untwisted) differential one-form $\alpha \in \mathbf{\Lambda}^1$ is a co-vector, the space in which it lives $\mathbf{\Lambda}^1 = \mathbf{V}^*$ is spanned by the coordinate differentials $\mathbb{d}x^i$, defined by their action on the coordinate differentials

$$\mathbb{d}x^i(\partial_j) = \delta^i{}_j \,. \tag{F.1}$$

A zero-form $f \in \mathbf{\Lambda}^0$ is just a scalar function.

Zero- and one-forms will be the starting point of much of the construction below.

Exterior product and r-forms For $\alpha, \beta \in \mathbf{\Lambda}^1$, their wedge product is the antisymmetrised tensor product,

$$\alpha \wedge \beta = -\beta \wedge \alpha \,. \tag{F.2}$$

From here one can define the (untwisted) differential $(r+1)$-forms by the wedge product of an one-form and an r-form, which are totally antisymmetric tensors of type $(0, r+1)$.

In general, the wedge product is defined for an arbitrary p- and q-form,

$$\wedge : \mathbf{\Lambda}^p \times \mathbf{\Lambda}^q \to \mathbf{\Lambda}^{p+q} \,. \tag{F.3}$$

For $\omega \in \mathbf{\Lambda}^p$, $\eta \in \mathbf{\Lambda}^q$,

$$\omega \wedge \eta = (-)^{pq} \eta \wedge \omega \,. \tag{F.4}$$

For a d-dimensional manifold, the non-empty spaces of forms are $\mathbf{\Lambda}^r$, $r = 0, 1, \ldots, d$.

Exterior derivative The exterior derivative $\mathbb{d}$ is a linear derivative operator that maps an r-form to an $(r+1)$ form, that acts on $f \in \mathbf{\Lambda}^0$ as the usual differen-

tial, and

$$\mathbb{d}(\mathbb{d}f) = 0\,. \tag{F.5a}$$

Moreover, for $\omega \in \mathbf{\Lambda}^p$, η another differential form,

$$\mathbb{d}(\omega \wedge \eta) = \mathbb{d}\omega \wedge \eta + (-)^p \alpha \wedge \mathbb{d}\eta\,. \tag{F.5b}$$

Interior product The interior product, or contraction $\lrcorner$, is a linear map

$$\lrcorner : \mathbf{V} \times \mathbf{\Lambda}^r \to \mathbf{\Lambda}^{r-1}\,. \tag{F.6}$$

In particular, for $v \in \mathbf{V}$, $\omega \in \mathbf{\Lambda}^p$, η an arbitrary form,

$$v \wedge \alpha = \alpha(v)\,, \tag{F.7a}$$

$$v \lrcorner (\omega \wedge \eta) = (v \lrcorner \omega) \wedge \eta + (-)^p \omega \wedge (v \lrcorner \eta)\,. \tag{F.7b}$$

Musical isomorphisms The musical isomorphisms [18, p. 21] are a convenient way to connect $\mathbf{V}$ and $\mathbf{V}^* = \mathbf{\Lambda}^1$ by using the metric. The flat operator takes vectors to one-forms

$$\flat : \mathbf{V} \to \mathbf{\Lambda}^1\,, \tag{F.8a}$$

$$(\partial_i)^\flat \mapsto g_{ij}\, \mathbb{d}x^j\,, \tag{F.8b}$$

whereas the sharp operator takes one-forms to vectors

$$\sharp : \mathbf{\Lambda}^1 \to \mathbf{V}\,, \tag{F.9a}$$

$$(\mathbb{d}x^i)^\sharp \mapsto g^{ij}\partial_j\,. \tag{F.9b}$$

Hodge star The Hodge star operator is a linear isomorphism

$$\star : \mathbf{\Lambda}^r \to \mathbf{\Lambda}^{d-r}\,, \tag{F.10}$$

$$\tag{F.11}$$

One can start the construction from the zero-form, the Hodge star of which is just the volume form

$$\star 1 = \sqrt{\left|\det g_{ij}\right|}\, \mathbb{d}x^1 \wedge \mathbb{d}x^2 \wedge ... \wedge \mathbb{d}x^d\,. \tag{F.12}$$

The Hodge star of higher forms is constructed inductively by the following identity

$$\star(\eta \wedge \alpha) = \alpha^\sharp \lrcorner \star\eta \,, \tag{F.13}$$

where $\alpha \in \mathbf{\Lambda}^1$, η an arbitrary form. In particular, the Hodge dual of coordinate differentials reads

$$\star \mathbb{d}x^i = \star(1 \wedge \mathbb{d}x^i) = \left(\mathbb{d}x^i\right)^\sharp \lrcorner \star 1 = g^{ij}\partial_j \lrcorner \star 1 \,. \tag{F.14}$$

The inverse of Hodge star is the Hodge star itself with additional signs. For $\mathsf{s} = \operatorname{sgn}\det g_{ij}$, ω an r-form,

$$\star^{-1}\omega := \mathsf{s}(-)^{r(d-r)} \star \omega \,, \tag{F.15a}$$

$$\star^{-1} \star \omega = \star \star^{-1} \omega = \omega \,. \tag{F.15b}$$

Inner product and codifferential Let $\alpha = \alpha_i \, \mathbb{d}x^i$, $\beta = \beta_i \, \mathbb{d}x^i$ be two one-forms. One can verify that

$$\alpha \wedge \star\beta = g^{ij}\alpha_i\beta_j \,. \tag{F.16}$$

In general, for $\omega, \eta \in \mathbf{\Lambda}^r$, their inner product is defined by

$$(\omega, \eta) = \int \omega \wedge \star\eta \,. \tag{F.17}$$

In the sense of this inner product, for $\omega \in \mathbf{\Lambda}^r$, $\lambda \in \mathbf{\Lambda}^{r-1}$, one can define the codifferential $\mathbb{d}^\dagger$ as the adjoint of the exterior differential

$$\mathbb{d}^\dagger : \mathbf{\Lambda}^r \to \mathbf{\Lambda}^{r-1} \,, \tag{F.18a}$$

$$(\omega, \mathbb{d}\lambda) =: \left(\mathbb{d}^\dagger\omega, \lambda\right) . \tag{F.18b}$$

One can show that for $\omega \in \mathbf{\Lambda}^r$,

$$\mathbb{d}^\dagger\omega = (-)^r \star^{-1} \mathbb{d} \star \omega \,. \tag{F.19}$$

References

[1] N. Aghanim et al. (Planck Collaboration), "Planck 2018 results, VI. cosmological parameters," Astronomy & Astrophysics **641**, A6 (2018), arXiv:1807.06209 [astro-ph.CO] (cit. on p. 7).

[2] C. R. Almeida, A. B. Batista, J. C. Fabris, and P. V. Moniz, "Quantum cosmology of scalar-tensor theories and self-adjointness," Journal of Mathematical Physics **58**, 042301 (2016), arXiv:1608.08971 [gr-qc] (cit. on p. 35).

[3] H. Anciaux, *Minimal submanifolds in pseudo-Riemannian geometry* (World Scientific, Nov. 2010), 184 pp. (cit. on pp. 61, 89).

[4] A. A. Andrianov, C. Lan, and O. O. Novikov, "PT symmetric classical and quantum cosmology," in *Springer proceedings in physics* (Springer International Publishing, 2016), pp. 29–44 (cit. on pp. 5, 6).

[5] A. A. Andrianov, C. Lan, O. O. Novikov, and Y.-F. Wang, "Integrable minisuperspace models with Liouville field: energy density self-adjointness and semiclassical wave packets," The European Physical Journal C **78**, 786 (2018), arXiv:1802.06720 [hep-th] (cit. on pp. vii, 5, 8, 9, 20, 21, 30, 43).

[6] A. A. Andrianov, O. O. Novikov, and C. Lan, "Quantum cosmology of multifield scalar matter: some exact solutions," Theoretical and Mathematical Physics **184**, 1224–1233 (2015), arXiv:1503.05527 [hep-th] (cit. on pp. 5, 9).

[7] V. S. Araujo, F. A. B. Coutinho, and J. F. Perez, "Operator domains and self-adjoint operators," American Journal of Physics **72**, 203–213 (2004) (cit. on p. 35).

[8] В. И. Арнольд, *Обыкновенные дифференциальные уравнения*, Russian, First edition published in 1984 (МЦНМО, 2012), 344 pp. (cit. on pp. 63, 66); trans. by R. Cooke as *Ordinary differential equations* (Springer, 1992).

[9] В. И. Арнольд, *Математические методы классической механики*, Russian, 6th ed., First edition published in 1974 (Ленанд, 2017) (cit. on pp. 11, 21, 28, 29, 81, 88); trans. by K. Vogtmann and A. Weinstein as *Mathematical Methods of Classical Mechanics* (Springer, 1989).

[10] R. L. Arnowitt, S. Deser, and C. W. Misner, "Dynamical structure and definition of energy in general relativity," Physical Review **116**, 1322–1330 (1959) (cit. on p. 89).

[11] V. G. Bagrov and D. M. Gitman, eds., *Exact solutions of relativistic wave equations*, Vol. 39, Mathematics and its Applications (Springer, Feb. 28, 1990), 334 pp. (cit. on p. 44).

[12] G. D. Barbosa and N. Pinto-Neto, "Noncommutative geometry and cosmology," Physical Review D **70**, 103512 (2004), arXiv:hep-th/0407111 [hep-th] (cit. on p. 8).

[13] C. Barceló, "Analogue black-hole horizons," Nature Physics **15**, 210–213 (2018) (cit. on p. 48).

[14] C. Barceló, S. Liberati, and M. Visser, "Analogue gravity," Living Reviews in Relativity **14**, 10.12942/lrr-2011-3 (2005), arXiv:gr-qc/0505065 [gr-qc] (cit. on p. 48).

[15] J. D. Barrow, "Cosmic no-hair theorems and inflation," Physics Letters B **187**, 12–16 (1987) (cit. on p. 7).

[16] C. M. Bender, S. Boettcher, and P. N. Meisinger, "PT-symmetric quantum mechanics," Journal of Mathematical Physics **40**, 2201–2229 (1998), arXiv:quant-ph/9809072 [quant-ph] (cit. on p. 2).

[17] C. M. Bender and S. A. Orszag, *Advanced mathematical methods for scientists and engineers I, Asymptotic methods and perturbation theory* (McGraw Hill, New York, 1978), 593 pp. (cit. on p. 22).

[18] M. Berger, P. Gauduchon, and E. Mazet, *Le Spectre d'une Variété Riemannienne*, French, Vol. 194, Lecture Notes in Mathematics (Springer, 1971) (cit. on p. 99).

[19] L. R. Berrone and H. Giacomini, "Inverse Jacobi multipliers," Rendiconti del Circolo Matematico di Palermo **52**, 77–130 (2003) (cit. on pp. 61, 63).

[20] L. Bianchi, "Sugli spazi a tre dimensioni che ammettono un gruppo continuo di movimenti," Italian, Memorie di Matematica e di Fisica della Società Italiana delle Scienze, 3rd ser. **11**, 267–352 (1898) (cit. on p. 6); trans. by R. Jantzen as "On the three-dimensional spaces which admit a continuous group of motions" (Dec. 2001).

[21] L. Bianchi, *Lezioni sulla teoria dei gruppi continui finiti trasformazioni*, Italian (Spoerri, Pisa, 1918) (cit. on p. 6).

[22] M. Blagojević and F. W. Hehl, eds., *Gauge theories of gravitation, A reader with commentaries*, with a forew. by T. W. B. Kibble (Imperial College Press, Oct. 14, 2012), 656 pp., arXiv:1210.3775 [gr-qc] (cit. on pp. 1, 88).

[23] R. Blumenhagen, D. Lüst, and S. Theisen, *Basic concepts of string theory* (Springer Berlin Heidelberg, 2013) (cit. on p. 85).

[24] I. Boettcher, P. Bienias, R. Belyansky, A. J. Kollár, and A. V. Gorshkov, "Quantum simulation of hyperbolic space with circuit quantum electrodynamics: from graphs to geometry," Physical Review A **102**, 032208 (2019), arXiv:1910.12318 [quant-ph] (cit. on p. 48).

[25] N. Bohr, "Über die Serienspektra der Elemente," Zeitschrift für Physik **2**, 423–469 (1920) (cit. on p. 53).

[26] G. Bonneau, J. Faraut, and G. Valent, "Self-adjoint extensions of operators and the teaching of quantum mechanics," American Journal of Physics **69**, 322–331 (2001), arXiv:quant-ph/0103153 [quant-ph] (cit. on p. 35).

[27] L. Brillouin, "La mécanique ondulatoire de Schrödinger; une méthode générale de resolution par approximations successives," French, Comptes rendus hebdomadaires des séances de l'Académie des sciences **183**, 24–26 (1926) (cit. on p. 21).

[28] A. Burd and J. D. Barrow, "Inflationary models with exponential potentials," Nuclear Physics B **308**, 929–945 (1988) (cit. on p. 7).

[29] W. L. Burke, *Applied differential geometry* (Cambridge University Press, May 1985) (cit. on pp. 59, 63, 98).

[30] R. R. Caldwell, "A phantom menace? cosmological consequences of a dark energy component with super-negative equation of state," Physics Letters B **545**, 23–29 (1999), arXiv:astro-ph/9908168 [astro-ph] (cit. on p. 6).

[31] R. R. Caldwell, R. Dave, and P. J. Steinhardt, "Cosmological imprint of an energy component with general equation of state," Physical Review Letters **80**, 1582–1585 (1997), arXiv:astro-ph/9708069 [astro-ph] (cit. on p. 6).

[32] L. Castellani, "Symmetries in constrained hamiltonian systems," Annals of Physics **143**, 357–371 (1982) (cit. on p. 85).

[33] A. Cayley, "Sur quelques propriétés des déterminants gauches.," Journal für die reine und angewandte Mathematik (Crelles Journal), 119–123 (1846) (cit. on p. 94).

[34] S. Chakraborty, "Boundary terms of the einstein–hilbert action," in *Gravity and the quantum*, Vol. 187, Fundamental Theories of Physics (Springer International Publishing, July 19, 2016), pp. 43–59, arXiv:1607.05986 [gr-qc] (cit. on p. 89).

[35] C. Chirenti, J. Skákala, and A. Saa, "Quasinormal modes from a naked singularity," in Relativity and gravitation, 100 years after einstein in prague, edited by J. Bičák and T. Ledvinka, Springer Proceedings in Physics (2014), pp. 339–346 (cit. on p. 35).

[36] C. Cisneros, R. P. Martínez-y-Romero, H. N. Núñez-Yépez, and A. L. Salas-Brito, "Comment on "quantum mechanics of the $1/x^2$ potential," by Andrew M. Essin and David J. Griffiths [Am. J. Phys. 74 (2), 109–117 (2006)]," American Journal of Physics **75**, 953–955 (2007) (cit. on p. 35).

[37] T. M. Cover and J. A. Thomas, *Elements of information theory*, 2nd ed. (Wiley, Apr. 2005), 792 pp. (cit. on p. 52).

[38] E. Czuchry, N. Kwidzinski, and W. Piechocki, "Comparing the dynamics of diagonal and general Bianchi IX spacetime," The European Physical Journal C **79**, 173 (2014), arXiv:1409.2206 [gr-qc] (cit. on p. 6).

[39] M. P. Dąbrowski, C. Kiefer, and B. Sandhöfer, "Quantum phantom cosmology," Physical Review D **74**, 044022 (2006), arXiv:hep-th/0605229 [hep-th] (cit. on pp. 6, 30).

[40] B. S. DeWitt, "Quantum theory of gravity. I. the canonical theory," Physical Review **160**, 1113–1148 (1967) (cit. on pp. 1, 2, 13, 15, 90).

[41] P. A. M. Dirac, "A new notation for quantum mechanics," Mathematical Proceedings of the Cambridge Philosophical Society **35**, 416–418 (1939) (cit. on p. 40).

[42] P. A. M. Dirac, *The principles of quantum mechanics*, 4th ed., International Series of Monographs on Physics (Clarendon Press, Jan. 7, 1981) (cit. on p. 87).

[43] P. A. M. Dirac, "The theory of gravitation in Hamiltonian form," Proceedings of the Royal Society of London, Series A. Mathematical and Physical Sciences **246**, 333–343 (1958) (cit. on p. 89).

[44] P. A. M. Dirac, *Lectures on quantum mechanics*, Vol. 2, Belfer Graduate School of Science Monographs Series (Yeshiva University, New York, 1964) (cit. on p. 13).

[45] F. W. J. Olver et al., eds., *NIST digital library of mathematical functions*, version 1.1.0, (Dec. 15, 2020) http://dlmf.nist.gov/ (cit. on pp. 20, 23, 35, 92, 93, 97).

[46] T. M. Dunster, "Bessel functions of purely imaginary order, with an application to second-order linear differential equations having a large parameter," SIAM Journal on Mathematical Analysis **21**, 995–1018 (1990) (cit. on pp. 14, 24, 93).

[47] J. Dutka, "On the early history of Bessel functions," Archive for History of Exact Sciences **49**, 105–134 (1995) (cit. on p. 92).

[48] D. Eberly, *Ridges in image and data analysis* (Springer, 1996), 228 pp. (cit. on pp. 55, 58, 61).

[49] A. Einstein, "Die Feldgleichungen der Gravitation," German, Sitzungsberichte der Königlich Preußischen Akademie der Wissenschaften zu Berlin, 844–847 (1915) (cit. on p. 88); trans. by A. Engel as "The field equations of gravitation" (Princeton University Press, Oct. 5, 1997).

[50] A. Einstein, "Hamiltonsches Prinzip und allgemeine Relativitätstheorie," German, Sitzungsberichte der Königlich Preußischen Akademie der Wissenschaften zu Berlin, 1111–1116 (1916) (cit. on p. 89); trans. by W. Perrett and G. B. Jeffery as "Hamilton's principle and the general theory of relativity" (Methuen, 1923).

[51] A. Einstein, "Näherungsweise Integration der Feldgleichungen der Gravitation," German, Sitzungsberichte der Königlich Preußischen Akademie der Wissenschaften zu Berlin, 688–696 (1916) (cit. on p. 1); trans. by A. Engel as "Approximative integration of the field equations of gravitation" (Princeton University Press, Oct. 5, 1997).

[52] A. Einstein, "Kosmologische betrachtungen zur allgemeinen relativitätstheorie," German, Sitzungsberichte der Königlich Preußischen Akademie der Wissenschaften zu Berlin, 142–152 (1917) (cit. on p. 5); trans. by W. Perrett and G. B. Jeffery as "Cosmological considerations in the general theory of relativity" (Methuen, 1923).

[53] A. M. Essin and D. J. Griffiths, "Quantum mechanics of the $1/x^2$ potential," American Journal of Physics **74**, 109–117 (2006) (cit. on p. 35).

[54] L. Evans, *Partial differential equations*, 2nd ed., Vol. 19, Graduate Studies in Mathematics (American Mathematical Society, 2010), 749 pp. (cit. on pp. 15, 28, 63).

[55] J. Feinberg and Y. Peleg, "Self-adjoint Wheeler–DeWitt operators, the problem of time, and the wave function of the Universe," Physical Review D **52**, 1988–2000 (1995), arXiv:`hep-th/9503073 [hep-th]` (cit. on p. 35).

[56] A. Friedman, "Über die Krümmung des Raumes," German, Zeitschrift für Physik **10**, 377–386 (1922) (cit. on p. 5); trans. by G. F. R. Ellis and H. van Elst as "On the curvature of space" (Dec. 1999).

[57] B. Friedrich and D. Herschbach, "Stern and Gerlach: how a bad cigar helped reorient atomic physics," Physics Today **56**, 53–59 (2003) (cit. on p. 37).

[58] T. F. Gallagher, *Rydberg atoms*, Cambridge Monographs on Atomic, Molecular and Chemical Physics (Cambridge University Press, Sept. 1994) (cit. on p. 48).

[59] I. A. García and M. Grau, "A survey on the inverse integrating factor," Qualitative Theory of Dynamical Systems **9**, 115–166 (2009), arXiv:0903.0941 [math.DS] (cit. on pp. 61, 62).

[60] H. García-Compeán, O. Obregón, and C. Ramírez, "Noncommutative quantum cosmology," Physical Review Letters **88**, 161301 (2001), arXiv:hep-th/0107250 [hep-th] (cit. on p. 8).

[61] U. H. Gerlach, "Derivation of the ten Einstein field equations from the semiclassical approximation to quantum geometrodynamics," Physical Review **177**, 1929–1941 (1969) (cit. on pp. 21, 28).

[62] W. Gerlach and O. Stern, "Über die Richtungsquantelung im Magnetfeld," Annalen der Physik **379**, 673–699 (1924) (cit. on p. 37).

[63] G. W. Gibbons and S. W. Hawking, "Action integrals and partition functions in quantum gravity," Physical Review D **15**, 2752–2756 (1977) (cit. on p. 88).

[64] D. M. Gitman, I. V. Tyutin, and B. L. Voronov, *Self-adjoint extensions in quantum mechanics* (Birkhäuser, 2012) (cit. on pp. 40, 44, 94).

[65] Д. М. Гитман and И. В. Тютин, *Каноническое квантование полей со связями*, Russian (Наука, 1986) (cit. on p. 81); trans. by D. M. Gitman and I. V. Tyutin as *Quantization of fields with constraints* (Springer, 1990).

[66] D. M. Gitman and I. V. Tyutin, *Quantization of fields with constraints*, trans. by D. M. Gitman and I. V. Tyutin, Springer Series in Nuclear and Particle Physics (Springer, 1990) (cit. on p. 39).

[67] D. Giulini, "What is the geometry of superspace?" Physical Review D **51**, 5630–5635 (1993), arXiv:gr-qc/9311017 [gr-qc] (cit. on p. 13).

[68] D. Giulini, "The superspace of geometrodynamics," General Relativity and Gravitation **41**, 785–815 (2009), arXiv:0902.3923 [gr-qc] (cit. on p. 5).

[69] M. Goodman, "Path integral solution to the infinite square well," American Journal of Physics **49**, 843–847 (1981) (cit. on p. 38).

[70] I. S. Gradshteyn and I. M. Ryzhik, *Table of integrals, series, and products*, edited by D. Zwillinger and V. Moll, 8th ed. (Academic Press, 2015), 1184 pp. (cit. on p. 17).

[71] R. L. Graham, D. E. Knuth, and O. Patashnik, *Concrete mathematics, A foundation for computer science*, 2nd ed., First edition published in 1988 (Addison-Wesley, Feb. 1, 1994), 672 pp. (cit. on p. 20).

[72] A. Gut, *An intermediate course in probability*, 2nd ed., Springer Texts in Statistics (Springer, 2009) (cit. on p. 31).

[73] B. C. Hall, *Quantum theory for mathematicians* (Springer, 2013) (cit. on pp. 37, 38, 94).

[74] J. J. Halliwell, "Scalar fields in cosmology with an exponential potential," Physics Letters B **185**, 341–344 (1987) (cit. on p. 7).

[75] J. J. Halliwell, "Introductory lectures on quantum cosmology," in Quantum cosmology and baby universes, Vol. 7, edited by S. Coleman, J. B. Hartle, T. Piran, and S. Weinberg (Aug. 1991), arXiv:0909.2566 [gr-qc] (cit. on pp. 53, 57).

[76] J. J. Halliwell and S. W. Hawking, "Origin of structure in the Universe," Physical Review D **31**, 1777–1791 (1985) (cit. on p. 6).

[77] P. Harremoes, "Binomial and Poisson distributions as maximum entropy distributions," IEEE Transactions on Information Theory **47**, 2039–2041 (2001) (cit. on p. 53).

[78] S. W. Hawking and D. N. Page, "Operator ordering and the flatness of the universe," Nuclear Physics B **264**, 185–196 (1986) (cit. on p. 21).

[79] D. Hilbert, "Grundlagen der Physik, Erste mitteilung," German, Nachrichten von der Koeniglichen Gesellschaft der Wissenschaften zu Goettingen, Math-physik. Klasse, 395–407 (1915) (cit. on p. 88).

[80] R. Jackiw, "Analysis on infinite-dimensional manifolds, Schrödinger representation for quantized fields," in Field theory and particle physics, edited by O. J. P. Eboli, M. Gomes, and A. Santoro (1990), pp. 78–143 (cit. on p. 90).

[81] C. G. J. Jacobi, "Theoria novi multiplicatoris systemati aequationum differentialium vulgarium applicandi," Latin, Journal für die reine und angewandte Mathematik (Crelles Journal), 199–268 (1844) (cit. on p. 63); "Theoria novi multiplicatoris systemati aequationum differentialium vulgarium applicandi, (cont. dissert. tom. XXVII)," Latin, Journal für die reine und angewandte Mathematik (Crelles Journal), 213–279 (1845).
"Theoria novi multiplicatoris systemati aequationum differentialium vulgarium applicandi, (cont. dissert.)," Latin, Journal für die reine und angewandte Mathematik (Crelles Journal), 333–376 (1845).

[82] E. Joos, "Decoherence through interaction with the environment," in *Decoherence and the appearance of a classical world in quantum theory*, 2nd ed. (Springer Berlin Heidelberg, 2003) Chap. 3, pp. 41–180 (cit. on p. 52).

[83] I. Jubb, J. Samuel, R. D. Sorkin, and S. Surya, "Boundary and corner terms in the action for general relativity," Classical and Quantum Gravity **34**, 065006 (2016), arXiv:1612.00149 [gr-qc] (cit. on p. 89).

[84] R. Kantowski and R. K. Sachs, "Some spatially homogeneous anisotropic relativistic cosmological models," Journal of Mathematical Physics **7**, 443–446 (1966) (cit. on pp. 6, 8).

[85] C. Kiefer and H. D. Zeh, "Arrow of time in a recollapsing quantum universe," Physical Review D **51**, 4145–4153 (1994), arXiv:gr-qc/9402036 [gr-qc] (cit. on p. 13).

[86] C. Kiefer, "Wave packets in minisuperspace," Physical Review D **38**, 1761–1772 (1988) (cit. on p. 6).

[87] C. Kiefer, "Non-minimally coupled scalar fields and the initial value problem in quantum gravity," Physics Letters B **225**, 227–232 (1989) (cit. on p. 13).

[88] C. Kiefer, "Wave packets in quantum cosmology and the cosmological constant," Nuclear Physics B **341**, 273–293 (1990) (cit. on p. 21).

[89] C. Kiefer, "Consistent histories and decoherence," in *Decoherence and the appearance of a classical world in quantum theory*, 2nd ed. (Springer, 2003) Chap. 5, pp. 227–258 (cit. on p. 3).

[90] C. Kiefer, "Decoherence in quantum field theory and quantum gravity," in *Decoherence and the appearance of a classical world in quantum theory*, 2nd ed. (Springer, 2003) Chap. 4, pp. 181–225 (cit. on pp. 3, 52).

[91] C. Kiefer, *Quantum gravity*, 3rd ed., International Series of Monographs on Physics (Oxford University Press, Apr. 2012) (cit. on pp. 1–3, 6, 12, 13, 15, 21, 22, 29, 89).

[92] C. Kiefer, "Quantum gravity," in *Springer handbook of spacetime*, edited by A. Ashtekar and V. Petkov, Springer Handbooks (Springer, Berlin, 2014) Chap. 33, pp. 709–722 (cit. on p. 1).

[93] C. Kiefer, N. Kwidzinski, and W. Piechocki, "On the dynamics of the general Bianchi IX spacetime near the singularity," The European Physical Journal C **78**, 691 (2018), arXiv:1807.06261 [gr-qc] (cit. on p. 6).

[94] C. Kiefer, N. Kwidzinski, and D. Piontek, "Singularity avoidance in Bianchi I quantum cosmology," The European Physical Journal C **79**, 10.1140/epjc/s10052-019-7193-6 (2019), arXiv:1903.04391 [gr-qc] (cit. on pp. 6, 20–22).

[95] C. Kiefer and T. Schmitz, "Singularity avoidance for collapsing quantum dust in the Lemaître–Tolman–Bondi model," Physical Review D **99**, 126010 (2019), arXiv:1904.13220 [gr-qc] (cit. on p. 5).

[96] N. Kiriushcheva and S. Kuzmin, "The Hamiltonian formulation of general relativity: myths and reality," Open Physics **9**, 10.2478/s11534-010-0072-2 (2008), arXiv:0809.0097 [gr-qc] (cit. on pp. 89, 90).

[97] J. J. Koenderink and A. J. van Doorn, "Local features of smooth shapes: ridges and courses," in Geometric methods in computer vision II, edited by B. C. Vemuri (June 1993) (cit. on pp. 55, 59, 61, 63, 64).

[98] J. J. Koenderink and A. J. van Doorn, "Two-plus-one-dimensional differential geometry," Pattern Recognition Letters **15**, 439–443 (1994) (cit. on pp. 55, 61).

[99] H. A. Kramers, "Wellenmechanik und halbzahlige Quantisierung," German, Zeitschrift für Physik **39**, 828–840 (1926) (cit. on p. 21).

[100] E. E. Kummer, "De integralibus quibusdam definitis et seriebus infinitis," Latin, Journal für die reine und angewandte Mathematik (Crelles Journal) **1837**, 228–242 (1837) (cit. on p. 97).

[101] D. N. Kupeli, "Degenerate submanifolds in semi-Riemannian geometry," Geometriae Dedicata **24**, 337–361 (1987) (cit. on p. 61).

[102] Kvale, "L^p Spaces," in *Encyclopedia of mathematics* (2016) (cit. on p. 15).

[103] N. Kwidzinski, D. Malafarina, J. Ostrowski, W. Piechocki, and T. Schmitz, "Hamiltonian formulation of dust cloud collapse," Physical Review D **101**, 104017 (2020), arXiv:2001.01903 [gr-qc] (cit. on pp. 5, 6).

[104] N. Kwidzinski and W. Piechocki, "Curvature invariants for the Bianchi IX spacetime filled with tilted dust," 10.1140/epjc/s10052-019-6701-z (2019), arXiv:1901.01790 [gr-qc] (cit. on p. 6).

[105] Л. Д. Ландау and Е. М. Лифшиц, *Квантовая механика, Нерелятивистская теория*, Russian, edited by Л. П. Питаевский, 6th ed., Vol. 3, 10 vols., Теоретическая физика (Физматлит, 2016) (cit. on pp. 21, 38, 96); trans. by J. B. Sykes and J. S. Bell as *Quantum mechanics, Non-relativistic theory* (Pergamon, 1977).

[106] Л. Д. Ландау and Е. М. Лифшиц, *Механика*, Russian, 7th ed., Vol. 1, 10 vols., Теоретическая физика (Физматлит, 2017) (cit. on pp. 28, 29); trans. by J. B. Sykes and J. S. Bell as *Mechanics* (Pergamon, 1976).

[107] Л. Д. Ландау and Е. М. Лифшиц, *Теория поля*, Russian, edited by Л. П. Питаевский, Vol. 2, 10 vols., Теоретическая физика (Физматлит, 2017) (cit. on pp. 6, 7, 60); trans. by M. Hamermesh as *The classical theory of fields* (Pergamon, 1975).

[108] Л. Д. Ландау and Е. М. Лифшиц, *Статистическая физика, Часть 1*, Russian, 6th ed., Vol. 5, 10 vols., Теоретическая физика (Физматлит, 2018) (cit. on p. 37); trans. by M. J. Kearsley as *Statistical physics*, Part 1 (Butterworth–Heinemann, 1980).

[109] G. Lemaître, "Un univers homogène de masse constante et de rayon croissant rendant compte de la vitesse radiale des nébuleuses extragalactiques," French, Annales de la Société Scientifique de Bruxelles, A **47**, 49–59 (1927) (cit. on p. 5); [Monthly Notices of the Royal Astronomical Society **91**, 483–490 (1931)].

[110] G. Lifschytz, S. D. Mathur, and M. E. Ortiz, "Note on the semiclassical approximation in quantum gravity," Physical Review D **53**, 766–778 (1994), arXiv:`gr-qc/9412040 [gr-qc]` (cit. on p. 21).

[111] J. Lim, H.-g. Lee, and J. Ahn, "Review of cold Rydberg atoms and their applications," Journal of the Korean Physical Society **63**, 867–876 (2013) (cit. on p. 48).

[112] J. Liouville, "Sur l'équation aux différences partielles $\frac{\mathrm{d}^2 \log \lambda}{\mathrm{d}u\,\mathrm{d}v} \pm \frac{\lambda}{2a^2} = 0$," French, Journal de Mathématiques Pures et Appliquées, 71–72 (1853) (cit. on p. 7).

[113] A. J. Maciejewski and M. Szydlowski, "On the integrability of Bianchi cosmological models," Journal of Physics A: Mathematical and General **31**, 2031–2043 (1997), arXiv:`gr-qc/9702045 [gr-qc]` (cit. on p. 79).

[114] W. Magnus, F. Oberhettinger, and R. P. Soni, *Formulas and theorems for the special functions of mathematical physics* (Springer, 1966) (cit. on pp. 23, 24).

[115] Y. I. Manin and A. A. Panchishkin, *Introduction to modern number theory, Fundamental problems, ideas and theories*, 2nd ed., Encyclopaedia of Mathematical Sciences, Russian version originally published in 1990 (Springer, 2005) (cit. on p. 116).

[116] B. Markoski, *Basic principles of topography*, Springer Geography (Springer, 2018) (cit. on p. 58).

[117] C. W. Misner, "Minisuperspace," in *Magic without magic, John Archibald Wheeler*, A collection of essays in honor of his sixtieth birthday, edited by J. R. Klauder (W. H. Freeman and Company, San Francisco, July 1972), pp. 441–474 (cit. on pp. 3, 5).

[118] C. W. Misner, K. S. Throne, and J. A. Wheeler, *Gravitation*, with a forew. by D. I. Kaiser, Originally published in 1973 (Princeton University Press, Oct. 24, 2017), 1280 pp. (cit. on p. 59).

[119] J. W. Moffat, "Scalar–tensor–vector gravity theory," Journal of Cosmology and Astroparticle Physics **2006**, 004–004 (2005), arXiv:gr-qc/0506021 [gr-qc] (cit. on p. 88).

[120] P. M. Morse, "Diatomic molecules according to the wave mechanics. II. vibrational levels," Physical Review **34**, 57–64 (1929) (cit. on p. 44).

[121] A. Mostafazadeh, "Pseudo-Hermitian representation of quantum mechanics," International Journal of Geometric Methods in Modern Physics **07**, 1191–1306 (2008), arXiv:0810.5643 [quant-ph] (cit. on p. 2).

[122] M. Nakahara, *Geometry, topology and physics*, 2nd ed., Graduate Student Series in Physics, First edition published in 1990 (Taylor & Francis Ltd, June 4, 2003), 596 pp. (cit. on p. 98); trans. by M. Delbrück as *Differentialgeometrie, Topologie und Physik* (Springer, 2015).

[123] Y. Nakayama, "Liouville field theory – a decade after the revolution," International Journal of Modern Physics A **19**, 2771–2930 (2004), arXiv:hep-th/0402009 [hep-th] (cit. on p. 7).

[124] J. A. Nelder and R. W. M. Wedderburn, "Generalized linear models," Journal of the Royal Statistical Society, A **135**, 370 (1972) (cit. on p. 54).

[125] J. von Neumann, "Allgemeine Eigenwerttheorie Hermitescher Funktionaloperatoren," Mathematische Annalen **102**, 49–131 (1930) (cit. on p. 94).

[126] J. von Neumann, *Mathematische Grundlagen der Quantenmechanik*, with a forew. by R. Haag, 2nd ed., First edition published in 1932 (Springer, 1996) (cit. on p. 35); trans. by R. T. Beyer as *Mathematical foundations of quantum mechanics* (Princeton University Press, Feb. 2018).

[127] Y. Ohkuwa and T. Kitazoe, "Wave packet in quantum cosmology and definition of semiclassical time," International Journal of Modern Physics A **12**, 859–871 (1996), arXiv:gr-qc/9606006 [gr-qc] (cit. on p. 21).

[128] S. Pal and N. Banerjee, "Addressing the issue of nonunitarity in anisotropic quantum cosmology," Physical Review D **90**, 104001 (2014), arXiv:1410.2718 [gr-qc] (cit. on p. 35).

[129] S. Pal and N. Banerjee, "Restoring unitarity in anisotropic quantum cosmological models," Physical Review D **91**, 044042 (2014), arXiv:1411.1167 [gr-qc] (cit. on p. 35).

[130] S. Pal and N. Banerjee, "Anisotropic models are unitary: a rejuvenation of standard quantum cosmology," Journal of Mathematical Physics **57**, 122502 (2016), arXiv:1601.00460 [gr-qc] (cit. on p. 35).

[131] A. Passian, H. Simpson, S. Kouchekian, and S. Yakubovich, "On the orthogonality of the MacDonald's functions," Journal of Mathematical Analysis and Applications **360**, 380–390 (2009) (cit. on p. 43).

[132] W. Pauli, *Ausgewählte Kapitel aus der Feldquantisierung*, German, edited by U. Hochstrasser and M. R. Schafroth (ETH Zürich, 1951) (cit. on p. 22); trans. by S. Margulies and H. R. Lewis as *Selected topics in field quantization* (MIT Press, 1973).

[133] M. E. Peskin and D. V. Schroeder, *An introduction to quantum field theory* (CRC Press, Oct. 2, 1995), 866 pp. (cit. on p. 85).

[134] W. Piechocki and T. Schmitz, "Quantum oppenheimer-snyder model," Physical Review D **102**, 046004 (2020), arXiv:2004.02939 [gr-qc] (cit. on p. 5).

[135] J. B. Pitts, "A first class constraint generates not a gauge transformation, but a bad physical change: the case of electromagnetism," Annals of Physics **351**, 382–406 (2013), arXiv:1310.2756 [gr-qc] (cit. on p. 81).

[136] L. Pochhammer, "Ueber die Differentialgleichung der allgemeineren hypergeometrischen Reihe mit zwei endlichen singulären Punkten," German, Journal für die reine und angewandte Mathematik (Crelles Journal), 76–159 (1888) (cit. on p. 97).

[137] D. N. Poenaru and A. Calboreanu, "Alexandru Proca (1897-1955) and his equation of the massive vector boson field," Europhysics News **37**, 24–26 (2006) (cit. on p. 81).

[138] E. Poisson, *A relativist's toolkit* (Cambridge University Press, May 2004) (cit. on pp. 89, 90).

[139] S. Popescu, A. J. Short, and A. Winter, "Entanglement and the foundations of statistical mechanics," Nature Physics **2**, 754–758 (2005), arXiv:quant-ph/0511225 [quant-ph] (cit. on p. 52).

[140] L. V. Prokhorov and S. V. Shabanov, *Hamiltonian mechanics of gauge systems* (Cambridge University Press, Sept. 2011), 486 pp. (cit. on p. 89).

[141] M. Reed and B. Simon, *Methods of modern mathematical physics, Fourier analysis, self-adjointness*, Vol. 2 (Academic Press, Nov. 5, 1975), 361 pp. (cit. on pp. 35, 39, 94, 95).

[142] M. Reed and B. Simon, *Methods of modern mathematical physics, Functional analysis*, Vol. 1 (Academic Press, Feb. 8, 1981), 416 pp. (cit. on pp. 35, 39).

[143] H. P. Robertson, "Kinematics and world-structure," The Astrophysical Journal **82**, 284 (1935) (cit. on p. 5); "Kinematics and world-structure III.," The Astrophysical Journal **83**, 257 (1936).

[144] H. J. Rothe and K. D. Rothe, *Classical and quantum dynamics of constrained Hamiltonian systems* (World Scientific, Apr. 2010) (cit. on p. 81).

[145] R. Rothe, "Zum Problem des Talwegs," German, Sitzungsberichte der Berliner Mathematischen Gesellschaft **14**, 51–68 (1915) (cit. on pp. 61–64).

[146] C. E. Rüter, K. G. Makris, R. El-Ganainy, D. N. Christodoulides, M. Segev, and D. Kip, "Observation of parity–time symmetry in optics," Nature Physics **6**, 192–195 (2010) (cit. on p. 2).

[147] M. P. Ryan, *Hamiltonian cosmology*, Vol. 13, Lecture Notes in Physics (Springer, 1972) (cit. on p. 6).

[148] B. de Saint-Venant, "Surfaces à plus grande pente constituées sur des lignes courbes," French, Extraits des procès-verbaux des séances. Société philomathique de Paris, 24–29 (1852) (cit. on pp. 58, 59).

[149] J. J. Sakurai and J. Napolitano, *Modern quantum mechanics*, 3rd ed., First edition published in 1985 (Cambridge University Press, Sept. 17, 2020) (cit. on p. 37).

[150] T. Schmitz, "Towards a quantum Oppenheimer–Snyder model," Physical Review D **101**, 026016 (2019), arXiv:1912.08175 [gr-qc] (cit. on p. 5).

[151] F. Schwabl, *Statistische Mechanik*, German, 3rd ed. (Springer, 2006) (cit. on p. 37).

[152] J. Shigeru, "Seki Kowa," in *Encyclopaedia of the history of science, technology, and medicine in non-western cultures*, edited by H. Selin, 2nd ed. (Springer, Dordrecht, 2008), pp. 1992–1994 (cit. on p. 20).

[153] N. Sibalic, *Rydberg physics* (IOP Publishing, 2018) (cit. on p. 48).

[154] E. D. Solomentsev and E. V. Shikin, "Laplace–Beltrami equation," in *Encyclopedia of mathematics* (2020) (cit. on p. 13).

[155] N. Y. Sonine, "Recherches sur les fonctions cylindriques et le développement des fonctions continues en séries," French, Mathematische Annalen **16**, 1–80 (1880) (cit. on p. 97).

[156] J. Steinhauer, "Observation of quantum Hawking radiation and its entanglement in an analogue black hole," Nature Physics **12**, 959–965 (2015), arXiv:1510.00621 [gr-qc] (cit. on p. 48).

[157] R. Szmytkowski and S. Bielski, "Comment on the orthogonality of the Macdonald functions of imaginary order," Journal of Mathematical Analysis and Applications **365**, 195–197 (2009), arXiv:0909.4232 [math.CA] (cit. on pp. 43, 92, 93).

[158] W. G. Unruh, "Experimental black-hole evaporation?" Physical Review Letters **46**, 1351–1353 (1981) (cit. on p. 48).

[159] J. H. Van Vleck, "The correspondence principle in the statistical interpretation of quantum mechanics," Proceedings of the National Academy of Sciences **14**, 178–188 (1928) (cit. on p. 22).

[160] M. Visser, "Van Vleck determinants: geodesic focussing and defocussing in Lorentzian spacetimes," Physical Review D **47**, 2395–2402 (1993), arXiv:hep-th/9303020 [hep-th] (cit. on p. 22).

[161] C. Waksjö and S. Rauch-Wojciechowski, "How to find separation coordinates for the Hamilton–Jacobi equation: a criterion of separability for natural Hamiltonian systems," Mathematical Physics, Analysis and Geometry **6**, 301–348 (2003) (cit. on p. 21).

[162] R. M. Wald, *General relativity* (University of Chicago Press, Chicago, 1984) (cit. on p. 90).

[163] A. G. Walker, "On milne's theory of world-structure," Proceedings of the London Mathematical Society **s2-42**, 90–127 (1937) (cit. on p. 5).

[164] 竹. 王 and 敦. 郭, 特殊函数概论, Chinese (Peking University Press, Beijing, May 2000) (cit. on p. 92); trans. by D. R. Guo and X. J. Xia as *Special functions* (World Scientific, Oct. 1989).

[165] S. Weinberg, *Cosmology* (Oxford University Press, Feb. 21, 2008), 624 pp. (cit. on p. 7).

[166] S. Weinfurtner, S. Liberati, and M. Visser, "Analogue model for quantum gravity phenomenology," Journal of Physics A: Mathematical and General **39**, 6807–6813 (2005), arXiv:gr-qc/0511105 [gr-qc] (cit. on p. 48).

[167] S. Weinfurtner, E. W. Tedford, M. C. J. Penrice, W. G. Unruh, and G. A. Lawrence, "Measurement of stimulated Hawking emission in an analogue system," Physical Review Letters **106**, 021302 (2010), arXiv:1008.1911 [gr-qc] (cit. on p. 48).

[168] G. Wentzel, "Eine Verallgemeinerung der Quantenbedingungen für die Zwecke der Wellenmechanik," German, Zeitschrift für Physik **38**, 518–529 (1926) (cit. on p. 21).

[169] J. A. Wheeler, "Superspace and the nature of quantum geometrodynamics," in *Battelle rencontre, 1967 lectures in mathematics and physics, 1967 lectures in mathematics and physics*, edited by C. M. DeWitt and J. A. Wheeler (W. A. Benjamin, Inc., 1968) Chap. 9, pp. 242–307 (cit. on p. 5).

[170] N. Wheeler, *Feynman quantization, An introduction to path-integral techniques*, (2000) https://www.reed.edu/physics/faculty/wheeler/documents/Quantum%20Mechanics/Class%20Notes/Chapter%203:PDF (visited on 01/23/2021) (cit. on p. 22).

[171] S. Wimberger, *Nonlinear dynamics and quantum chaos* (Springer International Publishing, 2014), 220 pp. (cit. on p. 21).

[172] T. T. Wu and C. N. Yang, "Concept of nonintegrable phase factors and global formulation of gauge fields," Physical Review D **12**, 3845–3857 (1975) (cit. on p. 1).

[173] J. Wudka, "Boundary conditions and the cosmological constant," Physical Review D **36**, 1036–1040 (1987) (cit. on p. 35).

[174] S. B. Yakubovich, "A distribution associated with the Kontorovich–Lebedev transform," Opuscula Mathematica **26**, 161–172 (2006) (cit. on p. 43).

[175] X. L. Yang, S. H. Guo, F. T. Chan, K. W. Wong, and W. Y. Ching, "Analytic solution of a two-dimensional hydrogen atom. I. nonrelativistic theory," Physical Review A **43**, 1186–1196 (1991) (cit. on p. 50).

[176] J. W. York, "Role of conformal three-geometry in the dynamics of gravitation," Physical Review Letters **28**, 1082–1085 (1972) (cit. on p. 88).

[177] B. Zaslow and M. E. Zandler, "Two-dimensional analog to the hydrogen atom," American Journal of Physics **35**, 1118–1119 (1967) (cit. on p. 96).

[178] H. D. Zeh, "Basic concepts and their interpretation," in *Decoherence and the appearance of a classical world in quantum theory*, 2nd ed. (Springer, 2003) Chap. 2, pp. 7–40 (cit. on p. 52).

Acknowledgement

To begin with, we would like to thank you, the reader, who has spent the precious time to read this section. The dissertation is doomed to lose its significance over time, but at least it stirs up tiny ripples in humanity when you read these lines.

We are grateful to our supervisor, Prof. Dr. Claus Kiefer, who has not only shared us his rich experience on quantum gravity, but also showed us many insights into general physics, history of science, philosophy and other aspects. Moreover, Claus offered us much help in affairs related to our study, and provided many opportunities to practise technical skills and expand our horizons. We feel happy and honoured to have worked with and been guided by him.

We would also like to thank Dr. Chen Lan (兰 晨) for his collaboration. We met Chen on `douban.com` (豆瓣网) years ago, which was originally a combination of goodreads, IMDB and spotify, and is not particularly intended for scientists. It is a miracle that technology brings people together, in one way or another.

We thank Prof. Dr. Friedrich W. Hehl, Dr. Branislav Nikolić, Dr. Nick Kwidzinski, Dr. Leonardo Chataignier, (almost Dr.) Tim Schmitz, Tatevik Vardanyan, Mario Montero, Alexander Hermanns, Anton Krieger, David Wichmann, Dennis Piontek, Anirudh Gundhi, Sebastian Arenas, Dimitrios Gkiatas, Sandeep Suresh, Ali Lezeik and Christina Kolifoti, for having you in our research group, so that we could enjoy our life both as people and as researchers. Friedrich, ich wünsche Dir beste Gesundheit! Leonardo and Tim, you genius, wish you good luck working in academia! David, 你中文很可以! Dimitris, diao! And we feel sorry for Atharva Rawte, Shreyas Tiruvaskar, Enes Aktas, Ayesha Khan and Willem van der Feltz, for that we have hardly spent time with you due to the pandemic.

Jun.-Prof. Dr. Nele Callebaut, Prof. Dr. Andreas Eckart and PD Dr. Rochus Klesse made the defence committee for us. Dr. Petra Neubauer-Guenther and Dr. Andreas Sindermann have provided us much help during our study.

In addition, Prof. Dr. Alexander A. Andrianov, Dr. Oleg O. Novikov, Dr. Huifang Geng (耿 惠芳) and Prof. Dr. Alexander Andreev have collaborated with us in publications, in which we also benefited from discussions with Dr. Ziping Rao (饶 梓平) and Dr. Chao Li (李 超).

In the end, we are thankful to Qinglan Liu (刘 青蓝), who stays together with us in these rough days. With your presence, we see the necessity of paving a way out towards a dynamic future, even if the quantum Universe is timeless itself. *Wir müssen es schaffen, wir werden es schaffen.* Don Jon and Cassie are also to be mentioned.

I have discovered a truly marvellous ending sentence, which this margin is too narrow to contain. [115, sec. 7.1.1]